

A dissertation submitted to the UNIVERSITÀ DEGLI STUDI DI NAPOLI FEDERICO II and produced in collaboration with the SWISS FEDERAL INSTITUTE OF TECHNOLOGY ZURICH



**ETH**

Eidgenössische Technische Hochschule Zürich  
Swiss Federal Institute of Technology Zurich

# Diesel Injection Analysis for New Premium Fuel Research and Emission Reduction

Presented for the degree of DOCTOR OF TECHNICAL SCIENCES by

**Stephan Caruso**

Master of Science – Mechanical Engineering

Università degli Studi di Napoli Federico II

Born June 26<sup>th</sup>, 1980

Citizen of Italy

Scuola di dottorato in Ingegneria Industriale Dottorato di Ricerca in Ingegneria dei Sistemi Meccanici XXIII Ciclo

Supervisors:

Prof. Dr. Mariano Migliaccio  
Dr. Bruno Schneider

Coordinator of the PhD school:

Prof. Dr. Fabio Bozza

2010

*to my father*

---

## Acknowledgment

This study has been carried out at the Aerothermochemistry and Combustion Systems Laboratory within the Institute for Energy Technology at the ETH Zurich even though my PhD study starts at the “Dipartimento di Energia Meccanica per l’Energetica” within the University of Naples “Federico II”. I felt particularly proud and lucky for having the chance to be part of these two first-rate universities and therefore want to thank professor Mariano Migliaccio and professor Konstantinos Boulouchos who both made this possible for me. The first for being so helpful and for offering me the opportunity to spend almost 2 years of my PhD studies abroad and the second for taking me aboard.

For different reasons I am very thankful to many persons and to some of them for more than one.

As to my dissertation and the time spent at the LAV I wish to give a special thank to Dr. Bruno Schneider who supervised all my work. He is an excellent scientist and he has been helpful, friendly and of great help till the end of this dissertation. I feel honoured to know such a great person!

My sincerest appreciation also goes to Wolfgang Kreutner, Jean Gilder, Yuri M. Wright and Panagiotis Kyratos who helped me to make this dissertation bearable - or dare I say, enjoyable - by helping me not only with the English.

I’d like to thank all my colleagues at LAV, with whom I spent some really good time together. I hope to keep in contact with all of you and, why not, keep having a few beers and definitely some nice rides. My thanks also go to the LAV technical and secretary staff who made my life that much easier. Despite my German improvement seems to show little desire to integration I have been fortunate enough to be surrounded by people who all leave wonderful memories. I hope I’ll be able to show you all my good will in learning German!

Regarding my work at the DIME I’d like to thank Dr. Ottavio Pennacchia, a friend with an exceptional intelligence and with an incommensurable patience that made me learn a lot. I also wish to express my gratitude to all the people of the DIME, for their encouragement and never-ending support.

I express my greatest gratitude to all those persons who pushed me into this experience abroad when I felt insecure. I clearly remember the moment when my brother told me to think what my father would have suggested. Those words had a strong effect. Thanks for saying these words at the right time. My family (and I’m saying **my entire family**), had a strong influence on my final decision and even though this meant moving away from them, they definitely supported this experience. You’re the most important people whom I simply will not be able to thank enough. I really love you with all my heart!

---

## Abstract

The objective of this study was to bring a scientific contribute in the problem of reducing diesel in-cylinder emissions, and releasing the diesel engine from its dependence on petroleum. The first two introductory chapters of this dissertation contain an overview of these two issues and the techniques used nowadays to address them respectively. In this context, the emphasis is on the injection system parameters and the most interesting petroleum-diesel alternatives. Improvements of the injection system parameters help to meet future more stringent exhaust gas limits and seem to become the decisive factor to reach further emission targets [1]. The search for alternatives to petroleum-based fuels is probably the only solution which, at the same time, may help to reduce the harmful exhaust emissions and to diversify energy sources, thus improving security of supply.

The first part of this work was dedicated to the design and implementation of a test bench for investigating the hydraulic injection behaviour of large diesel injectors (up to 1000 mg per stroke). This task was motivated by the need to develop the diagnostics for a new experimental 4-litres, single cylinder diesel engine. The test bench consists of an injection rate measuring system of the Bosch tube type that is able to completely define all injector characteristics as: Injection time (hydraulic start, end and corresponding delay from electric signal), injection rate and injected quantity. In the third chapter of this dissertation, first a brief overview is given of the state of the art of the injection system technology and of the physical measurement principle of the injection analyzer. Then, the design of the new injection meter is described. The implementation of the measurement setup with the data acquisition system and the development and implementation of the data processing algorithm are also presented. Some measurement results are shown to demonstrate the performances of the new injection analyzer.

The second part of this work aimed at contributing to a research project named “Future Fuels for Diesel Engines” and promoted by the FVV (Research Association for Combustion Engines), with partners the LAV and the Institute for Internal Combustion Engines and Automotive Engineering (Institut für Verbrennungsmotoren und Kraftfahrwesen, IVK)<sup>1</sup>. This project aimed on clarifying the influences of chemical and physical properties of synthetic fuels on combustion and emission behaviour at conventional diesel engine operation in order to define the basis for premium synthetic fuels. Therefore seven synthetic blends of components with different chemical structures and with a common matrix obtained by the Fischer-Tropsch (FT) process, were defined and investigated. Results were then compared to a reference diesel fuel following the requirements of EN 590. In last chapter of this dissertation an overview of the entire project is given. The main topic is, however, the investigation of these fuels’ behaviour with regard to injection through a commercial diesel injector. A study to identify dependencies of the injection rate profile on the fuel’s physical properties was conducted comparing the injection rate profiles obtained with the different fuels. This research was conducted using an injection test bench featuring a commercially available injection analyzer. Therefore a detailed description of this test rig, the experimental approach and the results obtained with this investigation are presented in chapter four.

---

<sup>1</sup> The IVK is part of the University of Stuttgart in Germany.

## Table of Contents

<b>Acknowledgment</b> .....	<b>i</b>
<b>Abstract</b> .....	<b>ii</b>
<b>1 Introduction</b> .....	<b>1</b>
1.1 The Spread of Diesel Engine .....	1
1.2 The Diesel Engine Issues.....	3
1.2.1 Emissions .....	3
<i>Unburned Hydrocarbons</i> .....	4
<i>Carbon Monoxide</i> .....	4
<i>Aldehydes</i> .....	5
<i>Particulate Matter (PM)</i> .....	5
<i>Nitrogen Oxides (NO<sub>x</sub>)</i> .....	6
1.2.2 Petroleum Scenario .....	9
1.3 Structure and Objective of this Research.....	12
<b>2 Literature Review – State of the Art</b> .....	<b>14</b>
2.1 Exhaust Gas After-Treatment Systems.....	14
2.1.1 PM reduction Technology .....	15
<i>Diesel Oxidation Catalyst (DOC)</i> .....	15
<i>Diesel Particulate Filter (DPF)</i> .....	15
2.1.2 NO <sub>x</sub> Reduction Technology .....	16
<i>Active Lean NO<sub>x</sub> Catalyst</i> .....	16
<i>NO<sub>x</sub> Adsorption Catalyst (NAC)</i> .....	17
<i>Plasma Converters (PC)</i> .....	17
<i>Selective Catalytic Reduction (SCR)</i> .....	18
2.2 In-Cylinder Combustion Optimization.....	18
2.2.1 Injection System Parameters .....	19
<i>High Pressure</i> .....	19
<i>Multiple Injections Strategies</i> .....	20
<i>Injection Rate Shaping</i> .....	22
2.2.2 Alternative Fuels.....	23
<i>Synthetic Fuel</i> .....	24

	<i>Biodiesel</i> .....	26
<b>3</b>	<b>Injection Analyzer</b> .....	<b>28</b>
3.1	Introduction and Objective .....	28
3.2	Injection System Technology.....	31
3.3	Injection Analyzer Measurement Principle .....	32
3.4	Design .....	35
3.4.1	Hydraulic Circuit .....	35
3.4.2	Measuring Tube.....	39
	<i>Length of the Measuring Tube</i> .....	39
	<i>Bore of the Measuring Tube</i> .....	40
3.4.3	Sensors Support and Injector Adaptors .....	41
3.4.4	Bleeding Valve .....	47
3.5	Setup.....	48
3.6	Signal Processing .....	51
3.6.1	Obtaining the Hydraulic Start and End of the Injection .....	52
3.6.2	Obtaining the Injection Rate and the Injected Fuel Mass from the Pressure Trace .....	55
3.6.3	Obtaining the Injected Fuel Mass from the Back Flow of the System .....	55
3.6.4	Obtaining the Data Processed.....	56
3.7	Measurement Results .....	57
3.8	Outlook.....	61
<b>4</b>	<b>Future Fuels for Diesel Engines</b> .....	<b>63</b>
4.1	Introduction and Objectives.....	63
4.1.1	Fuels .....	64
4.2	Project Framework Overview.....	65
4.2.1	IVK Experimental Approach.....	65
4.2.2	LAV Experimental Approach.....	67
4.3	Injection Analysis Approach .....	69
4.3.1	Test Bench .....	69
	<i>The IAV Injector Analyzer</i> .....	70
	<i>The injector Control System</i> .....	71

<i>Fuel Feeding System</i> .....	73
4.3.2 Working Points .....	74
4.3.3 Speed of Sound Determination .....	77
4.3.4 Investigational Procedure .....	80
4.4 Injection Analysis Results .....	80
<b>Indexes</b> .....	<b>90</b>
<b>Bibliography</b> .....	Error! Bookmark not defined.
Index of Symbols .....	94
Index of Abbreviations and Definitions .....	94
<b>Appendix</b> .....	<b>96</b>
(A) Some Details of the IVK's Motor Test Bench .....	96
(B) Some Details of the HTDZ Test Bench.....	96

# 1 Introduction

## 1.1 The Spread of Diesel Engine

Because of its unique combination of energy efficiency, power, reliability and durability, diesel technology plays a vital role in important sectors of the world economy. Due to these key factors diesel engine is and will be dominant for several decades to come.

There is a great variety of compression ignition engine designs in use in a wide range of applications: automobiles, buses, commercial vehicles, locomotive, marine transport, power generation. More than 90 % of commercial trucks are powered by diesel engines, as are two-thirds of all farm and construction equipment, and 100 % of all freight locomotives, river barges and other marine work vessels [2].

A great advantage of diesel-powered cars is the better fuel economy than equivalent gasoline engines and the lower production of greenhouse gases. Their greater economy is due to the higher energy per litre content of diesel fuel and the intrinsic efficiency of the diesel engine. While the higher density of petrodiesel results in higher levels of greenhouse gas emissions per litre compared to gasoline [EPA], the 20–40 % better fuel economy achieved by modern diesel-engined automobiles offsets the higher per litre emissions of greenhouse gases, and, moreover, a diesel-powered vehicle emits 10 % to 20 % less greenhouse gas than comparable gasoline vehicles [2].

In the context of global warming due to greenhouse gases like CO<sub>2</sub> (which contributes to the greenhouse effect in a percentage of 9-26 %), the emissions caused by private transport has attracted much media attention, and consequently, reducing those emissions has become a crucial issue.

As mentioned above, while diesel engines have been widely used in applications that require reliability and high torque output for a long time (such as trucks, heavy equipment and busses) their use in passenger cars in Europe has experienced a boom in the last decade, and the market share is still growing (figure 1.1) [3].

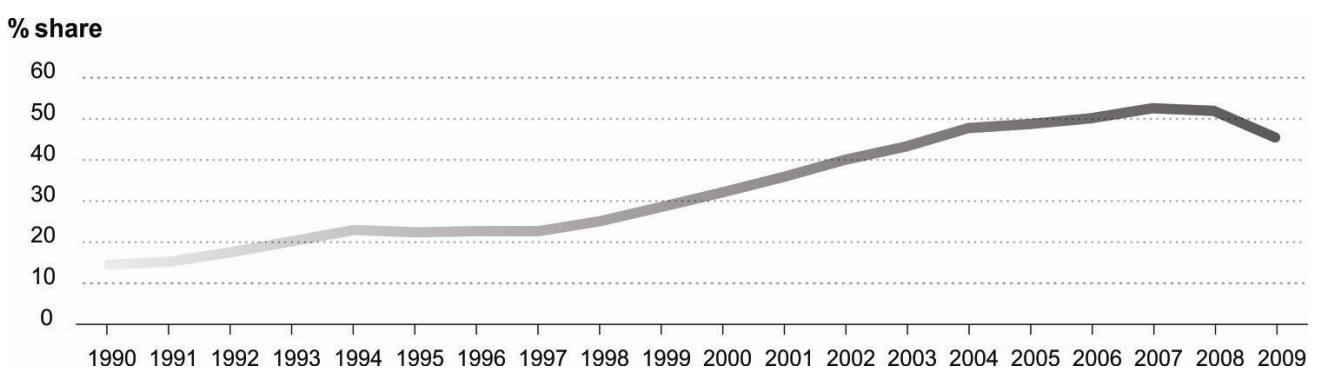


**Figure 1.1:** Share of diesel in new car registrations in the EU15+EFTA (% of new cars registered) [4].

The car is the preferred means of transport for Europeans and the average annual distance travelled by a car in Europe is about 22,000 km. There are more than 234 million vehicles on the European roads, or about 1 per 2 inhabitants (figure 1.2). Nearly 6 % of them are new vehicles (up to 1 year) and about 34 % are at least 10 years old (figure 1.3) [4]. In the last 10 years, Europe has represented a market of around 15 million new vehicles per year.

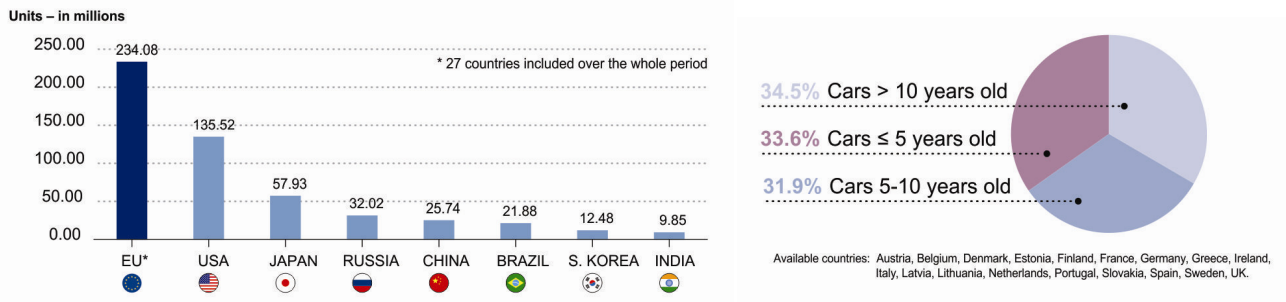


Figure 1.2 – Figure 1.3: Car fleet in millions, 2008; Car fleet composition, 2008 [4].

In 2008, diesel-powered cars account for 33.7 % of the total car fleet (figure 1.4) but due to the steep increase of the market share of diesel engines, the tax incentives offered by European Union for the purchase and operation of diesel cars and trucks, and to the greater public awareness of environmental problems (figure 1.5), the situation is rapidly turning around.

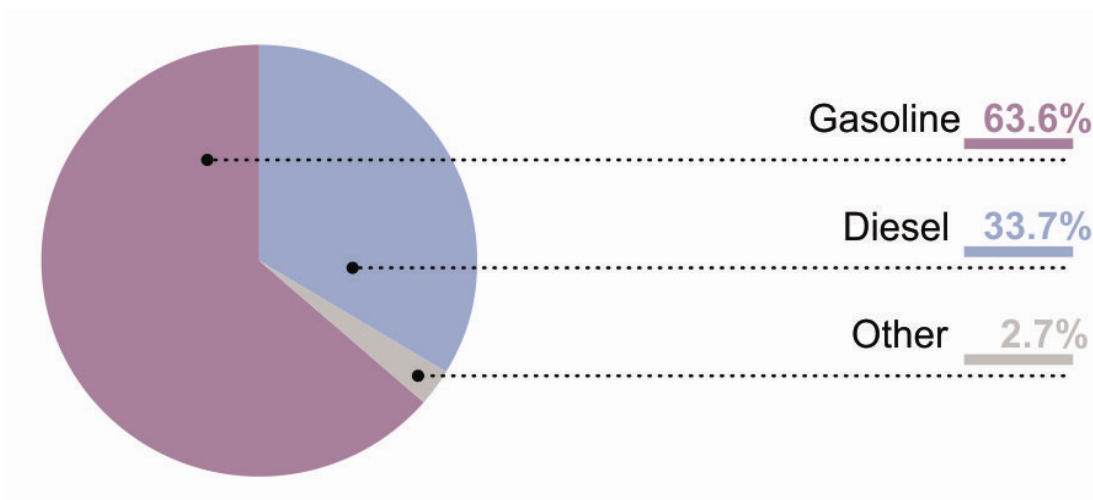


Figure 1.4: EU passenger car fleet according to fuel type (2008) [4].

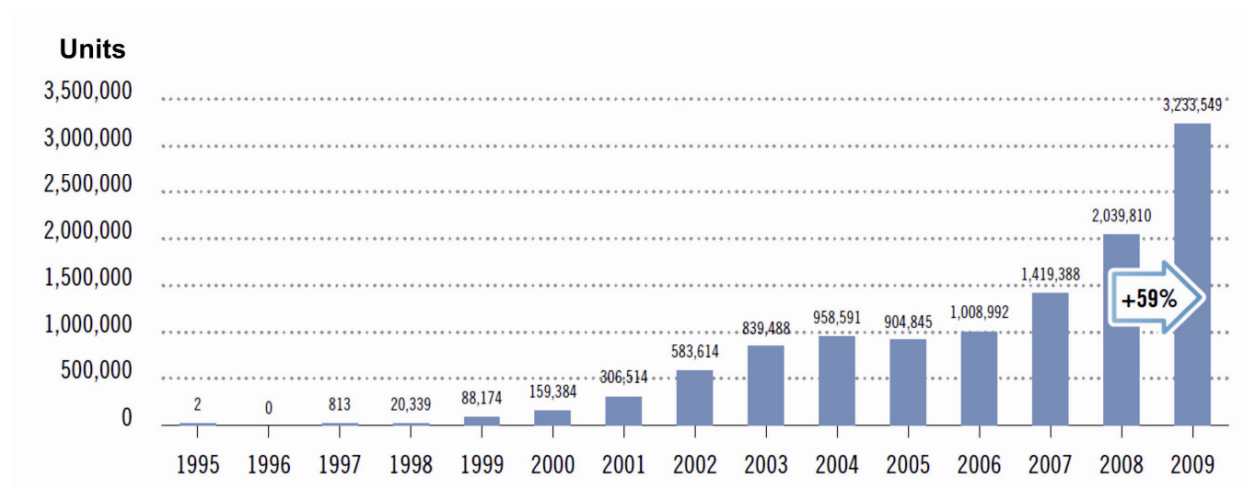


Figure 1.5: Demand for cars ≤ 120 gCO<sub>2</sub>/km [4].

In order to give an overview of the context in which this study brings its main contribute, the first part of this chapter focuses on the main limits of diesel, or at least, on the issues related to an increase of diesel engines in the market. The framework of this research project and its aims are detailed in the last part of this introductory chapter.

## 1.2 The Diesel Engine Issues

### 1.2.1 Emissions

Internal combustion engines contribute significantly to air pollution, which has a damaging impact on our health and on the environment, and has been implicated in global climate changes. The environmental benefits of diesels, such as the reduction of low greenhouse gas emissions indicated above, are balanced by growing concerns about the emission of nitrogen oxides and especially diesel particulates. This is reflected in the worldwide call for increasingly stricter environmental regulations for advanced emission controls and near-zero diesel emission levels [5]. Table 1.1 summarizes the European Union emission standards for light duty vehicles (passenger cars and light commercial vehicles).

This section contains an overview of the main constituents of DI-diesel engine pollutants and of the factors that most affect their production.

Tier	Date	CO	HC + NO <sub>x</sub>	NO <sub>x</sub>	PM
Euro 1†	1992.07	2.72 (3.16)	0.97 (1.13)	-	0.14 (0.18)
Euro 2, IDI	1996.01	1.0	0.7	-	0.08
Euro 2, DI	1996.01 <sup>a</sup>	1.0	0.9	-	0.10
Euro 3	2000.01	0.64	0.56	0.50	0.05
Euro 4	2005.01	0.50	0.30	0.25	0.025
Euro 5	2009.09 <sup>b</sup>	0.50	0.23	0.18	0.005 <sup>c</sup>
Euro 6	2014.09	0.50	0.17	0.08	0.005 <sup>c</sup>

\* At the Euro 1..4 stages, passenger vehicles > 2,500 kg were type approved as Category N1 vehicles  
† Values in brackets are conformity of production (COP) limits  
a - until 1999.09.30 (after that date DI engines must meet the IDI limits)  
b - 2011.01 for all models  
c - 0.0045 g/km using the PMP measurement procedure

**Table 1.1:** EU emission standards for passenger cars (category M1\*), g/km [5].

The combustion products of diesel fuels under ideal conditions (complete combustion) are carbon dioxide (CO<sub>2</sub>), water (H<sub>2</sub>O) and sulphur dioxide (SO<sub>2</sub>). However diesel engine exhaust gases contain carbon monoxide (CO), unburned or only partially oxidized hydrocarbons (HC), aldehydes, oxides of nitrogen (nitric oxide, NO,

and small amounts of nitrogen dioxide,  $\text{NO}_2$  - collectively known as  $\text{NO}_x$ ), diesel particulate matter (PM) and other organic compounds. The above-indicated partially burned or unburned components present in the exhaust of diesel engines are due to several factors that affect combustion, namely, the short time available for the mixture formation, the variable air/fuel ratio in the different regions of the fuel spray, the vicinity of the combustion chamber walls and intermittent combustion.

### Unburned Hydrocarbons

The unburned hydrocarbons in the diesel exhaust consist of either original or decomposed fuel molecules, or recombined intermediate compounds. Hydrocarbons originate in regions where the flame quenches on the walls and where excessive dilution with air prevents the combustion process from either starting or going to completion. Fuel that vaporizes from the nozzle sac volume during the later stages of combustion is also a source of HC

A small portion of these hydrocarbons originate from the lubricating oil left in a thin film on the cylinder wall, piston and perhaps on the cylinder head. These oil layers can absorb and desorb fuel hydrocarbon components, before and after combustion, respectively, thus permitting a fraction of the fuel to escape the primary combustion process unburned.

The mechanisms of formation and oxidation of the hydrocarbon molecules depend upon most of the engine operating variables, i.e., fuel-air ratio, injection time, swirl and of course injection system design, time and rate of injection.

### Carbon Monoxide

Carbon monoxide is one of the compounds formed during the intermediate combustion stages of hydrocarbon fuels. As combustion proceeds to completion, oxidation of CO to  $\text{CO}_2$  occurs through a recombination reaction between CO and the different oxidants. If these recombination reactions are incomplete because of lack of oxidants, low gas temperatures, or short residence time, CO will not be fully oxidized to  $\text{CO}_2$ . The CO formed during the combustion process as a ratio of the injected quantity, depends upon the fuel-air ratio. At low loads, this ratio is high because the gas temperature is low and very little oxidation takes place. An increase in load or fuel-air ratio results in lower CO emissions because of the increase in gas temperatures and elimination reactions. The increase in the fuel-air ratio beyond a certain limit may reduce the elimination reactions, despite the increase in temperature, because of the low oxidant concentration and the short reaction time. This results in high CO emissions with an increase in load, as shown in figure 1.6 [6].

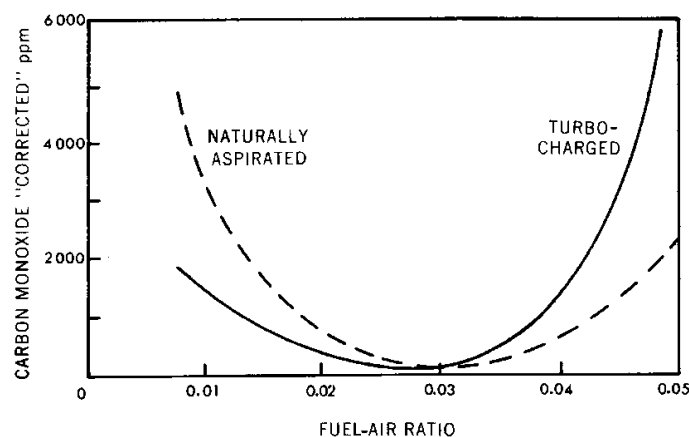


Figure 1.6: Effect of the fuel-air ratio on carbon monoxide emission in a DI-diesel engine [6].

Diesel engines are not a significant source of carbon monoxide because the load is controlled by the amount of fuel and these engines always operate lean.

### *Aldehydes*

Aldehydes are the product of partial oxidation of hydrocarbons. They consist mainly of formaldehyde and acrolein. Formaldehyde, at certain concentrations, is considered to be the cause of the odour and irritant property of diesel exhaust.

Aldehydes are highly oxygen concentration-dependent. As occurs for hydrocarbon formation, aldehydes originate in a region where the flame extinguishes: Wall quenching or quenching by excessive exhaust dilution are possible ways that can arise these oxygenated hydrocarbon molecules [6]. The use of alcohol fuels in diesel engines substantially increases aldehyde emissions. While these are not subject to regulation, aldehydes would be a significant pollutant if these fuels were to be used in quantities comparable to gasoline and diesel.

### *Particulate Matter (PM)*

Diesel particulate emissions are of increasing concern. They are small solid or liquid particles, mostly less than 2.5 microns in size, and consist of a complex mix of engine oils, sulphates and inorganic materials. Health experts have demonstrated that these particles contribute to a variety of lung-related illnesses including asthma, emphysema and bronchitis. The International Agency for Research on Cancer (IARC) considers particulate matter (PM) a probable human carcinogen. Based on the best available scientific evidence, the Mine Safety Health and Administration (MSHA) has determined that PM puts miners at an excess risk for diseases of the heart and lung, including lung cancer [7]. Consequently, the generation of PM is under intense study by researchers from various disciplines.

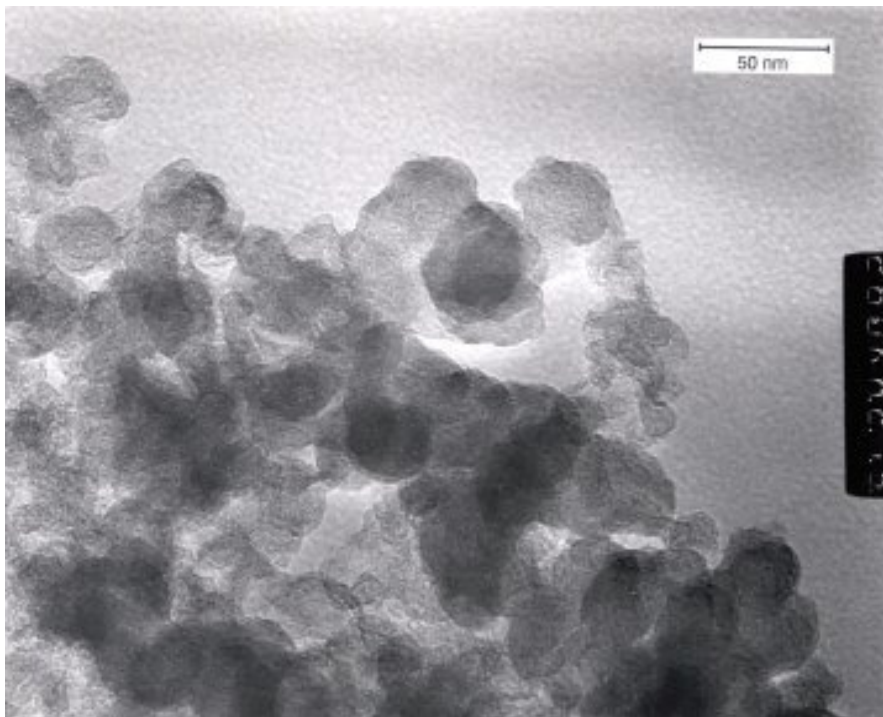


**Figure 1.7:** High-resolution transmission electron microscopy images of diesel soot particles obtained by the Argonne National Laboratory [8].

Different types of particulates are emitted from diesel engines under different modes and operating conditions. Particulate is often separated into a soluble and an insoluble or dry fraction called respectively *soluble or volatile organic fraction* (SOF or VOF)<sup>2</sup> and *soot* [9].

The soluble organic fraction of diesel particulates includes heavy hydrocarbons derived from the decomposition of a tiny fraction of the fuel and from the atomized and evaporated engine lubricating oil [10]; it may be accompanied by partially oxidized products. The term “soluble” originates from the analytical method used to measure SOF, which is based on the extraction of particulate matter using organic solvents.

Diesel particulate matter consists mainly of soot or black smoke (the fraction of soot in particulate from diesel exhaust varies, but is typically above 50%) and it is a product of the incomplete combustion of fuel hydrocarbons in locally fuel-rich regions. The chemical composition of soot particles depends on the temperature in the engine exhaust and on the particulate sampling system. At high temperatures (>500 °C), its composition is mainly elementary carbon (EC) and organic carbon (OC). Below 500 °C, the particles become coated with adsorbed and condensed high molecular weight organic compounds, among which, unburned hydrocarbons, aromatic and oxygenated hydrocarbons and inorganic species such as sulphur dioxide and sulphuric acid (sulphates). The structure of diesel soot samples seems to consist of collections of primary particles (spherules) agglomerated into aggregates forming spatial ramified chains as shown in figure 1.7. Clusters may contain as many as 4000 spherules with a diameter varying between 10 and 80 nm, although most are in the 15 to 30 nm range [11].

Soot production process consists of two principal events, namely soot formation and oxidation. These processes run in parallel in the cylinder. A more detailed description of soot is beyond the aim of this dissertation but can be found, for instance, in [9].

Like all the other pollutants, PM production is affected by the engine’s physical parameters. Considering the high complexity of combustion in compression ignition engines, the dependence between PM emission and the engine’s physical parameters is perhaps one of the most complex studies due to the difficulty of isolating the effects of individual parameters. To give an idea of the physical parameters that most affect soot production in a direct injection diesel engine, is possible to summarize them as the combustion chamber geometry, the intake temperature and pressure, the injection system (capability of the system to perform multiple injections, injection rate shaping, etc.), injection timing, cylinder temperature, air injection, engine transient and water emulsified fuels. Given the increasing legislation restricting soot production, the aim of many ongoing research projects is to discover the effects of engine parameters on soot emission.

### *Nitrogen Oxides (NO<sub>x</sub>)*

Nitrogen oxide can refer to a binary compound of oxygen and nitrogen, or to a mixture of such compounds. In the field of engines, the term “nitrogen oxide” (NO<sub>x</sub>) refers to nitric oxide (NO) and nitrogen dioxide (NO<sub>2</sub>). NO<sub>x</sub>, together with non-methane hydrocarbons (NMHC), is the main precursor of the formation of ground-level ozone (troposphere ozone) through complex and non-linear photochemical reactions in sunlight. A major source of NO<sub>x</sub> released in the atmosphere is the burning of fossil fuels in automotive engines; consequently the reduction of highway emissions may considerably change ozone levels. The NO<sub>x</sub> species also exert a direct toxic effect on human health. NO and NO<sub>2</sub> exert different toxic effects on the human body.

---

<sup>2</sup> Some authors (Zinbo *et al* 1990, 1993) observed a strong correlation between the SOF (Soxhlet extraction method) and the volatile organic fraction VOF (TGA method), but they should not be expected to be the same, because of some volatile particulate components that can remain after the solvent extraction.

NO is thought to be carcinogenic (like soot), and responsible for acid rain and smog. NO<sub>2</sub> is an irritant gas causing pulmonary edema [12]. Moreover, being liposoluble, NO<sub>2</sub> can penetrate deep in the lung air sacs where it damages the capillaries and cause extensive inflammation.

Nitric oxide is the predominant oxide of nitrogen produced inside the engine cylinder. The principal source of NO is the oxidation of atmospheric (molecular) nitrogen. However, if the fuel contains significant levels of nitrogen, the oxidation of the fuel nitrogen-containing compounds is an additional source of NO. NO forms in both the flame-front and the post-flame gases. In engines, however, combustion occurs at high pressure so the flame reaction zone is extremely thin (~ 0.1 mm) and residence time within this zone is short. In addition, the cylinder pressure rises during most of the combustion process, so that burned gases produced early in the combustion process are compressed to a higher temperature than they reached immediately after combustion. Thus, NO formation in the post-flame gases almost always dominates any flame-front-produced NO.

NO<sub>x</sub> species can be formed either during homogeneous reactions in the gas phase or during heterogeneous reactions in combustion systems containing solid fuel such as coal. According to literature, three primary sources of NO<sub>x</sub> have been identified in the homogeneous combustion processes: *thermal NO<sub>x</sub>*, *fuel NO<sub>x</sub>* and *prompt NO<sub>x</sub>* [12].

- *Thermal NO<sub>x</sub>*

Thermal NO<sub>x</sub> forms in the post-flame zone and is produced by the oxidation of atmospheric nitrogen at relatively high temperatures (T>1600 °C) in fuel-lean environments in a strongly temperature-dependent process. Thermal NO<sub>x</sub> reactions take place in a few tens of microseconds, and are highly dependent on temperature, residence time and atomic oxygen concentration [12]. It is generally agreed that the principal reactions governing the formation of thermal NO<sub>x</sub> from molecular nitrogen (and its destruction) are:



Yakov Borisovich Zel'dovich suggested the importance of the two first reactions whereas the third reaction has been shown to contribute to NO formation particularly in fuel-rich mixtures<sup>3</sup>. The forward and reverse rate constants for these reactions have been measured in numerous experimental studies; recommended values for the forward rate constants are given in table 2.2 [11].

Reaction (1.1) is the rate-determining step due to its high activation energy of breaking the triple bond of molecular nitrogen, and is temperature-sensitive. The temperature-dependence also results from the temperature sensitivity of the O atom equilibrium concentration [12].

A simplified formula for the initial NO formation rate may be written, as proposed by Heywood [11], as:

<sup>3</sup> There are new reaction schemes for NO<sub>x</sub> production attempting to better predict NO<sub>x</sub> formation level [7].

$$\frac{d[NO]}{dt} = \frac{c_1}{T^{1/2}} \cdot e^{\left(\frac{-c_2}{T}\right)} \cdot [O_2]^{1/2} \cdot [N_2] \quad [mol/cm^3 \cdot s]$$

where  $[ ]$  denote species concentrations in moles per cubic centimetre and  $c_1$  and  $c_2$  are two positive constants.

The strong dependence of NO formation rate on temperature in the exponential term is evident. High temperatures and high oxygen concentrations result in high NO formation rates.

Reaction	Rate constant [ $cm^3/(mol s)$ ]	Activation temperature [K]	Temperature range [K]
(1.1)	$7.6 \times 10^{13} \exp(-38000/T)$	38'000	2000 - 5000
(1.2)	$6.4 \times 10^9 \exp(-3150/T)$	3'150	300 - 3000
(1.3)	$4.1 \times 10^{13}$		300 - 2500

**Table 1.2:** Forward rate constants for NO formation mechanism

- *Fuel NO<sub>x</sub>*

Fuel NO<sub>x</sub> refers to NO<sub>x</sub> formed from the conversion of fuel-bound nitrogen to NO<sub>x</sub> during combustion of certain coals and oils. Although the formation kinetics is nowadays limited, it is usually assumed that fuel NO<sub>x</sub> is a source of nitrogen oxides via formation of precursors like ammonia (NH<sub>3</sub>), hydrocyanic acid (HCN) and cyanide radicals (CN). In fuel-rich regions, these nitrogen-containing species will typically be reduced to N<sub>2</sub>, and in fuel-lean regions they are generally oxidized to form NO. The amount of fuel nitrogen converted to NO is sensitive to the air/fuel ratio but only weakly dependent on temperature, in contrast to the strong temperature-dependence of NO formed from atmospheric nitrogen [11]. At a sufficient residence time in a very fuel-rich gas, the fuel-nitrogen converts to relatively small amounts of NO and large amounts of N<sub>2</sub>. The yield of NO from the coal nitrogen will increase for higher air/fuel ratios [12]. Fuel NO is formed more readily (occurring on a time scale comparable to that of combustion reactions) than thermal NO because the N-H and N-C bonds, which are very common in fuel-bound nitrogen, are much weaker than the triple bond in molecular nitrogen which must be broken for thermal NO formation. Controlling the local environment in which nitrogen is released from the fuel is a primary means of controlling NO emissions and although the amount of fuel NO in the diesel exhaust is negligible with the diesel fuel used today, its contribution to the total amount of NO<sub>x</sub> produced from the engine must be considered.

- *Prompt NO<sub>x</sub>*

The presence of a third mechanism leading to NO<sub>x</sub> formation was first identified by Fenimore and was termed "prompt NO<sub>x</sub>" or "Fenimore-NO<sub>x</sub>". Prompt NO<sub>x</sub> forms in the flame-reaction zone and is produced by the reaction of atmospheric nitrogen with hydrocarbon radicals (such as C, CH, and CH<sub>2</sub>) in fuel-rich regions of flames. This process results in the formation of fixed species of nitrogen such as NH (nitrogen monohydride), HCN (hydrogen cyanide), H<sub>2</sub>CN (dihydrogen cyanide) and CN- (cyano radical) which can then oxidized to form NO. Since the prompt NO<sub>x</sub> mechanism requires a

hydrocarbon to initiate the reaction with nitrogen, this mechanism is much more prevalent in fuel-rich than in fuel-lean hydrocarbon flames [12]. The contribution of prompt  $\text{NO}_x$  is normally considered negligible.

In general terms, the critical equivalence ratio for  $\text{NO}_x$  formation in high-temperature high-pressure burned gases, typical of DI-diesel engines, is close to stoichiometric. The critical period is when burned gas temperatures are at a maximum, i.e., between the start of combustion and shortly after the occurrence of peak cylinder pressure. Mixture which burns early in the combustion process is especially important since it is compressed to a higher temperature, thereby increasing the  $\text{NO}$  formation rate, as combustion proceeds and cylinder pressure increases. After the time of peak pressure, burned gas temperatures decrease as the cylinder gases expand. The decreasing temperature due to expansion and due to mixing of high-temperature gas with air or cooler burned gas freezes the  $\text{NO}$  chemistry. This second effect means that freezing occurs more rapidly in the diesel than in the spark-ignition engine, and there is much less decomposition of the  $\text{NO}$ . This mechanism is supported by different experiments, i.e., gas sampling from within the cylinder of normally operating diesel engines with special gas-sampling rapid-acting valves [11] or by applying the laser-induced fluorescence (LIF) technique (fig 2.3) [13].

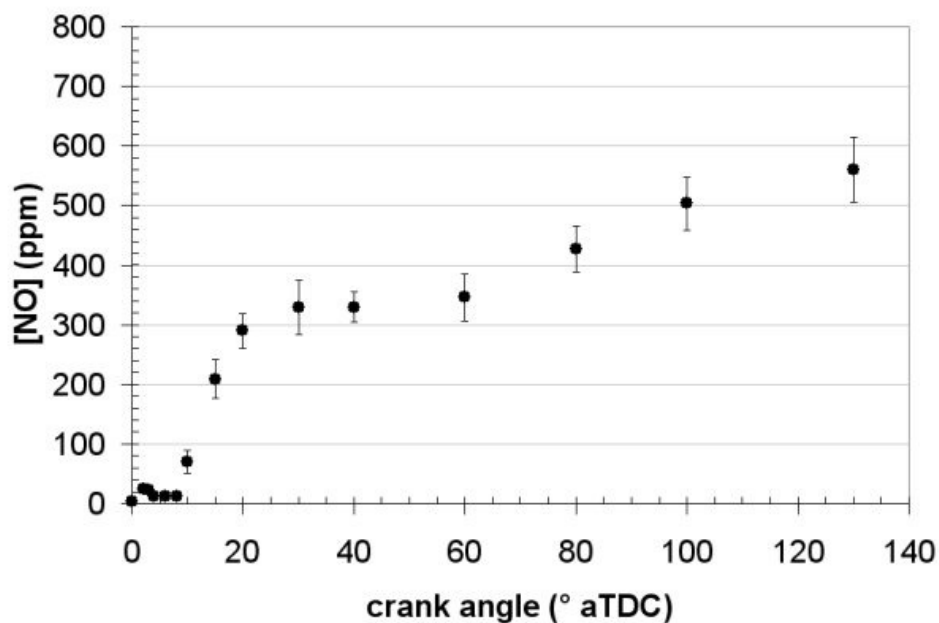


*Figure 1.8: In-cylinder  $\text{NO}$  measurements by means of the laser-induced fluorescence (LIF) technique [18].*

The parameters that most significantly affect the formation of  $\text{NO}_x$  in diesel engines are the in-cylinder gas temperature, the availability of oxygen, the cylinder pressure, as well as the residence time of the fuel/gas mixture in locations with favorable temperatures and oxygen concentration for the formation of nitric oxides [11]. All these parameters, in turn, depend on inlet air pressure, exhaust gas recirculation (EGR) rate, and on the earlier or later start of injection.

### 1.2.2 Petroleum Scenario

Given present demand, petroleum is one of the most important raw materials in the world. It is an easily transportable and usable energy source for most vehicles (cars, trucks, trains, ships, airplanes) and is a base

element for many chemical products. Consequently, access to petroleum has been and continues to be the principal cause of military conflict and political instability among nations.

The petrochemical industry was born in the USA on the initiative of Edwin Drake in 1850. It spread slowly until the beginning of the 20<sup>th</sup> century, after which the demand for petroleum increased exponentially with the advent of the internal combustion engine. Although coal was the most widely used combustible in the 1950s, petroleum met all the increasing energy demand of the following years to such an extent that it now satisfies 90% of the entire world fuel requirements [14]. The two petroleum crises of 1973 and 1979 (the second caused the price of a barrel to increase from 11 to 40 dollars) showed that this energy resource is not endless, and gave renewed impetus to research on new energy sources. The reaction of developed countries was to focus on alternative sources of energy and to reduce petroleum consumption by limiting importation from the OPEC countries. Despite the increase in the price of crude oil and the political instability in some of the major crude producer countries, petroleum remains the world's most widely used energy source (figure 1.9 – 1.10), and its extraction and purchase are still convenient given the limited availability of alternative energy resources.

According to the International Energy Agency (IEA), in 2009 more than 8 thousand million tons of oil equivalent<sup>4</sup> (Mtoe), namely fossil fuels, nuclear energy, hydroelectric energy and other sources, were consumed, and more than 40 % of the entire amount is real petroleum.

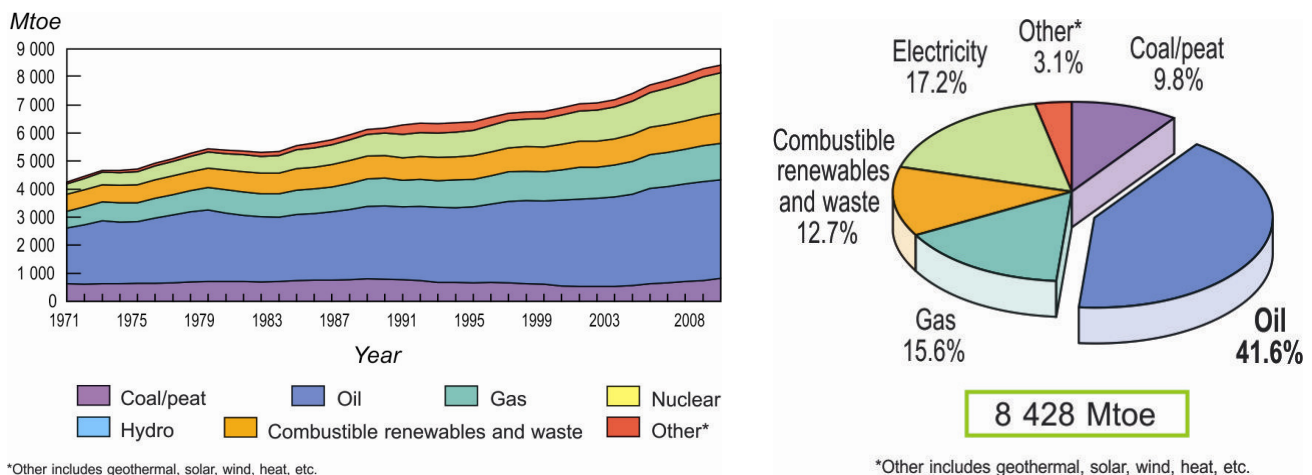


**Figure 1.9 – 1.10:** Evolution from 1971 to 2008 of world Total Primary Energy Consumption by fuel; Fuel share of Total Primary Energy Consumption in 2008 [15].

In the first decade of the second millennium the world consumption of oil has grown by an annual mean rate of almost 2 % per year (figure 1.11). IEA foresees an annual energy consumption increase of around 25 % (only in the transport sector) in the next 25 years, accompanied by a possible increase of more than 100 % in the price of crude oil<sup>5</sup> [16].

<sup>4</sup> The ton of oil equivalent (toe) is a unit of energy based on the approximate energy released by burning one ton of crude oil, approximately 42 GJ.

<sup>5</sup> Many factors influence this projection, and it has also been suggested [16] that the price of oil could remain low during the next 25 years even if the growth rate of fuel usage follows the previous trend.

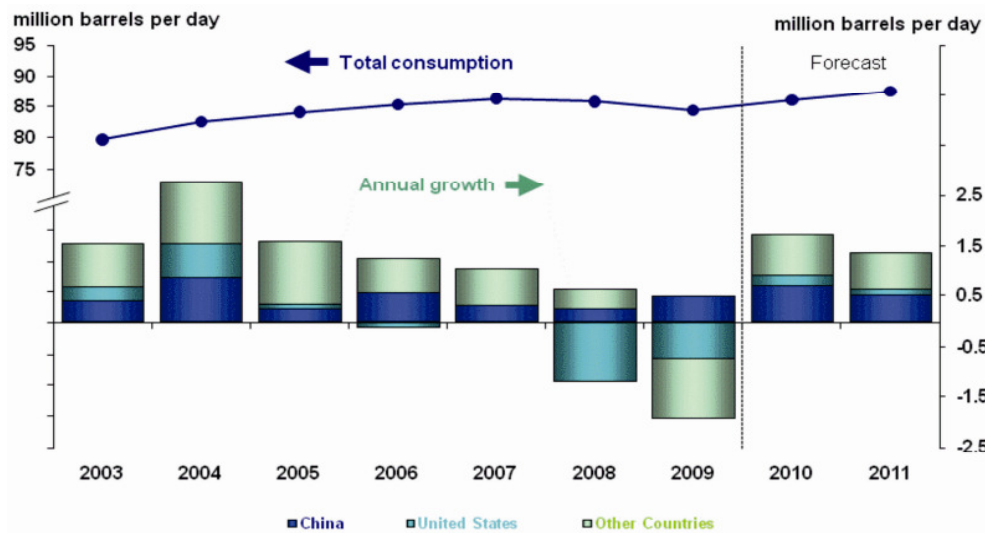


Figure 1.11: World liquid fuel consumption [16].

According to recent assessments, the world petroleum reserve is within the range of 1237 thousand million barrels (Association for the Study of Peak Oil & Gas: ASPO) and 1354 billion barrels (EIA).

Figure 1.12 shows the world's proven oil reserves according to geographic region, and, as over 50 % of the world's oil is concentrated in the Middle East, is clear that an unstable situation in that region can result in volatile prices.

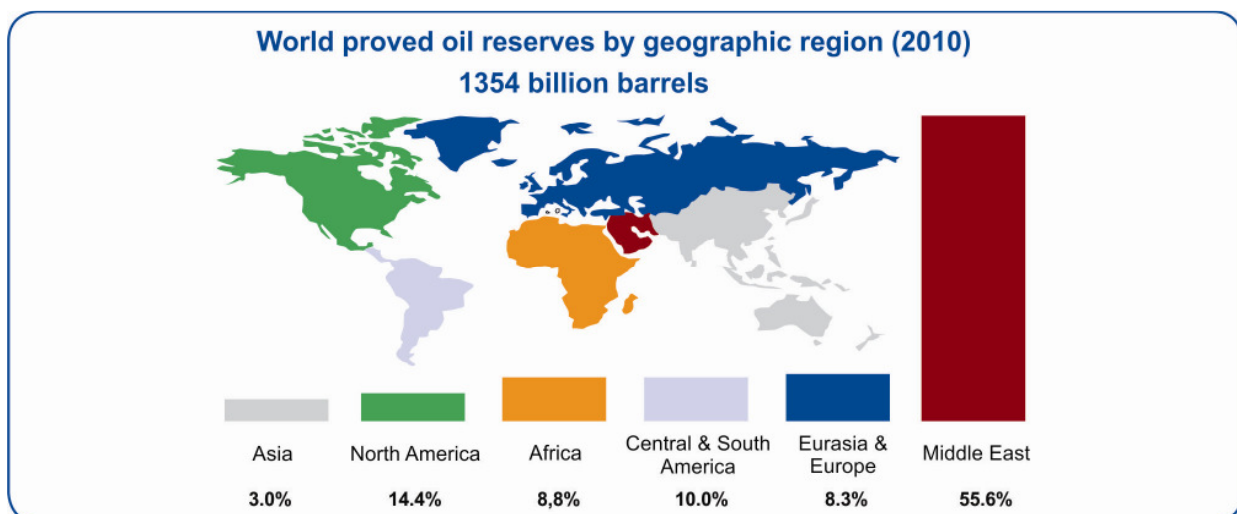


Figure 1.12: World proved oil reserves by geographic region (2010) [16].

The future availability of petroleum can be calculated with the reserve/production ratio: using the positive forecast of a reserve of 1,354 billion barrels and a constant production of 80 million barrels per day (~30 billion barrels per year), it will be possible to count on petroleum for 45 years.

Obviously, calculations of the future availability of petroleum based on a constant supply of crude oil may not be reliable. Furthermore, the data about reserves may be misleading because of the objective difficulty in estimating the real amount of crude in the oilfields, which the oil companies estimate as a likelihood ratio, and because of many strategical, political and economic factors regarding the elaboration and diffusion of

these assessments by the various oil companies and by producer countries [14]. However, there is clearly a physical limit to the amount of oil that is in the ground and, as existing reserves become depleted and new finds become less frequent and more difficult to extract, prices must increase thus creating immeasurable economical problems.

From this scenario, it is clear that the very nature of oil as a non-renewable resource implies future depletion. Therefore, advancements in the field of fuel technologies are likely to be not only beneficial but also necessary. Apart from relieving fossil fuel dependence, the development of alternative fuels also has several secondary benefits. Alternative fuel usage could have a tremendous impact on reducing pollution since many types of alternatives have significantly lower emissions. Equally important, the decreased need for oil could have a positive impact on the foreign policies of governments.

### 1.3 Structure and Objective of this Research

The objective of this study is to bring a scientific contribute by a twofold ways: (i) reducing diesel in-cylinder emissions, and (ii) releasing the diesel engine from its dependence on petroleum. The approach of this research was essentially experimental, but few mathematical algorithms were also implemented to process and analyze the measurement results.

The first part of this work is dedicated to the design, at LAV (Laboratorium für Aerothermochemie und Verbrennungssysteme, Department of Mechanical and Process Engineering at ETH Zurich), of a Bosch tube-type injection rate measuring system ordered to make an in-depth study of the hydraulic injection behaviour (injected mass, injection rate shape, injection timing and injection delays) of the common-rail (CR) injection system of a single cylinder, 4-liter diesel engine. This engine represented the starting point of a test bench set up at LAV in order to yield reproducible and reliable measurement data for the development and validation of new or improved numerical models. This part of the work focuses on the design of the hardware and of the software of this instrument. Some measurements and first results are also presented.

In the second part of this work, according to the acquired knowledge, another test bench equipped with a commercial injection analyzer was set up at LAV to contribute in a two-partners research project named "Future Fuels for Diesel Engines".

This project aims on clarifying the influences of chemical and physical properties of synthetic fuels on combustion and emission behaviour during conventional diesel engine operation in order to define the basis for premium synthetic fuels. A reference diesel fuel, following the requirements of EN 590 and seven synthetic blends of components with different chemical structures and with a common matrix obtained by the Fischer-Tropsch (FT) process were defined and investigated. This study was jointly conducted by the IVK (Institut für Verbrennungsmotoren und Kraftfahrwesen, University of Stuttgart) and the LAV, resulting in a multiple-sided research approach. To enable an in-depth interpretation of the experiments conducted at the IVK on a single cylinder engine, fundamental investigations were performed at the LAV. Here, besides the above mentioned injection analyzer test bench, a high temperature / high pressure constant volume combustion chamber (HTDZ) was used to define spray penetration depth, spray propagation, evaporation, points of ignition and soot formation.

The focal interest of the second part of this dissertation is the study conducted by means of the injection analyzer test bench. At the moment of this writing the HTDZ measurements were still in course,

consequently an in-depth analysis to correlate the data resulted from the three experimental approaches was not done yet. Nevertheless, a study to identify dependencies of the injection rate profile on the fuel's physical properties was conducted by comparing the injection rate profiles obtained with the different fuels. A detailed description of the injection analyzer test rig, the experimental approach and the results obtained with this study are presented in last part of this work.

## 2 Literature Review – State of the Art

As mentioned in the introduction of this manuscript, internal combustion engines contribute significantly to air pollution and in order to regulate engine's emission, the tailpipe emission standard<sup>6</sup> was initiated in California in 1959 specifically to control CO and HC emission from gasoline engines. Nowadays the main limitation of compression ignition engines is the emission of PM and NO<sub>x</sub>. With the aim of reducing these two pollutants and to fulfil future more stringent exhaust gas regulations, two different approaches can be followed:

- Exhaust gas after-treatment systems
- In-cylinder combustion optimization

The main diesel engine issue is not only the degradation of the environment; the present petroleum scenario will not improve in the near future and therefore the fuel used to power IC engines is highly limited to feedstock availability. To counter the issue of diesel fuel availability, as in the early 1980s, research with alternative fuels is again on the increase. Even though earlier work on alternative fuels centred on their suitability to power diesel engines, most of the current work focuses on evaluating their potential to reduce engine emissions.

This chapter contains an overview of the diesel engine technology presently in practice to improve emission/air quality, fuel consumption, petroleum independence, and the balance of trade. In particular, it contains an overview of the diesel engine in-cylinder and after-treatment systems used to reduce NO<sub>x</sub> and PM emissions but, as mentioned previously, its main emphasis is given to the following promising in-cylinder measures:

- Injection system parameters
- Alternative fuels

### 2.1 Exhaust Gas After-Treatment Systems

The use of in-cylinder measures to reduce diesel engine emissions usually results in a trade-off between NO<sub>x</sub> improvements and PM improvements; to control NO<sub>x</sub> emissions, lower combustion temperatures are necessary, while PM emission reduction generally results from higher combustion temperatures [17]. Numerous research projects are currently addressing this topic but, since in-cylinder measures presently still do not satisfy the new European emission standards such as EURO V or lower, exhaust gas after-treatment technology has nevertheless progressed very rapidly in the last ten years. Diesel engine exhaust after-treatment devices are fitted to vehicles either during manufacture or retrofitted<sup>7</sup> as part of the exhaust system to reduce harmful emissions.

---

<sup>6</sup> Tailpipe emission standards specify the maximum amount of pollutants allowed in exhaust gases discharged from internal combustion engines.

<sup>7</sup> Retro-fitment programs have been implemented in many countries that are seeking a reduction in pollutants but which generally employ older vehicle technology. The London bus program, for example, has been very effective. Factors to be evaluated when considering DPF retrofit for a specific vehicle or piece of equipment include engine-out PM emission levels, the engine duty cycle and the resulting exhaust temperatures, available space and fuel sulphur levels.

### 2.1.1 PM reduction Technology

The most commonplace after-treatment systems used to reduce PM emission in diesel engines are the *diesel oxidation catalyst (DOC)* and the *diesel particulate filter (DPF)*.

#### *Diesel Oxidation Catalyst (DOC)*

The diesel oxidation catalyst has been used in some engines since the 1990s to reduce the amount of carbon monoxide (CO), particulate matter (PM) and hydrocarbon (HC) emissions released into the atmosphere. A diesel oxidation catalyst (DOC) is a flow through device that consists of a canister containing a honeycomb-like structure or substrate. The substrate has a large surface area that is coated with an active catalyst layer. This layer consists of a small, well dispersed amount of precious metals such as platinum or palladium. As the exhaust gases traverse the catalyst, carbon monoxide, gaseous hydrocarbons and liquid hydrocarbon particles (unburned fuel and oil) become oxidized, thereby reducing harmful emissions.

These devices have proven effective by reducing PM emissions by up to 25 % or more. Despite being robust and requiring little or no maintenance, they will not allow engine manufacturers to fulfil recent PM emission standards [17]. Oxidation catalysts have not been widely used in heavy duty vehicles with the exception of urban buses. Furthermore they are not necessary to meet HC and CO requirements of future European heavy duty emission regulations.

#### *Diesel Particulate Filter (DPF)*

One of the leading technologies for meeting future PM emission standards is the diesel particulate filter, or DPF. These devices generally consist of a wall-flow type filter positioned in the exhaust stream of a diesel vehicle. As the exhaust gases pass through the system, particulate emissions are collected and stored. Owing to the volume of diesel particulates collected by the system filling up and possibly blocking the filter, a method for controlling trapped particulate matter and regenerating the filter is needed. Even if DPF system has previously suffered from regeneration, reliability, and durability problems, this technology has demonstrated its effectiveness in reducing particulate emissions by more than 85%. Most of the particulate matter on the filter is carbon which can react with oxygen to form carbon dioxide. However, the reaction of carbon with exhaust gases in the particulate filter only occurs at around 600°C, and for many diesel engines, the exhaust gas temperature is insufficient to regenerate the filter. There are therefore two practical strategies for regenerating filters. These differ in their regenerating time, which can be “continuous” or “periodic”:

- The “continuous strategy” provides the lowering of the temperature at which the PM reacts. This is achieved either through the use of a catalyst (coated on the filter surface or added to the fuel) or by letting the carbon particles react with NO<sub>2</sub>. This latter patented continuously regenerating trap (CRT) technology uses a catalyst in front of the filter to generate NO<sub>2</sub>. The NO<sub>2</sub> then flows through the filter, reacting with the carbon particles at temperatures above 260°C producing both NO and CO<sub>2</sub> as well as cleaning the filter (figure 2.1). The oxidation catalyst also removes CO and HC and oxidizes some of the NO in the exhaust gasses to NO<sub>2</sub>. Particular requirements of this system are a significant proportion (~50%) of the operating time with an exhaust temperature higher than 250°C, the maximum sulphur content in the fuel (50 ppm) in order to minimize catalyst deactivation by sulphur poisoning and the NO<sub>x</sub>/PM engine out ratio which has to be greater than 25/1 [18], [19].

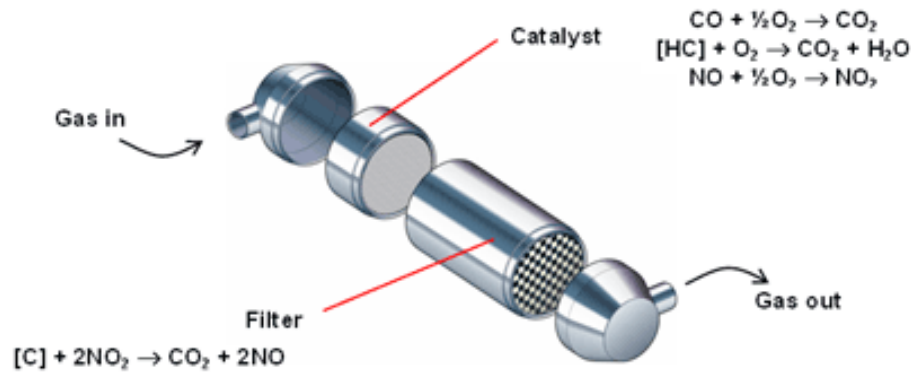


Figure 2.1: The CRT system [18].

- The “periodic strategy”, on the other hand, regenerates the trap by increasing the temperature of the gas passing through the filter. This is achieved by implementing post-injection combustion strategies through the use of electrical exhaust gas heating or by intake air throttling at low and medium engine load [20].

Depending on the application these two strategies can be implemented separately or combined.

Most of the systems that have been developed use filters based on ceramic monoliths (ceramic internals), but the key factor to achieve commercial practicality is the development of regeneration methods to “burn” off the trapped PM, either periodically or continuously, in order to avoid build up of excessive exhaust back pressure. This technology allows very high PM reduction and, for this reason is considered essential to satisfying future PM emissions standards. Typically, there is however a fuel consumption penalty with the application of these traps as the regeneration technique relies on the fuel energy to burn the PM off the catalyst, and sometimes require periodic operation of the engine in an inefficient manner during the regeneration cycle [21].

### 2.1.2 NO<sub>x</sub> Reduction Technology

The most well known diesel engine after-treatment systems used to reduce NO<sub>x</sub> are the *active lean NO<sub>x</sub> catalyst (ALNC or LNC)*, *NO<sub>x</sub> adsorption catalysts (NAC)*, *plasma converters (PC)* and *selective catalytic reduction (SCR)*.

#### *Active Lean NO<sub>x</sub> Catalyst*

The designation “lean NO<sub>x</sub>” refers to technologies that reduce nitrogen-oxides by using hydrocarbons under the excess of oxygen. This method requires reasonable amounts of hydrocarbons in the exhaust gas. DI-diesel engines are lean burning engines and the hydrocarbon concentration in the emissions is quite low, and not sufficient for NO<sub>x</sub> conversion, therefore hydrocarbons have to be added to the exhaust gas, i.e., post injection or secondary fuel injection<sup>8</sup>. It is crucial that the hydrocarbons are sufficiently atomized to provide adequate reactant surface and also prevent hydrocarbon slip to the tailpipe [22].

<sup>8</sup> The term “active” is used to differ this technology from the “passive lean NO<sub>x</sub> system” that uses only the hydrocarbons in the raw engine exhaust as a reductant. Unfortunately, the hydrocarbon concentration in Diesel exhaust is inherently low and, thus, maximum NO<sub>x</sub> conversion with passive systems is currently limited to approximately 15 % [56].

There are several types of lean NO<sub>x</sub> catalysts currently under development by many catalyst companies. The general trend is to use two types of catalysts so as to cover the temperature range between 200 °C to 500 °C, as shown in figure 2.2 [23].

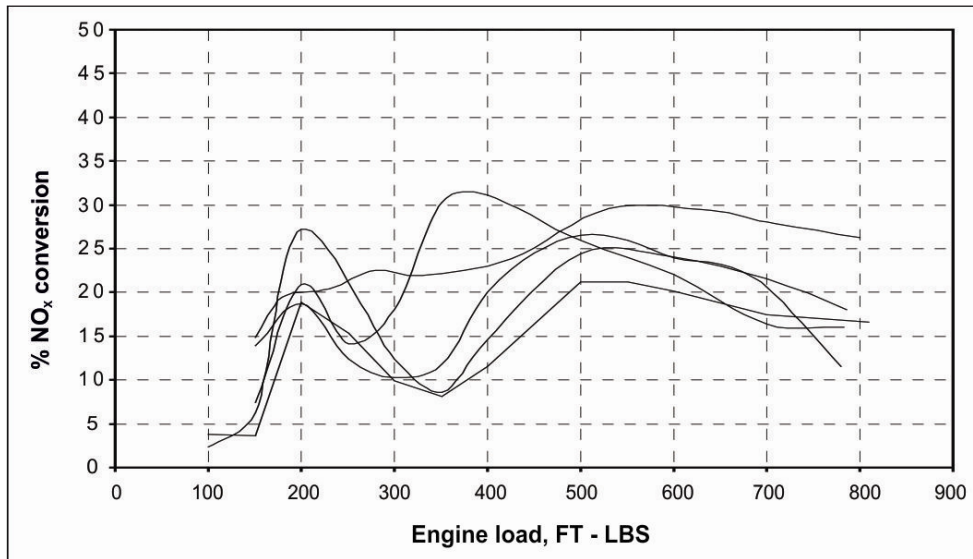


Figure 2.2: Combining precious metal and base metal catalysts to increase NO<sub>x</sub> reduction over a wide temperature range [23].

*NO<sub>x</sub> Adsorption Catalyst (NAC)*

The NO<sub>x</sub> adsorption catalyst method consists of capturing NO<sub>x</sub> in a trap during engine lean operation. When the trap is full, the exhaust is cycled to operate rich to release and reduce the trapped NO<sub>x</sub> [24]. The removal of the NO<sub>x</sub> from a lean gas stream is achieved by chemical adsorption onto a catalyst (hence the term NO<sub>x</sub> adsorber catalyst) with CO<sub>2</sub> release (figure 2.3). When the trap is regenerated by changing to a rich gas stream two main reactions happen: firstly, the catalyst releases the NO<sub>x</sub> and is thereby regenerated, followed by the NO<sub>x</sub> being reduced to nitrogen (figure 2.4) [18].

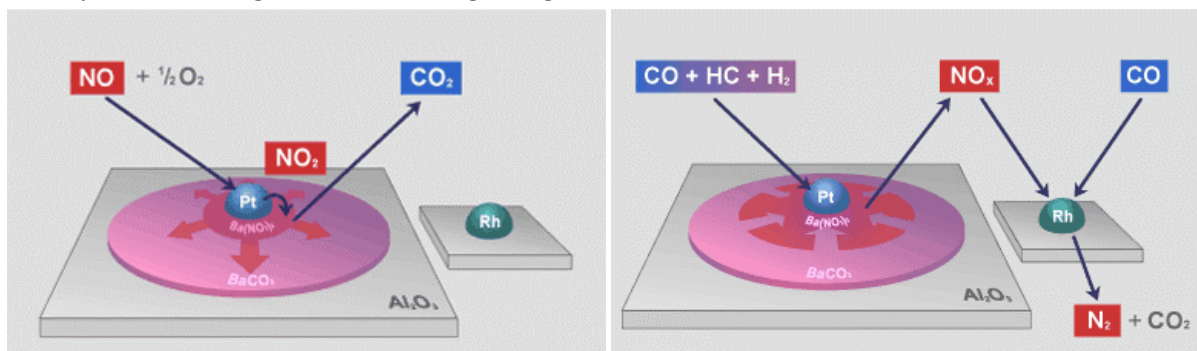


Figure 2.3 – 2.4: NO<sub>x</sub> adsorber catalyst (lean condition); NO<sub>x</sub> adsorber catalyst (rich condition) [18].

*Plasma Converters (PC)*

A catalytic plasma converter combines oxidation and reduction of exhaust gas emissions, namely HC, CO, NO and NO<sub>x</sub>, by providing a pair of catalytic metallic porous elements, such as electrically conductive metal matrix material, spaced apart to define an intermediate reaction chamber. High voltage electric charges of opposite polarity applied to the two elements generate a gas plasma in the exhaust gases passing through the converter reaction chamber. The passage of gases through the catalytic elements oxidizes CO and HC

emissions present in the exhaust gases, whilst the gas plasma in the reaction chamber causes the reduction of NO and NO<sub>x</sub> and further reaction of HC and CO exhaust emissions [25].

### *Selective Catalytic Reduction (SCR)*

The selective catalytic reduction selectively reduces the amount of nitrous-oxides to nitrogen N<sub>2</sub> (a naturally occurring atmospheric gas) using ammonia or urea as a reductant (figure 2.5). With this approach, exhaust temperature and reductant rates are extremely important for maximizing NO<sub>x</sub> conversion efficiencies and minimizing ammonia slip. Specifically, low exhaust temperature (below 240 °C) generally leads to low NO<sub>x</sub> conversion efficiency, while high reductant rates may lead to ammonia slip [26]. Therefore, extensive control of the system components is required in order to optimize this technology with special regard to transient engine operation. This highly effective technology has been used for many years in industrial processes and stationary engines, but its use in vehicle applications has been limited due to the large size of the device, the complexity of the technology and safety concerns around ammonia-slip into the environment. This technology is now being developed for the mobile fleet and is favoured by many heavy-duty European and a few North American companies [19]. It is likely that this technology will see widespread use in heavy duty applications and larger passenger cars in future. This technology is generally not sensitive to fuel or lubricant sulphur [21].

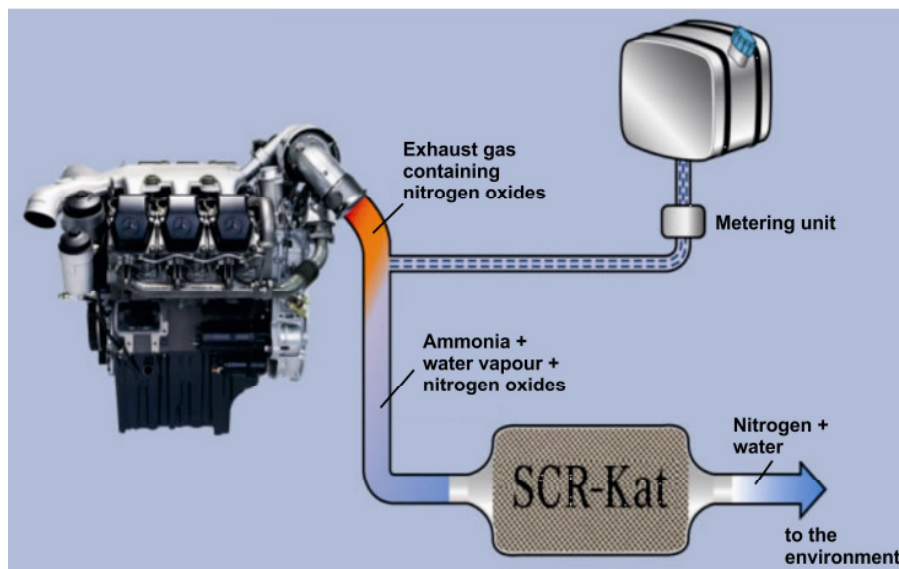


*Figure 2.5: Selective catalytic reduction.*

## 2.2 In-Cylinder Combustion Optimization

In the last 20 years, the reduction of regulated emission of about 80 % has been achieved through advances in diesel combustion technology, mainly by the optimization of engine components including turbo-charging, after-cooling, combustion chamber optimization, exhaust gas recirculation, injection system equipment and alternative fuels [19].

Turbochargers reduce both NO<sub>x</sub> and PM emissions by approximately 33 % when compared to naturally aspirated engines. After-cooling with turbo-charging provides even larger NO<sub>x</sub> and PM reductions by decreasing the temperature of the charged air after it is heated by the turbocharger [17]. Adding EGR to a diesel engine produces a trade-off between NO<sub>x</sub> reduction and PM increase: the insertion of combustion gases into the cylinder, increases the specific heat capacity of the cylinder contents (lowering the adiabatic flame temperature) and decreases oxygen partial pressure. On one hand these two effects reduce the

amount of produced  $\text{NO}_x$ , but on the other hand the decreased availability of oxygen causes an increase in particulate emission (the oxidation of soot is poorer) and HC if boost is not increased (to keep lambda constant) (figure 2.6 – 2.7). However, with a good EGR actuation strategy, benefit from EGR rates as high as 50 % (at idle, where there is otherwise a very large amount of excess air) in controlling  $\text{NO}_x$  emissions will be possible.

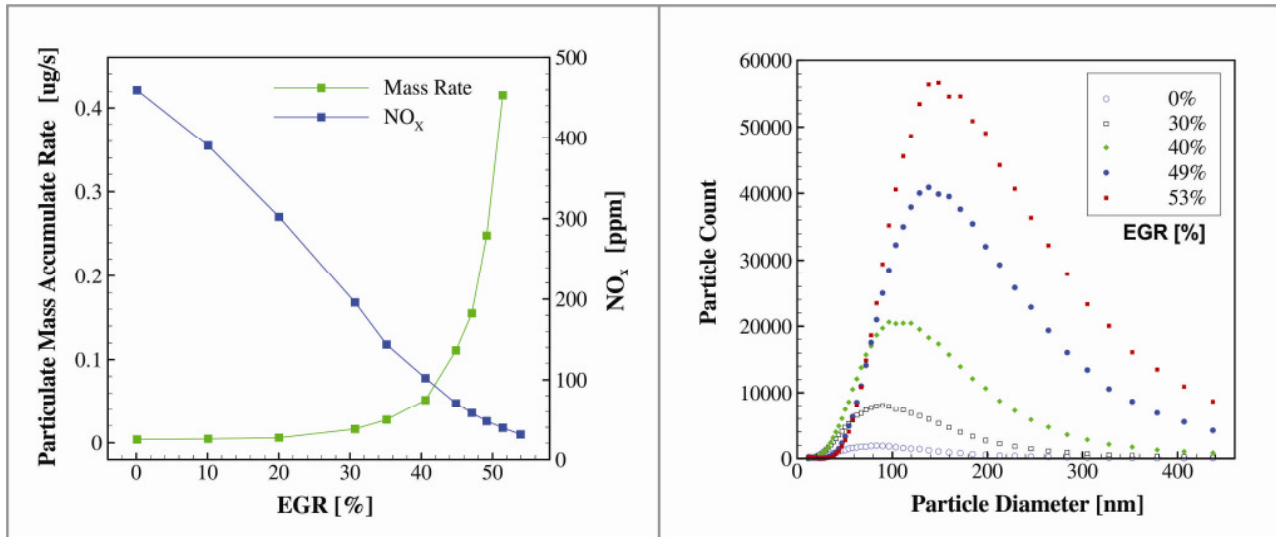


**Figure 2.6 – 2.7:** Ultimate EGR limit is delineated by a sudden increase of PM [27]; With increasing EGR particle count increase, median and large particles (> 100 nm) increase, and small particles (< 100 nm) decrease [27].

The optimization of the combustion chamber affects emissions mainly by affecting the in-cylinder turbulence and consequently the fuel/air mixing. A clear example is the re-entrant piston bowl designs used principally on medium-duty diesel engines; the re-entrant bowl causes a better fuel/air mixing that improves combustion and decreases both PM and HC emissions. Combustion chamber improvements are ongoing in the industry and result in improved fuel economy and emission reductions.

### 2.2.1 Injection System Parameters

The diesel injection system assists the engine development to fulfil future more stringent exhaust gas limits and becomes the decisive factor to reach additional emission targets [1]. It influences mixture formation, combustion, exhaust emissions, engine noise and, depending on the type, allows the implementation of after-treatment technologies.

As confirmed by a great number of technical research projects, in order to solve the trade-off between  $\text{NO}_x$ , PM, fuel consumption and noise a flexible high-pressure fuel injection systems that has multiple injection and rate-shaping capabilities, combined with a very high injection pressure is needed.

#### High Pressure

High injection pressures are required primarily to enable effective mixing of fuel with the air charge and thus reduce soot emission; this is particularly important during the operation with exhaust gas recirculation [28] and whether turbo-charging is used [29]. In the last 30 years a shift towards high-pressure fuel injection systems has been observed, with an increase of maximum injection pressure from 800 up to 1800 bar. Current production injection systems are capable of pressures of this order. Research into still higher pressure systems is ongoing but an upper useful limit is expected to be around 2000 bar [19]. Increased

interest is now directed in the improved use of the available pressure, by implementing new strategies for advanced combustion concepts [19].

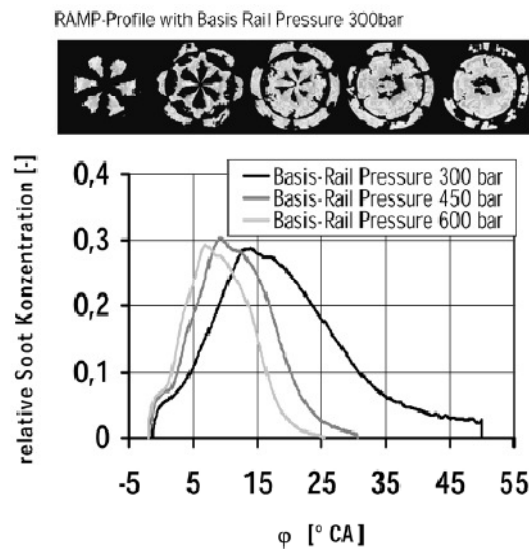


**Figure 2.8:** Effect of injection pressure on relative soot concentration in the combustion chamber (single cylinder research engine) [30].

Figure 2.8 shows how increasing rail pressure has a positive effect on accelerated and more complete soot oxidation.

### Multiple Injections Strategies

Multiple fuel injection strategies during the compression and expansion stroke of a diesel engine are being widely studied in an attempt to reduce the exhaust emissions and noise of diesel engines. Research has shown that multiple injections can slow down and/or delay heat release (i.e. splitting the heat release into several parts), thus lowering maximum heat release rate and combustion noise (figure 2.9).

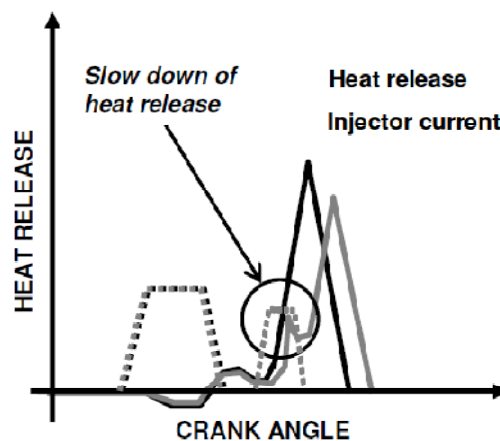


**Figure 2.9:** Slow down of heat release thanks to double injection [31].

Pilot injections can be very effective in reducing combustion noise through the shortening of ignition delay, and thus the reduction of the premixed combustion phase and the rapid pressure rise that is the primary cause of such noise. Since most  $\text{NO}_x$  is formed during premixed combustion, pilot injection has also been extensively investigated as a means of obtaining lower  $\text{NO}_x$  emissions. The corresponding increase in soot

emissions, due to the reduced proportion of premixed combustion, can be mitigated by a more flexible control of the fuel injected and by the use of post injection strategies. Significant improvements in the trade-off between particulate and NO<sub>x</sub> emissions can therefore be obtained (figure 2.10) [32].

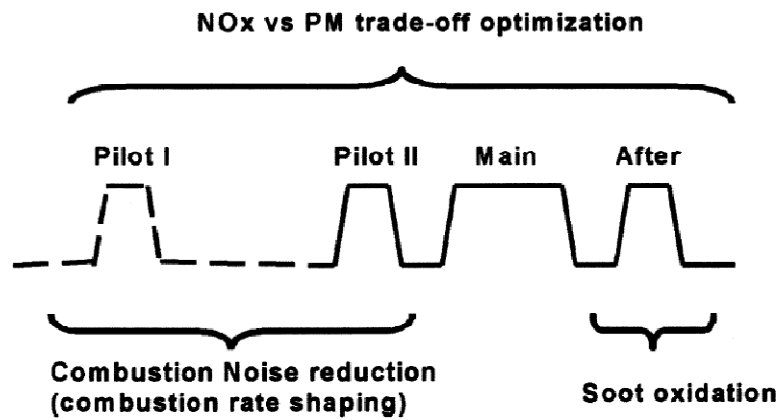


Figure 2.10: Common-rail multiple injections for the control of emissions and noise [32].

Various experiments have highlighted that beneficial effects on the combustion process for particular engine conditions such as low compression ratio and high EGR rate, could be achieved via multiple injections strategies. By means of the cooling effect<sup>9</sup>, the double injection strategy may increase ignition delay and thereby improving fuel/air mixture, decreasing local equivalence ratio and resulting in less soot formation (figure 2.11). When compared to the single injection case, this capability can be used at medium loads to improve fuel consumption since it allows increasing the EGR rate and advancing the combustion timing closer to TDC without combustion noise or soot penalty [31].

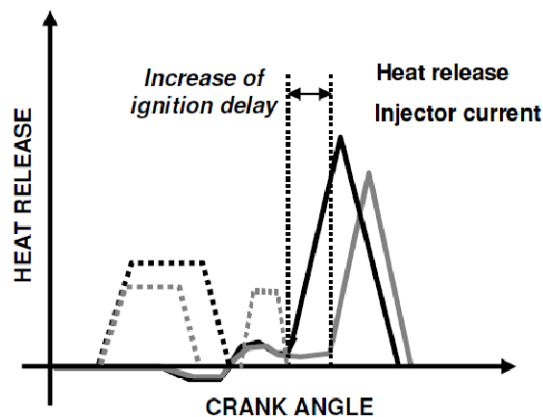


Figure 2.11: Increase of ignition delay thanks to double injection at identical EGR rate [31].

Multiple injections strategies also lead to better fuel distribution resulting in a most efficient use of the fresh air available in the combustion chamber, particularly at high engine load conditions [31].

<sup>9</sup> The cooling effect is the temperature decrease due to latent heat of vaporization of injected fuel. This effect is of particular interest when it is purposely used by adequately injecting a additional fuel quantity while fuel injected in the previous injection is just about to ignite, or is in a cool flame oxidation process or is starting to burn.

Nevertheless, multi injection strategies also bring some drawbacks as most of the injection strategies require a very accurate control of the fuel delivery (timing and quantity). As a matter of fact, the major challenge today is to obtain a fast-reacting injection system with good repeatability to perform all the necessary one-cycle injections and that allows an accurate control of the injected fuel quantities on each injection event (despite common-rail pressure waves which can strongly affect secondary and later injections).

### Injection Rate Shaping

Fuel injection rate shaping, which is a temporal variation of the injection rate during each single injection, is considered to have a great influence on the formation of the combustible mixture, because it controls spray temporal and spatial distributions. Therefore it is believed that an optimization of the injection rate shaping will be the key factor in improving spray combustion and reducing  $\text{NO}_x$  and particulates.

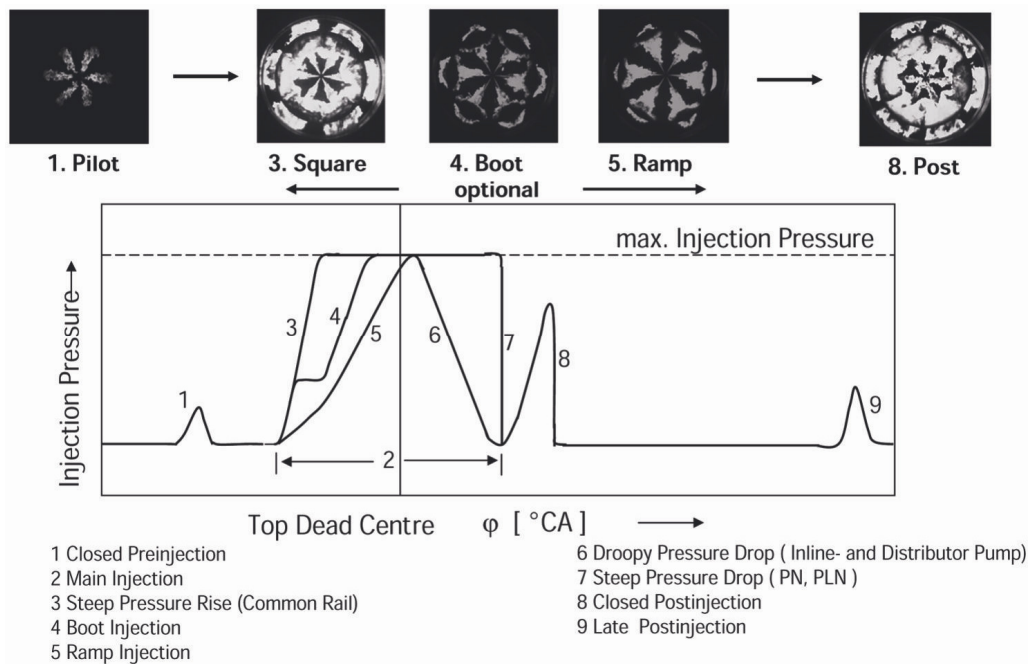


**Figure 2.12:** “Fully flexible” injection rate [30].

Many experiments have shown that every single injection shape may improve engine efficiency and reduce emissions depending on the engine state. Therefore a “fully flexible” injection system that is capable of injection rate shaping at each point of the engine operating map will offer the best compromise between emission trade-off and fuel consumption. For example, when using exhaust gas recirculation, a rectangular type main injection with high injection pressures at full load is recommended (shape no.3 in figure 2.12). On the other hand, without EGR and in the same point of the engine map, a boot or ramp shape (shape no.4 in figure 2.12) injection rate leads to better emissions with an unchanged or improved fuel consumption [1].

In a conventional common-rail system the injection pressure is constant throughout the injection period, resulting in a nearly rectangular injection rate shape and offering no control of the injection rate. For this reason there are many ongoing research projects focusing on controlling the injection rate shape during the injection. An example of the effort spent on this direction is the “Next-generation common-rail System (NCRS)”, which was conceptualized, designed, and fabricated in Japan and presented at the Seoul 2000 FISITA World Automotive Congress (figure 2.13) [33]. The NCRS has two rails, for low and high pressure fuel, and switches the fuel pressure supplied to the injector from the low to the high pressure rail during the injection period, resulting in control over the injection rate shape. The effects of the injection rate shape on

the exhaust emissions and fuel consumption were then investigated through experiments with this new system.

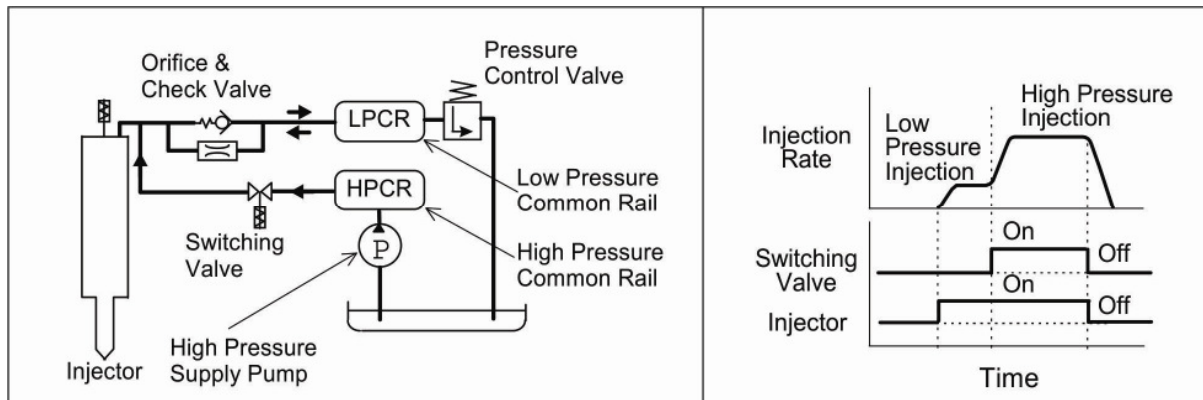


Figure 2.13: NCRS schematic and timing characteristics [33].

Figure 2.14 shows the improvement obtained with the NCRS, in terms of exhaust emissions and fuel consumption, compared to the conventional common-rail system in some reference engine points; at constant  $NO_x$ , fuel consumption was reduced by 2.6 % and PM by 39 %, while at constant ISFC (indicated specific fuel consumption),  $NO_x$  was reduced by 22 %, and PM by 54 %.

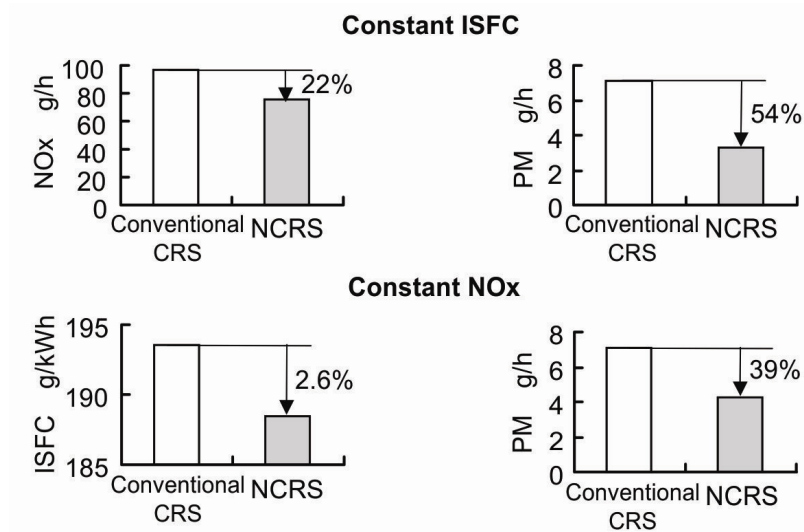


Figure 2.14: Improvement of fuel consumption and  $NO_x$  and PM emissions [33].

### 2.2.2 Alternative Fuels

As energy demand continues to rise, so does concern over the future availability of conventional fuels. There is a growing need to find alternative fuel options and future petroleum availability is not the only reason. As clearly presented in the previous section of this dissertation, the environmental problems concerning diesel pollutant emission need to be controlled and this is why research with alternative fuels is again on the increase. The key factor for the alternative fuels is the capability of the fuel to reduce harmful exhaust emission and to spread as a valid petrodiesel alternative, diversifying energy sources and improving security of supply. Synthetic liquid fuels and Biodiesel are the fuels that seem to appear the most in current literature and reports, probably because of the relatively small modification of the engine and the fuelling

infrastructure necessary. Other alternative fuels that have been investigated for use in diesel engines include ethers, alcohols, naphtha, and various gaseous fuels. Each of these has some advantage (such as reduced engine emissions) associated with its use. However, much work remains to be done with these fuels, including building a distribution infrastructure, before they can be widely used in diesel engines [34]. This section contains a brief description of the advantages and disadvantages resulting from fueling diesel engine with the most promising petrodiesel alternatives: Synthetic fuels and Biodiesel.

### *Synthetic Fuel*

The term “synthetic fuel” has several different meanings and it may include different types of fuels. The most general definition was given by the Energy Information Administration (EIA) that defines synthetic fuels in its Annual Energy Outlook 2006, as fuels produced from coal, natural gas, or biomass feedstocks through chemical conversion into synthetic crude and/or synthetic liquid products [35].

The synthetic fuels production process begins with a feedstock, which is a carbonaceous (rich in carbon) substance that is used as a source material to directly produce synthetic fuel (direct conversion) or by creating first a synthetic gas (indirect conversion). The three main feedstocks that can be used for synthetic fuel production are natural gas, coal and biomass.

- **Coal** has been used as a feedstock for many years and is currently in large-scale synthetic fuel production in South Africa. Countries with small oil and gas but large coal reserves can reduce reliance on petroleum imports by developing synthetic fuels from coal [36]. China, which has the world's third largest coal reserves after the United States and Russia, has shown particular interest in this process [37].
- **Natural gas** is currently used as a feedstock for synthetic fuels production in Malaysia and offers a good alternative to all those countries with abundant natural gas resources hard to bring to market<sup>10</sup>.
- **Biomass** is seen as a significant future feedstock for synthetic fuels. The U.S. Department of Energy and the U.S. Department of Agriculture have estimated that up to 1.3 GT (giga-tons) of dry biomass may be sustainably produced for energy and bioproduct production in the U.S. – enough to potentially displace 30 percent of current U.S. petroleum consumption [36].

There are numerous processes that can be used to produce synthetic fuels (direct, indirect and Biofuel processes) but the process with the widest deployment worldwide, probably because of its proven and well-known state of technology, is the indirect conversion. Indirect conversion refers to a process in which natural gas, coal, biomass, or bitumen from oil sands are converted into a liquid fuel (synthetic fuel respectively called GTL, CTL, BTL and OTL). All four processes, usually known as gas-to-liquid (GTL), consist of three separate technological processes. In the first step carbon feedstock is reacting with oxygen and steam inside of gasifier/reformer generating a mixture of hydrogen and carbon monoxide ( $H_2 + CO$ ) called syngas. This syngas generation can be used in many processes like fertilizer, methanol and specialty chemical production. In addition, generated waste heat could produce steam-derived electricity in IGCC (integrated gasification combined cycle) power plants as a by-product of the GTL process which could increase the overall energy efficiency, thereby helping to amortize the large cost of the equipment. After that, the syngas is processed

---

<sup>10</sup> Globally, there is more than 5,500 Trillion cubic feet (Tcf) of natural gas available. It is estimated that more than 2,500 Tcf is stranded natural gas. This means that the gas resource has been identified (usually discovered while drilling for oil), but there is no economical way to bring it to market. One Tcf of natural gas is potentially equal to 100 million barrels of FT fuel, and doing the math translates to immense possible revenues for the oil companies [57].

into a liquid transportation fuel using one of a number of different conversion techniques depending on the desired end product. The primary technology that produces synthetic fuel from syngas is the Fischer-Tropsch synthesis. During the Fischer-Tropsch process the resultant syngas is then fed to the FT reactor where, under the right process conditions and in contact with either a cobalt or iron catalyst, forms a long chain of carbonhydrogen molecules named FT wax, or paraffin. The third step splits these long chain molecules into shorter-length hydrocarbon molecules (diesel, naphtha, kerosene, LPG) in a hydrocracking stage that is almost identical to crude oil refining. The FT process offers the potential to produce a range of products such as middle distillates fuels, as well as lubricants and waxes [38]. The complete process, including input and outputs is illustrated in figure 2.15.

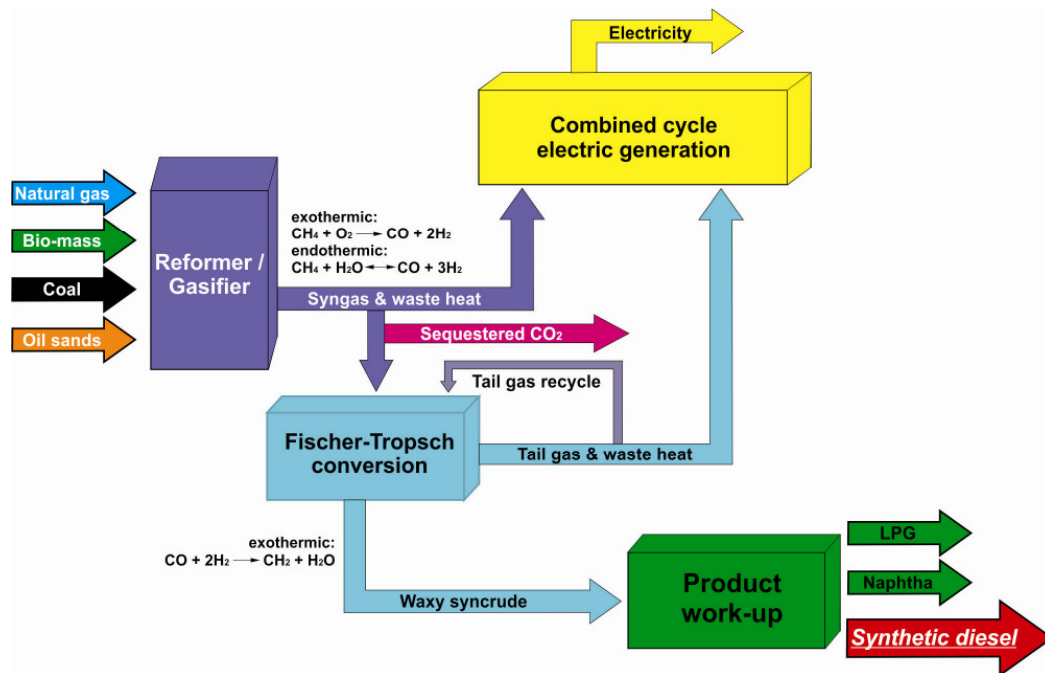
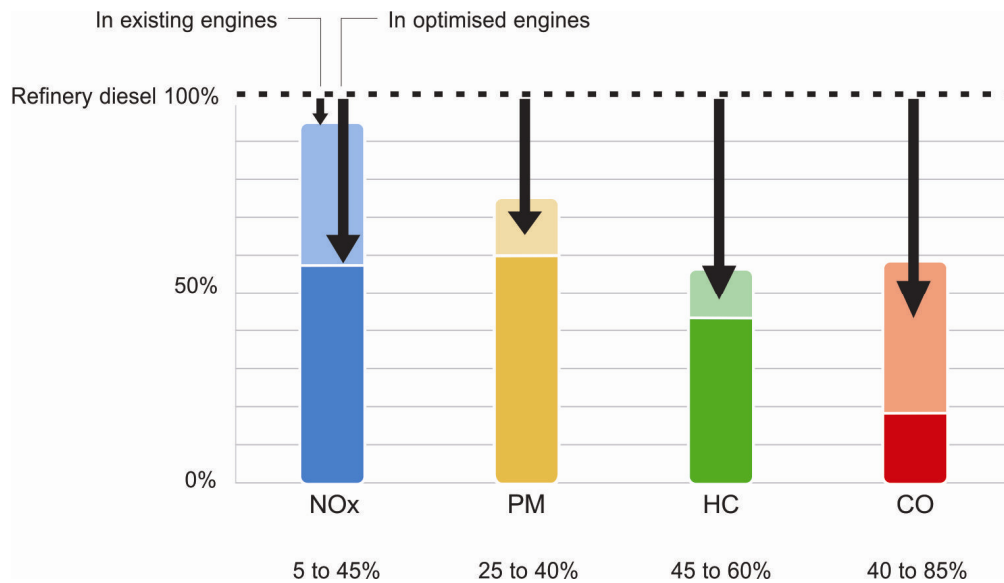


Figure 2.15: Gas-to-Liquid technological process with Fischer-Tropsch synthesis reactor.

Fischer-Tropsch technology, as the entire GTL process is usually called, results in a fuel that is colourless, odourless, low in toxicity and that has high cetane number<sup>11</sup>, no aromatic compounds and no sulphur. According to the available results, there are no significant differences in Fischer-Tropsch fuels' performance versus petrodiesel fuels. In fact, the higher cetane number of Fischer-Tropsch diesel fuel may result in improved combustion; it is virtually interchangeable with conventional diesel fuels and can be blended with diesel at any ratio with little or no modification [37].

Road trials of synthetic fuels in several European capitals and elsewhere demonstrate that they offer important emissions benefits compared with diesel, reducing nitrogen oxide, carbon monoxide, unburned hydrocarbon and particulate matter. Whereas the application of successive Euro-standards applies to new vehicles only, the introduction of synthetic fuels will have an immediate positive impact on the local emissions from the existing vehicle fleet, particularly in urban areas. When engines are optimized to run on synthetic fuels further reductions of nitrogen oxides can be achieved (figure 2.16) [39].

<sup>11</sup> The cetane number is a primary measure of diesel fuel quality and often FT diesel fuels have a cetane number greater than 70 cetane [34].



**Figure 2.16:** Emissions benefits vary depending on: Vehicle type and technology level (Euro 1 to Euro 4), base fuels (low sulphur diesel (350 to 500 ppm sulphur) or “zero” sulphur diesel (10 ppm sulphur)) [39].

Furthermore, while many alternative fuels require completely separate distribution systems, Fischer-Tropsch fuels have a great compatibility with currently existing vehicle technologies and fuel distribution systems. Synthetic diesel can be transported through existing pipelines, dispensed at existing fuelling stations, and used to fuel today's diesel powered vehicles [37]. A limited investment will be required, however, to maintain the fuel's purity during distribution.

Fischer-Tropsch fuels are however slightly less energy dense than petrodiesel, which may result in lower fuel economy and power [37]. Another significant potential problem is the low lubricating capability offered from these fuels; FT fuels may have poor lubricity properties. Some elastomer/seal swell problems, especially in older fuel systems, may also result from the use of these fuels since they have no aromatic compounds [34].

Synthetic fuels are one of the few economically viable and industrially scalable alternatives to petroleum capable of providing a major source of the liquid transportation fuels required to run the economy, and the only known non-petroleum source of aviation fuel. Currently, several oil companies are researching large-scale production of Fischer-Tropsch fuels. At least four major companies have announced plans to build pilot plants to produce synthetically derived Fischer-Tropsch diesel fuels.

### Biodiesel

Biodiesel is a clean-burning alternative fuel produced from domestically grown renewable resources such as animal or vegetable materials.

Biodiesel is commonly produced by the transesterification of vegetable oil or animal fat feedstock. The process involves reacting vegetable oils or animal fats catalytically with short-chain aliphatic alcohols (typically methanol or ethanol<sup>12</sup>) resulting in two products: fatty acid esters, the chemical name for biodiesel, and glycerol, a valuable by-product usually sold for use in the production of soap. There are several methods for carrying out this transesterification reaction including the common batch process, supercritical processes [40], ultrasonic methods [41], and even microwave methods [42].

<sup>12</sup> The finesched biodiesel derives approximately 10 % of its mass from the reacted alcohol. The alcohol used in the reaction may or may not come from renewable resources [34].

Many products, including peanut oil, hemp oil, corn oil and tallow (beef fat) have been used as feedstocks for the transesterification process. Today, the most common sources for biodiesel are [43]:

- plants: soybeans, peanuts, rapeseed, palm, corn, sorghum, canola, sunflower and cottonseed.
- animal fats: tallow, white grease, poultry fats and fish oils.
- recycled greases: used cooking oils and restaurant frying oils.

Biodiesel contains no petroleum products, but can be blended at any concentration with petrodiesel to create a blend; much of the world uses a system known as the "B" factor to state the amount of biodiesel in any fuel mix (100 % biodiesel is referred to as B100, 20 % biodiesel is labelled B20, and so on). Biodiesel (B100) is nontoxic, has good lubricity properties and contains essentially no sulphur or aromatics. However, biodiesel has a relatively high pour point, which could limit its use in cold weather<sup>13</sup> and it is also more susceptible to oxidative degradation than petroleum diesel [34].

An accurate analysis of biodiesel effects on the formation of harmful emissions requires engine type (light or heavy duty) and engine condition (load, speed, temperature, etc.) specification as the emissions of the engine fuelled with biodiesel are strongly affected by these parameters. It is however possible to show that blending more than 20 % biodiesel with petroleum (B20 - B100) causes a significant reduction in PM emissions but may also cause NO<sub>x</sub> emissions to increase by 1 to 3 percent [44].

The biodiesel production requires higher costs compared with fossil fuel (i.e. in Italy these costs are three times higher than the fossil diesel prices), but the advantages deriving from the use of this fuel induced many European governs to encourage biodiesel production by lowering taxes and by assisting the plantation of rapeseed, soybean and sunflower [14]. A possible solution to reduce the production cost of biodiesel comes from recycling cooking oils and restaurant frying oils, and using them as a feedstock for biodiesel production; unfortunately, their high free fatty acid content enhances the technological problems of biodiesel production [14]. Searching for new efficient and high oleaginous contents sources, algae emerged as one of the most promising source for biodiesel production. Algae are single-celled organisms that, like plants, produce energy through the process of photosynthesis, converting water, sunlight and carbon dioxide into "food" in the form of an oil. This algae oil can be used to produce biodiesel for engines. Algae are highly flexible: They can be grown in most climates, and do not require arable land for production. According to the National Renewable Energy Laboratory (NREL), "microalgae systems use far less water than traditional oilseed crops" algae can be grown in brackish water, seawater and even wastewater [43]; so far, there have not been large scale experimentations and are not known neither the possible illness due to so large monocultures nor the plant costs [14].

Many analysts state their doubts regarding the efficiency of the chemical process involved in biodiesel production. Some possible reasons that, so far, keep biodiesel from spreading as a clean diesel fueling alternative are summarized below:

- Need to reconvert large amounts of land to new cultivation
- Risk of creating high competition with alimentary cultivation
- Higher prices for the customers
- Production process still not efficient enough

---

<sup>13</sup> Using alcohols of higher molecular weights during the transesterification process improves the cold flow properties of the resulting ester, at the cost of a less efficient transesterification reaction.

## 3 Injection Analyzer

### 3.1 Introduction and Objective

One of the main research topics at the LAV/ETH are the physical and chemical mechanisms involved in the fuel injection/mixing/ignition and combustion processes in internal combustion engines. For the development and validation of new or improved numerical models a medium size (bore  $\varnothing 165$  mm) diesel engine test bench has been built in the laboratory. The setup of the test bench focuses on fully adjustable and controllable boundary conditions over a wide range of temperatures, pressures, loads etc. in order to yield reproducible and reliable measurement data. The advantage of having such a test bed within the same group as the numerical modellers gives the opportunity to closely cooperate the model development and the corresponding experimental measurements. The starting point of the test bench is a single cylinder, four stroke direct injected, engine manufactured by the German company MTU; the engine has been modified and equipped with laboratory devices to obtain the prearranged goals. The swept volume amounts to roughly four litres, further details of the test bench data are given in table 3.1.

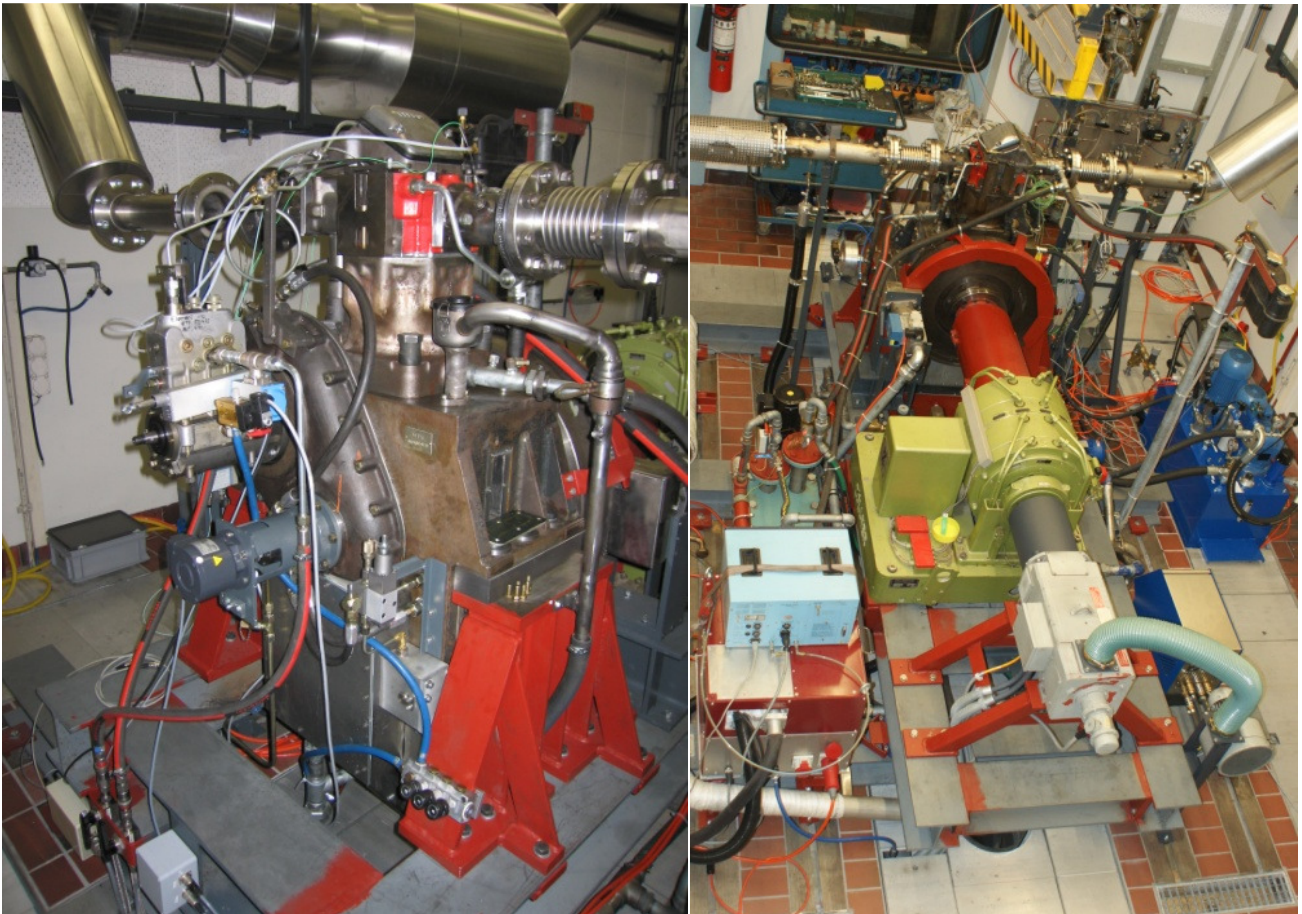


*Figure 3.1 - 3.2: Two different views of the MTU single cylinder engine test bench.*

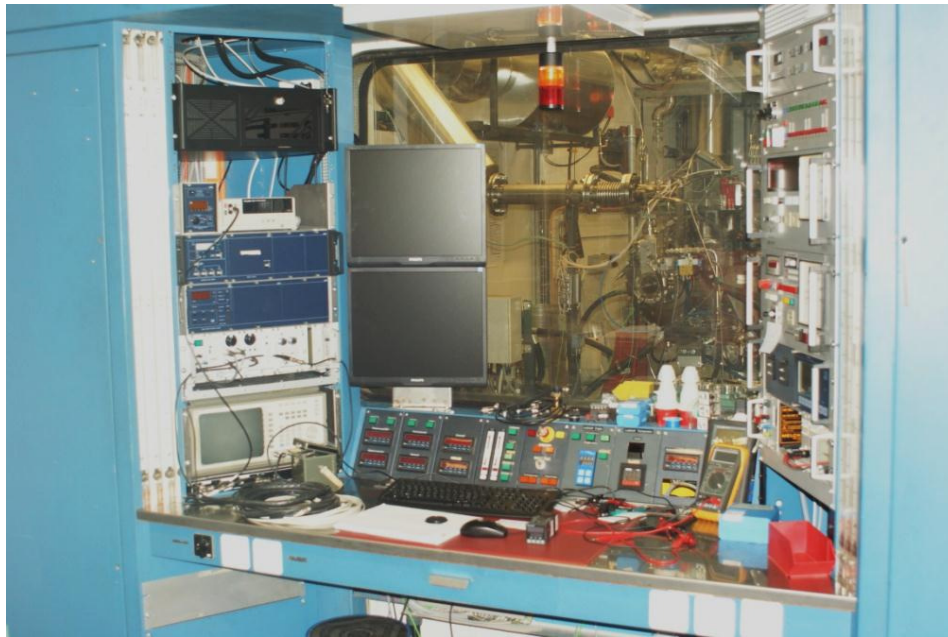


**Figure 3.3:** MTU engine test bench control room.

	<b>Test bench</b>	<b>Original engine</b>
<b>Nominal speed</b>	900 – 1500 rpm	2100 rpm
<b>Torque</b>	1000 Nm	700 Nm
<b>Bore / Stroke</b>	165 / 185 mm	165 / 185 mm
<b>Injection system</b>	Common-rail system, max. 1800 bar, (pump 2000 bar); 6 and 8 hole injectors with variable hole configurations	Cam-driven injector system, max 600 bar; 6 hole injector
<b>Inlet</b>	External compressor: 0 – 4.5 bar (above 6 bar), 20 – 100°C; Pressure sensors and thermocouple	Turbo charged (maximum relative pressure 4.5 bar)
<b>Exhaust</b>	FSN / Micro Soot sensor (Pass); AMA 1000 for exhaust gas analysis; Pressure sensors and thermocouple	
<b>EGR</b>	External system (controlled temperature, pressure and mass flow of the recirculated exhaust gas)	
<b>Cylinder pressure</b>	Pressure sensor flush mounted in the head	
<b>Additional Cylinder access</b>	Multifunctional adaptor (replaces one exhaust valve) for optical light probes, sampling valves or other sensors	
<b>Starter</b>	Pneumatic starter motor	
<b>Brake system</b>	Eddy current dynamometer	
<b>Electrical motor</b>	Used to drive the engine for measurements without combustion (or at the ignition/combustion limits)	

**Table 3.1:** Engine test bench data.

Access to the cylinder is obtained by the removal of one of the two exhaust valves of the engine. In this valve a seat to fit a multifunctional adaptor is realized. This modification allows for example the introduction of a

fast sampling valve with an actuation time of less than 1 ms, used to collect in-cylinder gas at a certain time / crank angle during each single engine cycle.



**Figure 3.4 - 3.5:** The MTU cylinder head before and after the modification to the exhaust valve.



**Figure 3.6 - 3.7:** The MTU cylinder with the injector and the fast sampling valve.

In the same multifunctional adaptor, alternatively an experimental optical light probe can also be installed. The optical probe used here is a prototype manufactured by Kistler/Sensoptic from an on-going collaboration between those companies and the LAV. The LAV task is to gain experience and provide further experimental data in order to develop this probe into a commercial instrument to measure in-cylinder soot formation and oxidation. The analysis of the provided experimental data requires a very detailed knowledge of all the boundary conditions, including the injection process: Particularly the exact calculation of the heat release rate and the formation of the pollutants (by using a quasi-dimensional, phenomenological modelling approach developed by the LAV itself). This is the reason why an in-depth study of hydraulic injection behaviour is absolutely necessary in order to know the exact injection timing and injection rate profile under all engine conditions encountered in the engine experiments.

Basing on the knowledge acquired by people from the LAV in earlier projects (which already had some previous experience) and after a detailed study of injection analyzer state of the art, a Bosch tube type injection rate measuring system was chosen to be design for this purpose.

Part of the work of this dissertation is the realization of this system (starting from some leftover hardware of former experiments). Such a measuring instrument must be able to completely define all injector characteristics as injection time (hydraulic start, end and corresponding delay from electric signal), injection rate and injected quantity (up to 1000 mg per stroke).

Before designing the injection analyzer test bench an in depth study to understand the measurement principle was made. Then the missing parts for the injection analyzer setup and the injector mounting were designed and manufactured. The realization of the measurements setup with the data acquisition system and the development and implementation of the data processing algorithm followed.

In this chapter, after a brief overview of the state of the art of the injection system technology and of the physical measurement principle of the injection analyzer, the design of the new injection meter is described including some measurement results.

### 3.2 Injection System Technology

The performance of modern diesel engines is highly dependent on the fuel injection equipment used on the engine and the accuracy of the control of fuel injection events. The fuel-injection system is responsible for supplying the engine with diesel fuel at the correct time and with the correct amount.

The injection pump generates the pressure required for fuel injection; the pressurized fuel flows through the high-pressure fuel-injection tubing to the injector and – during the injection events – to the injection nozzle which then injects it into the combustion chamber. Different kinds of fuel systems are available today which can be grouped as follows: in-line pumps, distribution pumps, unit-injectors and common-rail injection systems.

Since the first in-line fuel injection pump was produced by Bosch in 1927, countless numbers of them have reliably kept diesel engines in motion. These “classics of diesel fuel-injection technology” are still in use nowadays, but today’s passenger cars with DI-diesel engines are almost exclusively equipped with the distributor pump, the unit-injector and the common-rail injection system types.

There are two different types of distributor pumps – axial piston and radial piston types – both consist of one single plunger-and-barrel assembly for all the engine’s cylinders (in opposition to the in-line pump that has a set of cam-driven plungers for each cylinder). Distributor pumps have a mechanical (flyweight) governor or an electronic control with integrated timing device that allows a variable injection timing (to some degree). A great advantage of these injection systems is their proven technology but, even though the latest models are equipped with electronic control that offer a higher flexibility, this technology doesn’t permit the implementation of all the modern injection strategy (i.e. injection rate shaping and multiple injection per cycle).

In the unit-injector system the injection pump and injection nozzle form a single unit. One of these units is installed in the engine’s cylinder head for each engine cylinder and is driven directly by a tappet or indirectly from the engine’s camshaft through a valve lifter. Compared to the in-line and distributor injection pumps a considerably higher injection pressure (up to 2000 bar) is possible due to the omission of the high-pressure lines. Such high injection pressures coupled with the electronic map-based control of the duration of injection (or injected fuel quantity) including the shape of the injection rate profile permitted a considerable reduction of the diesel engine’s toxic emissions [45]. Electronic control concepts add a variety of additional

functions, but due to the inherent design limitations unit-injector systems will always be less flexible than common-rail systems.

As shown in various publications (i.e. [46], [47]) and demonstrated by thousands of common-rail systems installed on new DI-diesel cars, common-rail technology offers a number of advantages: One of the fundamental differences of the CR system compared to cam-controlled injection systems is the high flexibility in terms of injection timing and that the injection pressure is independent of the engine speed. Figure 3.8 shows the fuel pressure of the cam-controlled injection systems in comparison with the CR system at different engine speeds. The diagram clearly shows the low injection pressure of the distributor pump and the unit injection system at low engine speed. With lower fuel quantities, the effective injection pressure also decreases so that especially at part load conditions and at low engine speed there is less injection pressure to support the mixture formation [46].

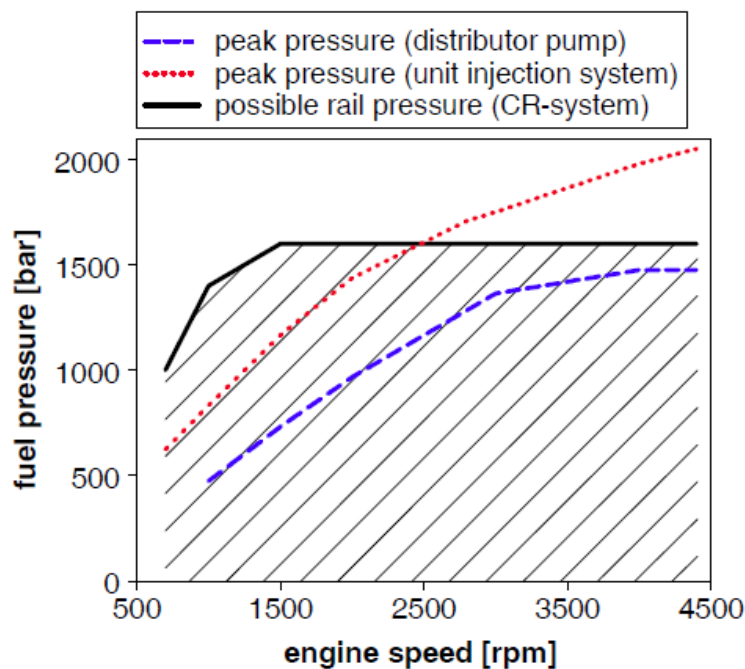


**Figure 3.8:** Possible fuel pressure of different injection system.

A further advantage of the common-rail system is the constant fuel pressure at the nozzle during the injection period. The cam-controlled injection systems reach their maximum injection pressure only for a short period (due to the pump piston motion). The fuel pressure at nozzle of the CR system levels off during the injection period (which includes the pilot and the main injection) [46].

According to the latest state-of-the-art, it is unquestionable that common-rail injection system offer great advantages compared to all the other systems.

### 3.3 Injection Analyzer Measurement Principle

There are several methods for the measurement of the injection hydraulic behaviour, such as: momentum method [48], pressure-lift method [48], Bosch's method [49], and Zeuch's method [50]. This section describes the measurement principle and the measurement system based on the principle of the Bosch's method.

The Bosch tube type injection rate measurement system records the rate of discharge by measuring the pressure wave that is produced by an injector when it injects into a predetermined length of a hydraulic tube filled with calibrated diesel fuel. In figure 3.9 the schema of this measurement device as described in [49] is shown.

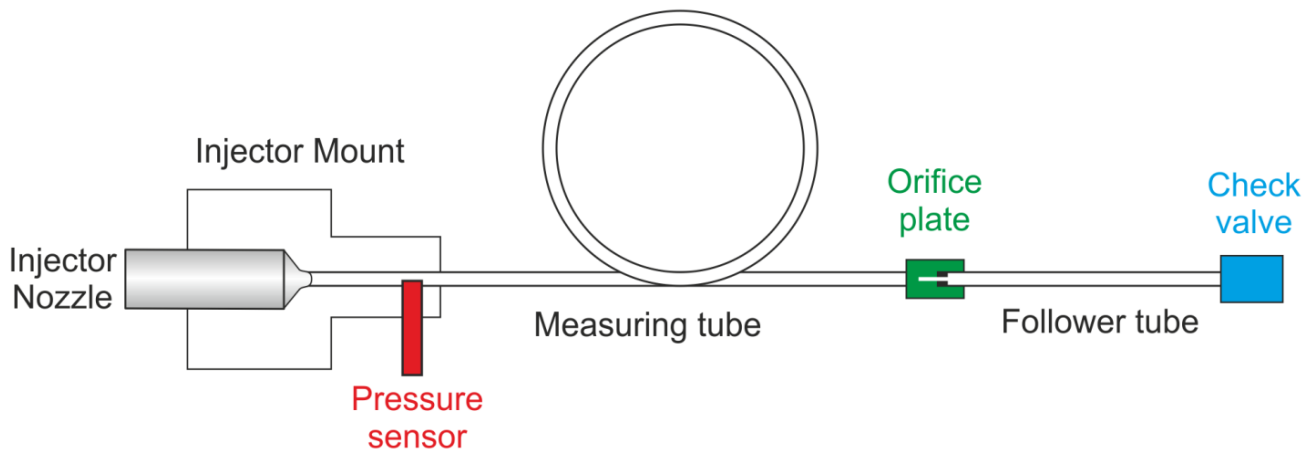


*Figure 3.9: Sketch of the Bosch tube type injection rate measuring system.*

The device consists of an injector mount, a measuring tube, an orifice, a follower tube and a check valve. The injector mount holds the injector so that the injector nozzle is positioned at the beginning of the measuring tube; it also holds the pressure sensor which is used to record the pressure signal. Between the measuring tube and the follower tube is an orifice (usually an orifice plate adapter with orifice plates). The size of the orifice determines which part of the fuel transported with the pressure wave is reflected and which part enters the follower tube. If the orifice is too large, the majority of the transported fuel passes through the orifice and a negative pressure wave is reflected back into the measuring tube. The inside diameter of the measuring tube determines the magnitude of the pressure waves (for a given injection rate) while the length of the measuring tube affects the attenuation efficiency of the device and the measurable injection frequency. A check valve located at the end of the follower tube adjusts the back pressure in the enclosed volume (injector mount, measuring tube and follower tube) so that an injection back pressure comparable to the conditions in the engine can be used when testing an injector [51], [49].

The function of the fuel rate indicator is based on the theory that for a one-dimensional flow in a rigid tube, the mass flow rate is determined by the velocity of flow through a known flow area<sup>14</sup>, expressed by the formula:

$$\dot{m} = \rho \cdot A \cdot v \tag{3.1}$$

where:

$\dot{m}$  = Mass flow rate

$\rho$  = Fluid density

$A$  = Tube cross section area

---

<sup>14</sup> This is obtained from the continuity equation of mass for steady one-dimensional flow in a rigid tube [52].

$v$  = Fluid velocity

Since the tube has a constant and known cross section area the determination of the rate of discharge (injection rate) is solely based on the calculation of the flow velocity during the injection.

The injection of the fluid into the tube produces a prompt change of pressure that propagates at the velocity of sound ( $a$ ) and produces a corresponding change of density and of velocity inside the flow.

The flow is **steady** when referred to a coordinate system moving with velocity  $a$ , which brings the pressure pulse to rest<sup>15</sup>. This is the flow relative to an observer moving with the pressure pulse [52]. The fluid flows towards the observer with velocity  $a$ , pressure  $p_0$  and density  $\rho_0$  and is suddenly slowed down to velocity  $a - dv$  with corresponding pressure  $p_0 + dp$  and density  $\rho_0 + d\rho$  (figure 3.10) [52].

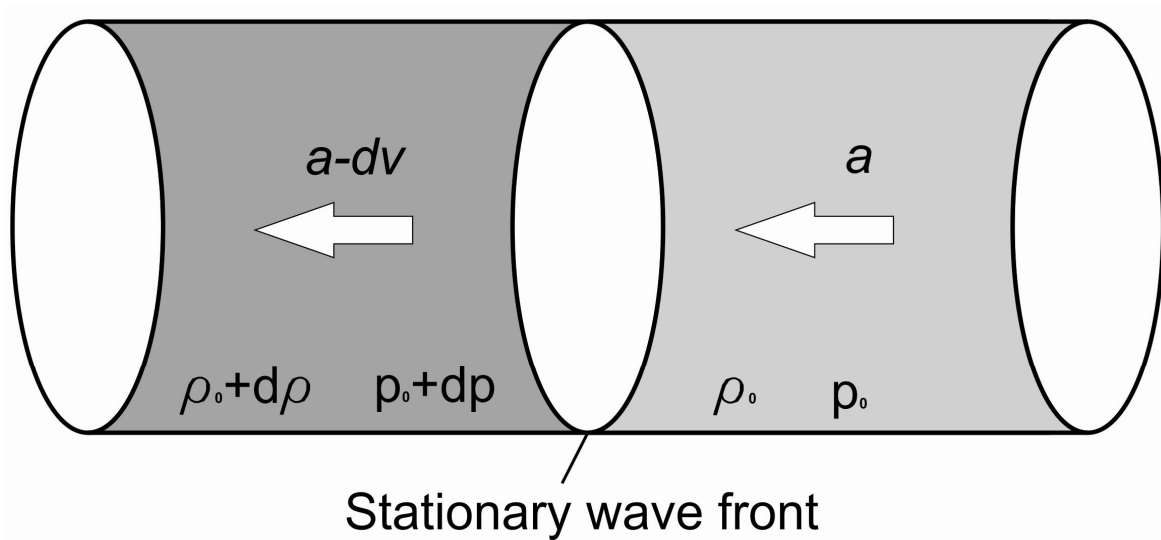


**Figure 3.10:** Flow relative to an observer moving with the pressure pulse.

According to the mass's continuity equation applied to the differential element of the flow (shell) containing the pressure wave, the mass entering the shell is equal the mass issuing from it<sup>16</sup>.

The mass entering the shell per unit of time:

$$m_{enter} = \rho \cdot a \cdot A$$

and corresponding mass leaving the shell:

$$m_{exit} = (\rho + d\rho) \cdot (a - dv) \cdot A$$

By equalizing both equations and after the elimination of the magnitudes of second order ( $dv \cdot dp$ ) the density increase is obtained:

$$d\rho = \rho \cdot \frac{dv}{a} \tag{3.2}$$

<sup>15</sup> If the wave front is accelerating, this procedure would not be correct.

<sup>16</sup> This is possible because the shell moves with velocity  $a$ , which makes the flow to be steady.

Without considering the friction of the fluid with the wall of the tube and applying the conservation of momentum to obtain the shell balance (rate of momentum in – rate of momentum out + sum of all forces = 0):

$$(\rho + d\rho) \cdot (a - dv)^2 \cdot A - \rho \cdot a^2 \cdot A = -A \cdot dp$$

after elimination of magnitudes of second order, the pressure increase is obtained:

$$dp = 2 \cdot \rho \cdot a \cdot dv - a^2 \cdot dp \tag{3.3}$$

Substituting the density increase (3.2) in equation (3.3):

$$dv = \frac{dp}{\rho \cdot a} \tag{3.4}$$

This equation proves that the flow velocity variation is proportional to the pressure variation of the fluid inside the tube. Since the pressure sensor measures the pressure variation of the fluid during the injection, equation 3.4 is numerically integrable (the assumption of  $v = 0$  at the start of the injection is necessary but also probable if the time between one injection and the following is enough for the wave to dissipate all its energy). The previous integration results in the velocity of the flow at the beginning of the tube.

$$v(t) = \frac{p(t)}{\rho \cdot a} \tag{3.5}$$

The combination of (3.1) and (3.5) returns the equation that produces the injection rate from the pressure signal:

$$\dot{m} = \frac{A}{a} \cdot p(t) \tag{3.6}$$

If the injected fuel mass per stroke is to be calculated, equation (3.6) has to be integrated between the start and end of the injection:

$$M_{stroke} = \frac{A}{a} \cdot \int_{inj.start}^{inj.end} p(t) \cdot dt \tag{3.7}$$

## 3.4 Design

### 3.4.1 Hydraulic Circuit

Some hardware left over from former experiments has been reused in the design of the new injection analyzer (figure 3.11 – 3.12). This part consists of a hydraulic circuit that can easily be adapted as the termination element of the hydraulic tube in the new instrument. Figure 3.13 shows the hydraulic schema of this element.

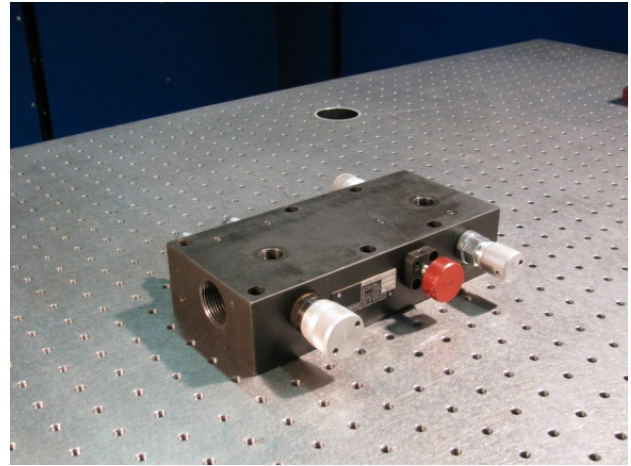
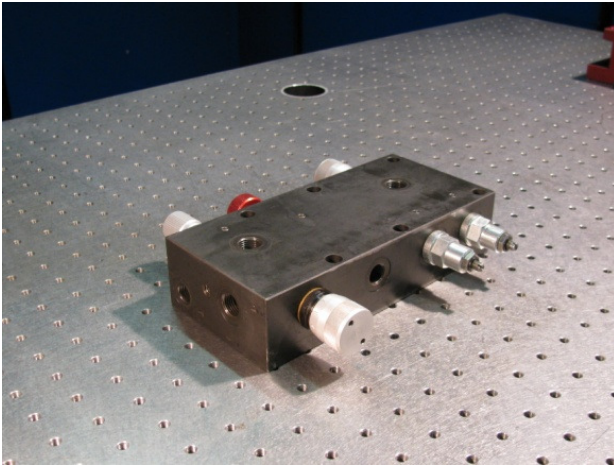
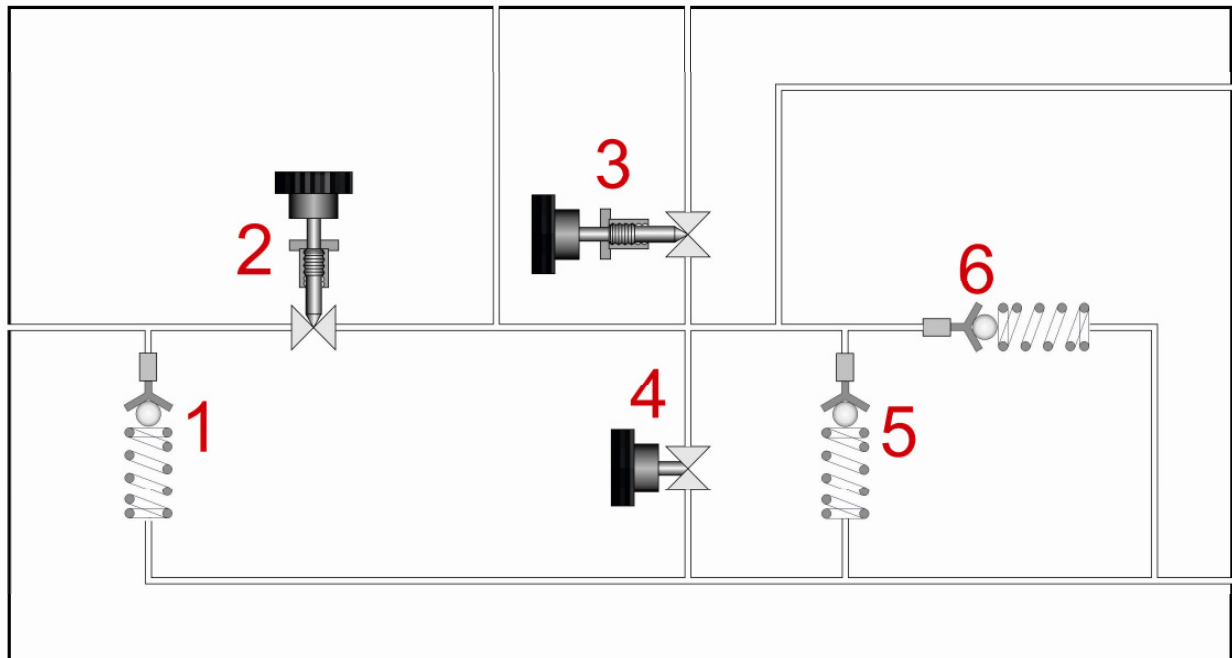


**Figure 3.11 – 3.12:** The leftover hardware from some former experiments for the injection analysis at the LAV.



**Hydraulic elements:**

- 1,5,6; Manually adjustable spring load valve
- 4; Dump valve
- 2,3; Needle valve

**Figure 3.13:** Hydraulic schema of the leftover hardware.

The elements numbered 1, 5 and 6 in figure 3.13 denote the three manually adjustable spring loaded pressure regulating valves. The spring load of each valve can be adjusted to guarantee a maximum tube pressure of 350 bar. The elements 2 and 3 are two needle valves with a range of adjustment that could vary the flow section diameter between 0 and 3 mm. Element number 4 is a valve used to dump the oil in the tube.

In order to reuse this hydraulic circuit as the termination element of the injector analyzer it must serve for different purposes:

- In order to prevent the reflected pressure waves to distort the pressure trace measured in front of the injector, the first requirement of this element is to attenuate the pressure waves oscillating between the ends of the tube between the injections. Even though the attenuation of the pressure wave is of course greatly assisted by the dampening effect of the surface friction on the inner wall of the measuring tube, the terminal section of the tube must be dimensioned to permit a complete smoothing of the pressure trace inside the tube before the next injection. To achieve this, the needle valve number 2 is used as a variable orifice. In this way the cross sectional area at the end of the measuring tube can be adjusted between 28.3 mm<sup>2</sup> and 0 mm<sup>2</sup> by manually adjusting the needle valve.
- The second requirement for the hydraulic circuit is to keep the pressure in the measuring tube to an adjustable constant value in order to reproduce internal combustion engine conditions. For this reason two possible configurations of the hydraulic circuit were taken into account.

The draft in figure 3.14 shows the first of the two considered setup configurations:

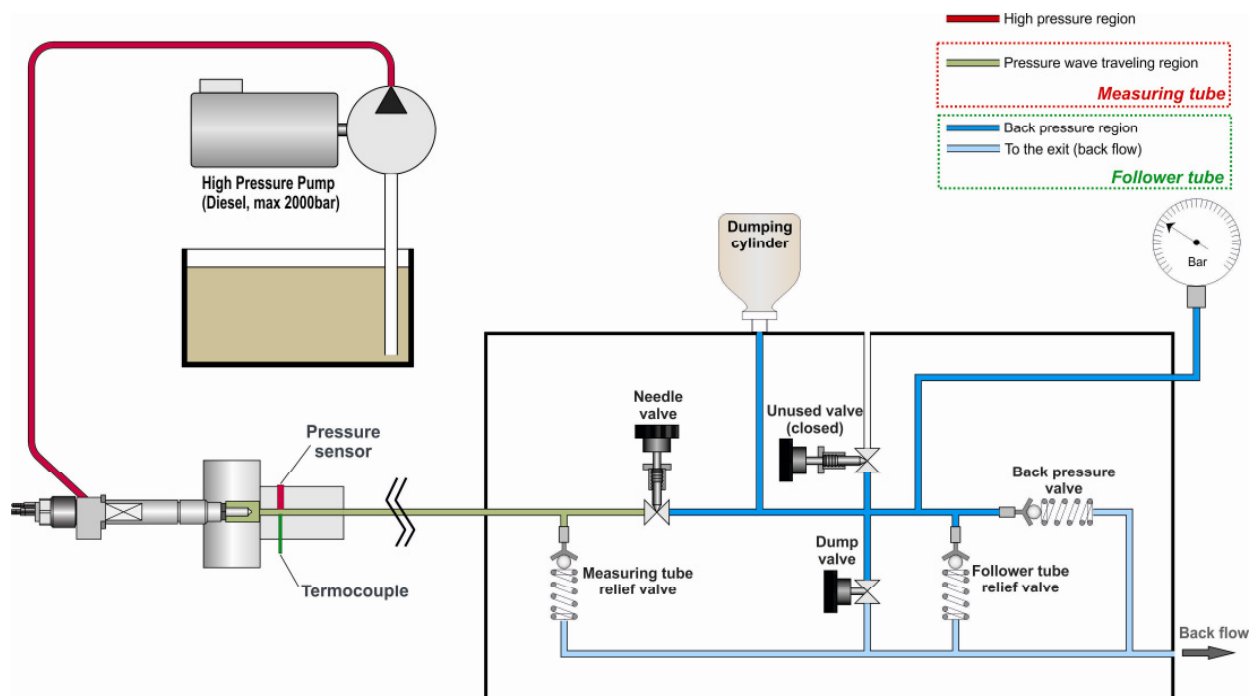


**Figure 3.14:** First possible configuration of the hydraulic circuit; different colours for the tubes are used to point out different hydraulic conditions.

In this first configuration a dumping cylinder containing nitrogen at 60 bar (separated from the fluid by a diaphragm) is used to damp the pressure oscillations in the region of the tube following the needle valve number 2 (follower tube). The pressure oscillations in this region could cause an erratic actuation of the pressure regulating valve number 6 (intermittent operation); the spring load of this valve is manually adjusted in order to obtain the desired value of pressure in the follower tube (back pressure).

Since a stable value of the back pressure is essential to obtain steady measurement signals, the measurement setup could also be modified. With an additional constant inflow into the back pressure region, a constant flow over the back pressure regulating valve could be achieved which would guarantee a stable operation of the valve and thus a stable back pressure value. The second possible configuration with the additional constant inflow is shown in figure 3.15:

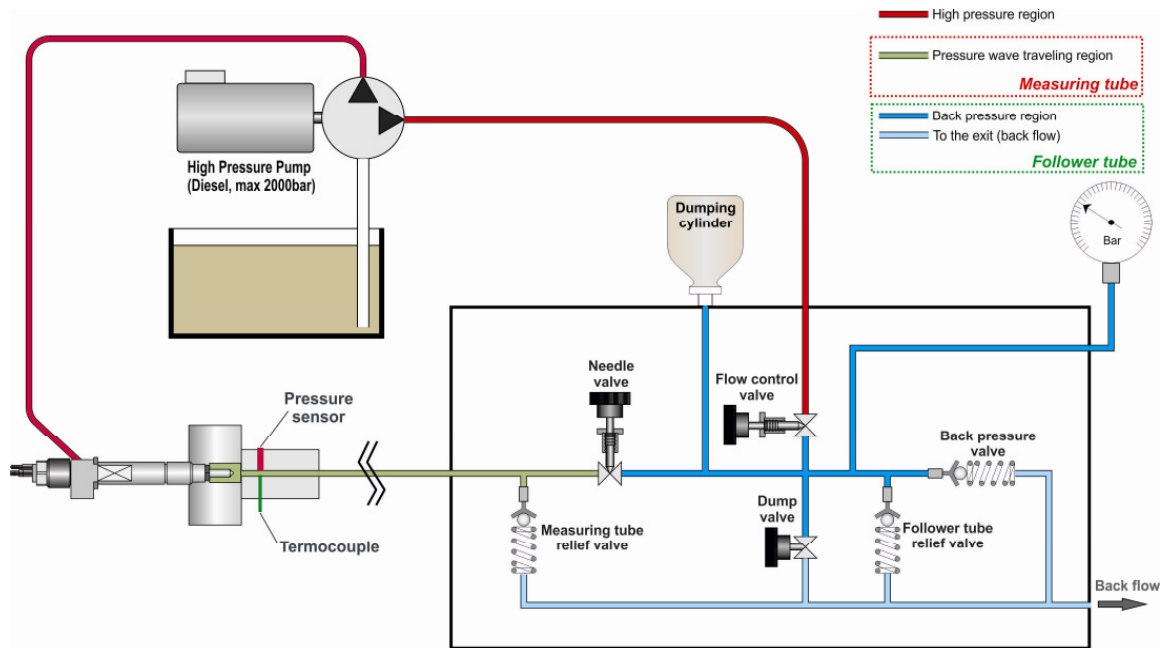


**Figure 3.15:** Second possible configuration for the hydraulic circuit.

In this configuration the high pressure pump used to supply the high pressure fuel to the injector is also used as a supply for the additional constant inflow which can be regulated by the needle valve number 3. The control of the flow is here necessary in order to reduce pressure to a more consonant value compared to the pressure reigning in this region of the analyzer (back pressure region, figure 3.15). By the simultaneous adjustment of the flow control valve and the back pressure valve, a stable pressure in the follower tube and therefore a constant regime of the analyzer back flow is achieved. However, since the stable equilibrium could be obtained with the first setup, this second alternative setup was actually never used for the measurements.

In both configurations the spring loaded valve number 2 (the measuring tube relief valve) and number 3 (the follower tube relief valve) are used to avoid any overpressure (>250 bar) in the measuring tube and the follower tube; the dump valve is only used to quickly discharge the pressurized fuel from the system if needed. In order to have the back pressure value under control during the experiment and to have a feedback during its adjustment, a pressure gauge is placed on one of the two free exits (figure 3.16 and 3.17).

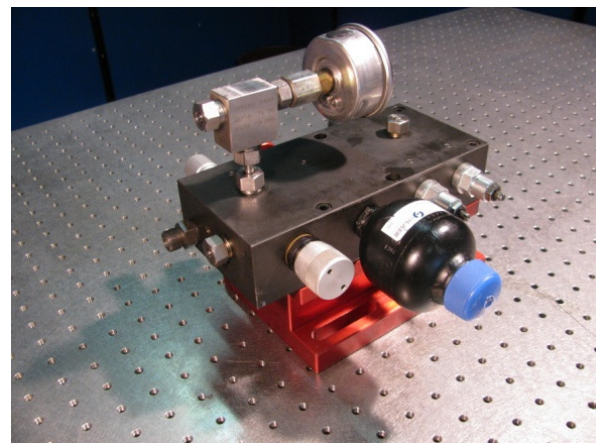
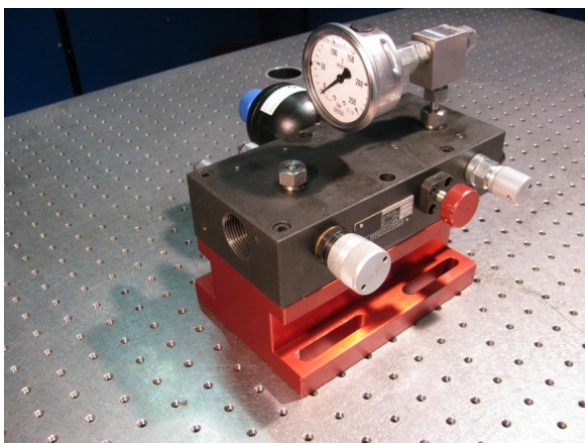


**Figure 3.16 – 3.17:** The hydraulic circuit fully equipped with the dumping cylinder and the additional pressure gauge.

## 3.4.2 Measuring Tube

The two important parameters of the measuring tube are the length and the bore diameter of the tube.

### *Length of the Measuring Tube*

In order to characterize injector performances, the original wave generated in the tube by the injection event, must be carefully analyzed over the whole injection duration and therefore possible pressure noise or the interference of reflected pressure waves during this time must be absolutely avoided. Considering the possibly lower value for the speed of sound in the testing tube (due to the possibly higher temperature and the lower pressure of the fuel in the measurement tube) and the maximum actuation time for the injector, the tube must be long enough to prevent the return of reflected wave to the pressure transducer during the injection event. Taking into account a safety factor of at least 30%<sup>17</sup> for the time between the end of the original pressure wave induced by the injection and the arrival of the reflected pressure wave, the minimum tube length can be calculated by the following formula:

$$T_{max} \cdot (1.30) = T_{2L} [s]; \quad T_{max} \cdot (1.30) = 2 \cdot \frac{L_{min}}{a} [s];$$

$$L_{min} = \frac{T_{max} \cdot a \cdot (1.30)}{2} [m] \tag{3.8}$$

where:

$T_{max}$  = maximum injection period [s]

$L$  = length of the tube [m]

$a$  = speed of sound in the testing fuel [ $\frac{m}{s}$ ]

$T_{2L} = \frac{2L}{a}$  = twice the transient time (corresponds to the time that the wave needs to travel twice through the tube) [s]

The measuring tube length calculated by means of equation (3.8) guarantees no interference between the original pressure wave and the first reflected wave. Another requirement to obtain reliable measurement signals is the total dissipation of the pressure waves inside the tube before starting the next injection so that a flat pressure signal is achieved in the tube.

Common-rail solenoid injectors greatly simplify the determination of the measuring tube length as the injection frequency is not imposed by the engine / conventional injection pump speed but is completely independent. As this test rig is designed to characterize the performance of solenoid injectors only, the injection frequency can be chosen in order to have a full damping of the pressure signal inside the measuring tube before the next injection.

If the real injection frequency needs to be reproduced in the injection test rig, then the maximum engine speed must be considered as well. As the MTU engine speed is limited to 1500 rpm an injection frequency of at least 12.5 Hz must be possible.

---

<sup>17</sup> A safety margin of at least 30% is necessary because of the difference between the electric actuation time of the injector and the real hydraulic injection duration.

Former experiences with Bosh tube type injection measuring systems had shown that a longer tube length is advantageous; with longer measuring tubes the time between reflections increases and the attenuation of the pressure waves within the tube between the injections is greatly enhanced by the dampening effect of the surface friction on the inner tube wall [49]. Considering that 4-5 reflected waves are usually enough to completely smooth a pressure signal<sup>18</sup> generated by an injection of 500 mm<sup>3</sup> in a 5 m long tube, two connected tubes of 5 meters length each were chosen in order to easily adjust the total tube length as desired.

With this measuring tube length it is easily possible to measure injections occurring with the real engine injection frequency for all engine operating conditions.

### *Bore of the Measuring Tube*

The inner diameter of the tube determines the amplitude of the pressure wave for a given injection rate. Therefore this parameter must be chosen in order to provide a reasonable measurement range for the differential pressure transducer. To ensure that the pressure in the injection rate meter is of a similar order to that in the engine, the opening pressure value of the back pressure valve had to be set equal to the pressure in the combustion chamber of the engine at the time of the injection.

A more accurate determination of the inner diameter of the measuring tube may offer the possibility to adjust the pressure wave amplitude to fit the pressure difference between cylinder pressure at the start and the end of the injection event; but this is difficult / impossible to achieve for all engine conditions!

Indicating with:

- $A_{tube}$  = Area of the tube section [mm<sup>2</sup>]
- $\rho$  = Density of fuel [kg/m<sup>3</sup>]
- $a$  = Speed of sound in the fuel [m/s]
- $\Delta t$  = Injection duration [ms]
- $\Delta p_{max}$  = Maximum pressure change during injection [bar]
- $q_{max}$  = Maximum injection rate [mm<sup>3</sup>/ms]
- $Q$  = Maximum injected quantity [mm<sup>3</sup>]

The inner tube bore is calculated by means of the following equation:

$$A_{tube} = \frac{\rho \cdot a \cdot q_{max}}{10^5 \cdot \Delta p_{max}} [mm^2] \quad (3.9)$$

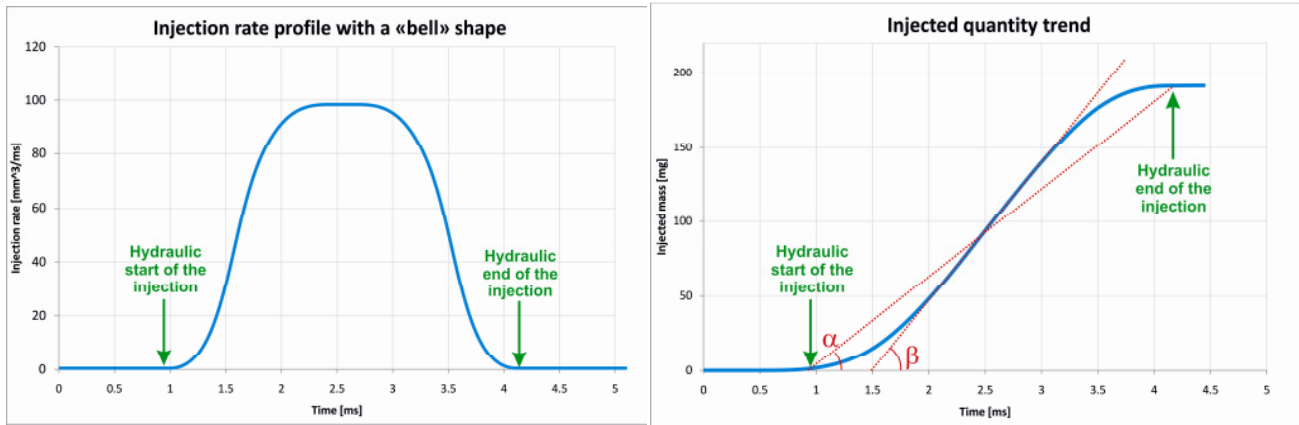
where:

$$q_{max} = 1.5 \cdot \frac{Q}{\Delta t} \left[ \frac{mm^3}{ms} \right]$$

---

<sup>18</sup> The dampening is also influenced by the needle valve adjustment

As the real maximum value of the injection rate ( $q_{max}$ ) is unknown, an approximation is done using a value 1.5 times larger than the maximum injected fuel quantity divided by the electrical injection duration. This approximation is correct if injection rate profile has a shape of a perfect “bell” (figure 3.18). In this case the first derivative of the injection rate has a similar shape to the one in figure 3.19 and  $\beta$  ( $\beta = q_{max}$ ) is equal to  $\alpha$  ( $\alpha = Q/\Delta t$ ) multiplied by 1.5.



**Figures 3.18 – 3.19:** An injection rate profile characterized by a “perfect bell” shape and its first derivative.

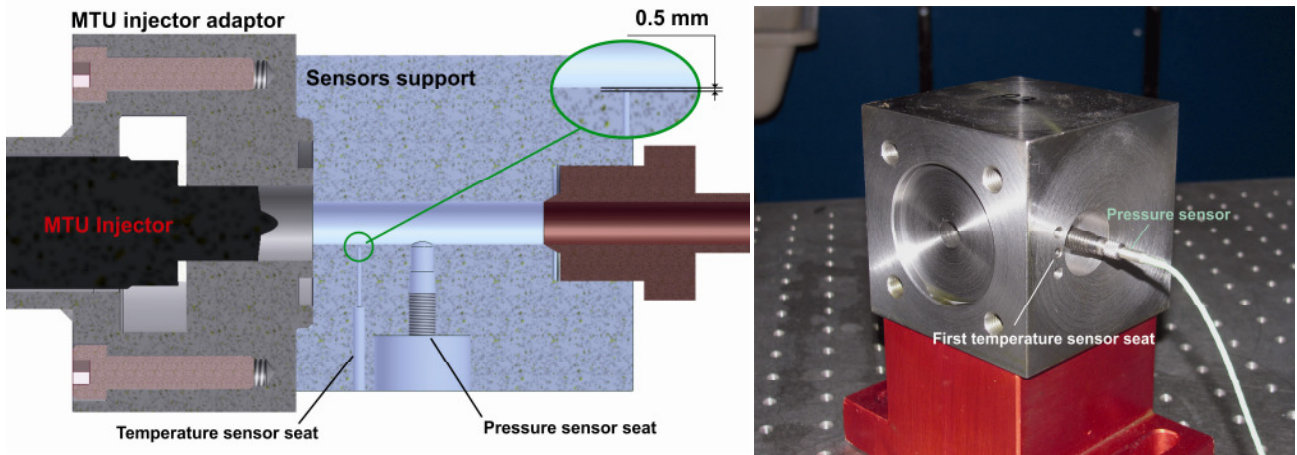
With an measurement range of 0-200 bar of the dynamic pressure sensor and in order to have a back pressure inside the measuring tube in the same order as the pressure inside the cylinder of the real engine during the injection period, a back pressure around 50 bar with a maximum peak of 100 bar was chosen for the calculation of the measuring tube inner bore diameter. Using the difference of these values as a  $\Delta p_{max}$ , and assuming a value of 5 ms for the maximum electrical injection time ( $\Delta t$ ) and of 1000 mm<sup>3</sup> for the maximum injected quantity ( $Q$ ), equation (3.9) returns an inner tube diameter of around 10 mm.

### 3.4.3 Sensors Support and Injector Adaptors

As mentioned in the beginning of this chapter, the aim of this project was to design and realize a device that could be used to fully characterize the MTU engine injector. However, in order to obtain a flexible measuring device that could be easily readapted for other injector types, the sensors support and the injector adaptor were designed as separate elements.

The sensor support was designed in a way that the internal contours are as smooth as possible. This helps reduce the unwanted noise in the pressure signal caused by pressure wave reflections on all irregular contour elements. With this in mind the first version of the sensor support had the temperature sensor element not directly in the fuel but separated from it by 0.5 mm of steel (figures 2.20 – 3.21).

However, a comparison between the temperature of the back flow (out of the injection analyzer) and the fuel temperature measured directly in the sensor support showed great discrepancies, due to the high temperature gradients in the fuel inside the sensor support the effective fuel temperature cannot be measured without a direct contact between fuel and temperature sensor. In the second version of the sensor support the temperature sensor was moved opposite the pressure sensor with a direct contact between the fuel and the sensor. (figure 3.22 – 3.23). The thermocouple was moved to the opposite side of the pressure sensor to minimize the effects of the pressure wave reflections caused by the thermocouple on the measured pressure signal.



Figures 3.20 – 3.21: First version of the sensor support.

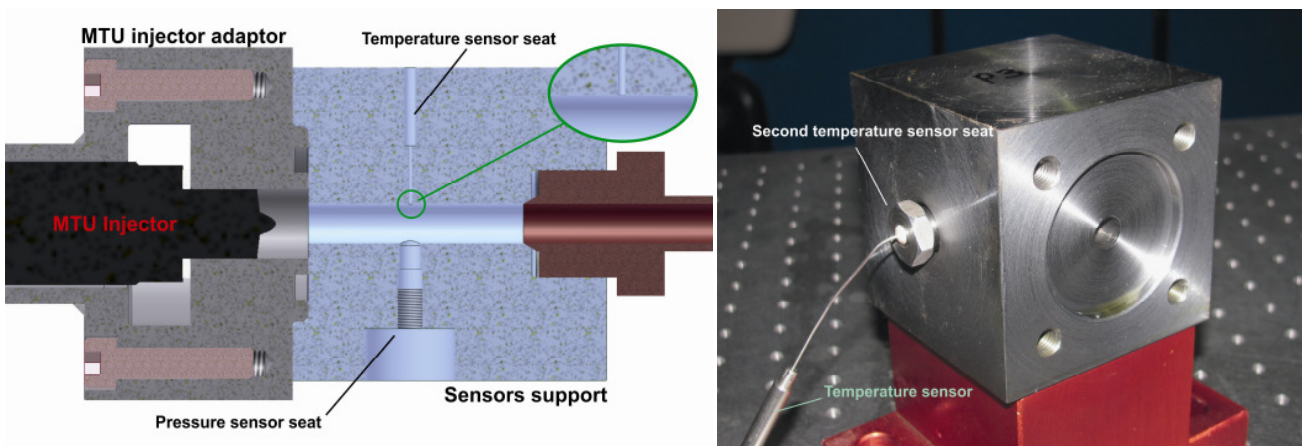


Figure 3.22 – 3.23: Revision of the sensor support. With this new element there is contact between the thermocouple and the fuel.

In both 3D sensor support sketches of figure 3.20 and 3.22, there is a brown element on the right side of the sensor support (on the opposite site of the injector position). This element is used to connect the sensors support to the measuring tube. It is a Nova Swiss high pressure cone to cone connection and allows the smoothest possible transition of the internal surfaces between the parts. The same type of connection is also used to join the end of the measuring tube with the follower tube.

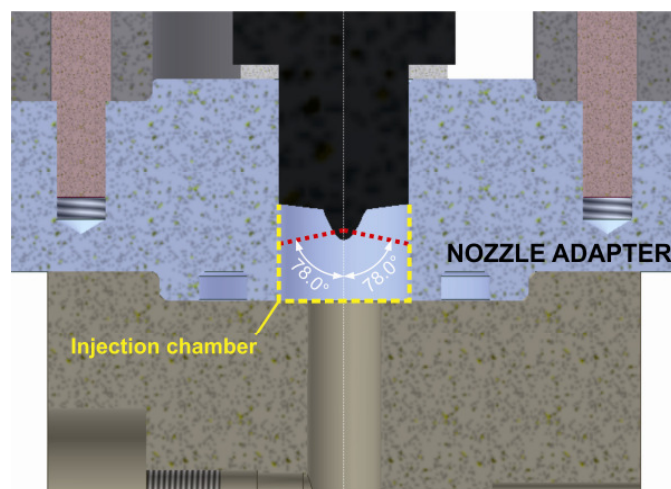


Figure 3.24: MTU injector spray cone angle

A constant value of the internal flow diameter (from the injector nozzle tip to the end of the measuring tube) is desirable but cannot be achieved in case of the MTU injector because of its large injector nozzle tip diameter ( $\varnothing$  17.8 mm). During the design of the injection analyzer system the influence of an injection chamber (figure 3.24) with a different diameter compared to the measuring tube internal diameter (where the pressure wave signal is measured) was not known. To allow for a wide range of configurations w.r.t “injection chamber” shapes/sizes and varying distances between the injector nozzle tip and the pressure sensor seat, a separate *nozzle adapter* part that could easily be modified was realized (figure 3.24).

The first nozzle adapter was designed under consideration of the cone angle of the injected fuel sprays (red lines in figure 3.24) and the values quoted in the literature for the distance between injector tip and pressure sensor [53] (see figure 3.24). For the sealing between the sensor support and the nozzle adaptor an o-ring with an external diameter of 40 mm and a thickness of 5 mm is used, while a copper sealing disk (thickness 2 mm) is used to seal the injector from the environment.

The first version of the injector support was designed in the form of two main assemblies (lower tube and higher tube), each consisting of three elements (two flanges and the tube) that are welded together. However, in the final version each assembly was realized in one piece (without welding).

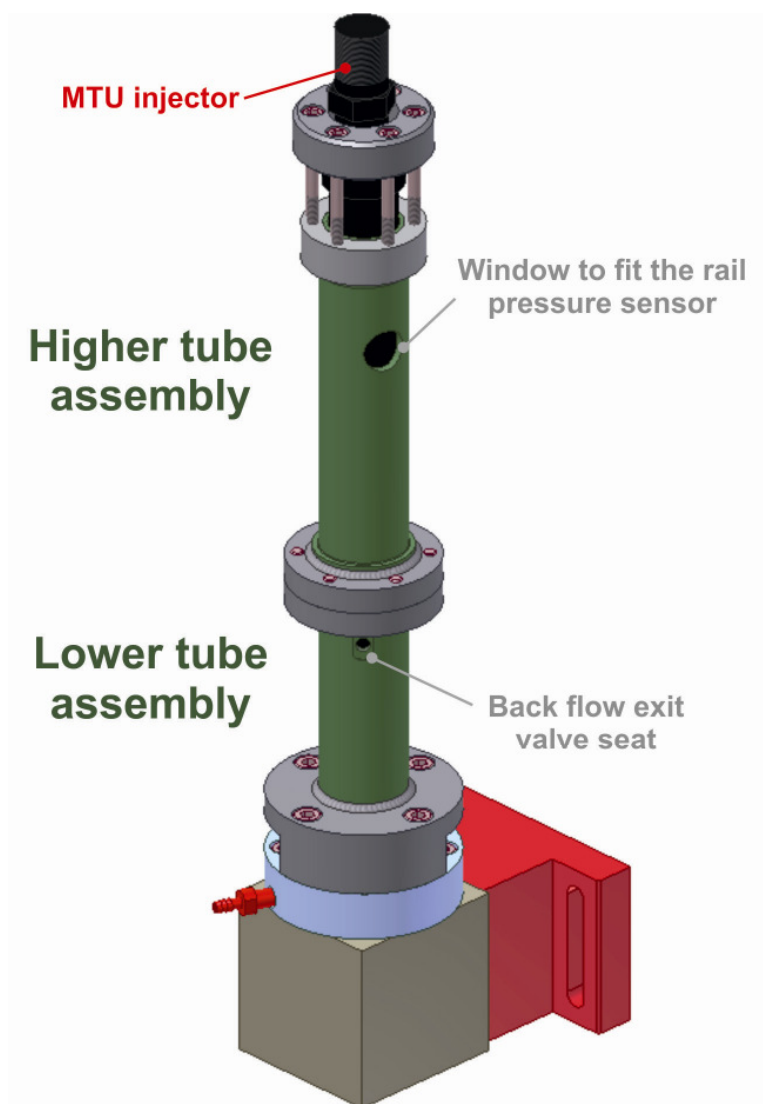
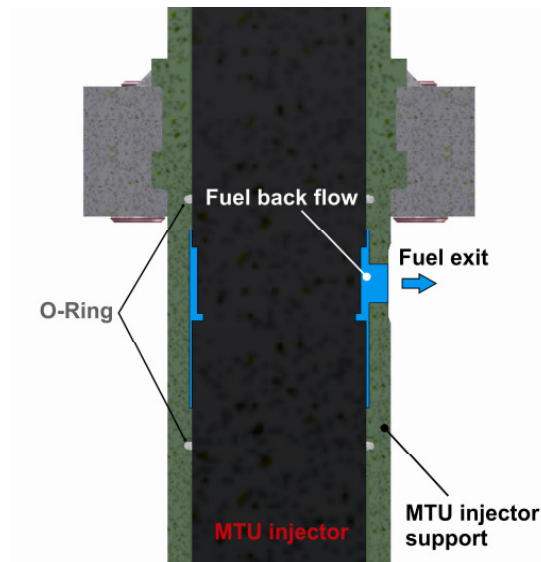


Figure 3.25: MTU injector adaptor.

The first priority of the injector support is of course the ability to clamp down the injector firmly and to position it in the centre of the measuring device, but for the MTU injector it also needs to catch the fuel flowing back from the injector (due to the injection actuation and unavoidable leakages). The back flow of the injector exits the lower part of the injector body from a small hole; in order to collect this fuel a small sac volume on the inside of the injector support was realized. The sac volume is sealed from the environment with o-rings above and below; a small hole in the tube assembly is used to collect the back flow (figure 3.25 and 3.26).



**Figure 3.26:** Section view of the back flow region of the MTU injector adaptor.

The MTU injector is a solenoid injector with an integrated accumulator rail in the upper part of its body. To be able to measure the fuel pressure directly in the rail, a window on the upper limit of the support (on the higher tube assembly) was realized to be able to mount the Kistler rail pressure sensor collar also used on the engine. Figure 3.27 shows a section of the modified MTU cylinder head and the collar used to fix the rail pressure sensor on the injector.

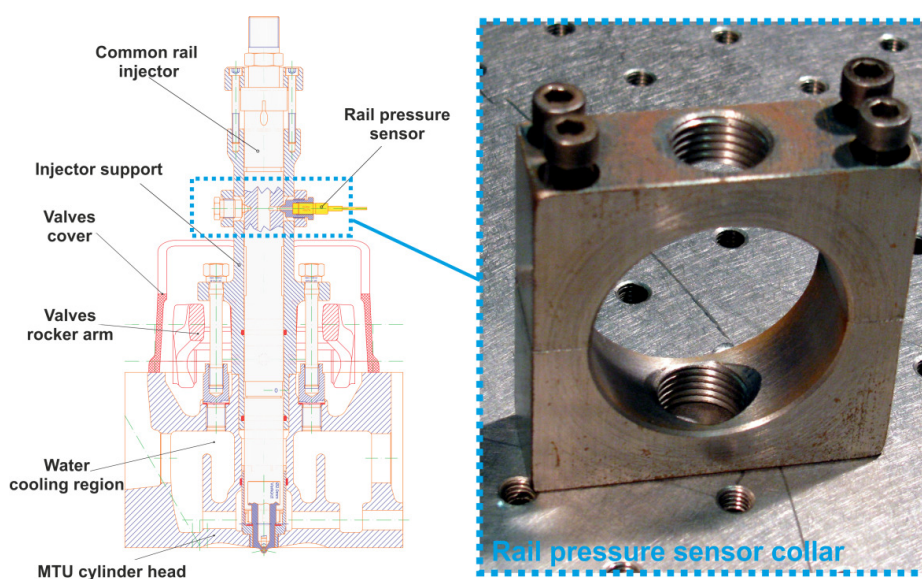


**Figure 3.27:** A section of the MTU cylinder head after the modification to fit the new injector and the collar used to support the rail pressure sensor.

During the design of the injector support for the MTU injector a new project in collaboration with the Paul Scherrer Institute<sup>19</sup> required the characterization of another type of a common-rail injector<sup>20</sup>. This project mainly concentrates on determining the predictive capability of a phenomenological combustion and emission model<sup>21</sup> when the inlet charge thermodynamic state changes significantly. This is done by using in-cylinder and exhaust gas measurements from a Wärtsilä 6L20 common-rail, 4-stroke, medium speed marine diesel engine (table 3.2 and figure 3.28) to calibrate the combustion and emission models. These models are used within a 1-D simulation program to simulate the performance and emissions from the engine when equipped with advanced inlet valve closure (Miller valve timing) and two-stage turbocharging. The simulation results are then compared with experimental results obtained from the same engine with identical hardware changes.

DATA	UNITS	VALUE
<b>Bore:</b>	<i>mm</i>	<b>200</b>
<b>Stroke:</b>	<i>mm</i>	<b>280</b>
<b>Number of Cylinder:</b>		<b>6</b>
<b>Compression Ratio:</b>		<b>16</b>
<b>Nominal Speed:</b>	<i>rpm</i>	<b>1000</b>
<b>Rated Power:</b>	<i>kW</i>	<b>1080</b>



**Table 3.2 / Figure 3.28:** Important data of the Wärtsilä 6L20 engine test bench / View of the Wärtsilä test engine.

Comparable values for the maximum injected fuel quantity and for the maximum actuation time of the new injector allowed the use of all already designed and manufactured injection analyzer parts except for the nozzle adapter and the injector support itself that always need to be adapted to the individual injector.

Contrarily to the MTU injector, the L'Orange injector has the high pressure fuel supply inlet placed on the side of the injector body (and not on the top), exactly on the opposite side of the back flow exit (figure 3.29).

<sup>19</sup> The PSI is the largest research centre for natural and engineering sciences within Switzerland.

<sup>20</sup> The injector is manufactured by the German company l'Orange.

<sup>21</sup> The model has the capability to capture changes in combustion caused by altering the injection timing, duration and pressure, by the introduction of multiple injections, as well as changes in the chemical and thermodynamic state of the inlet charge.

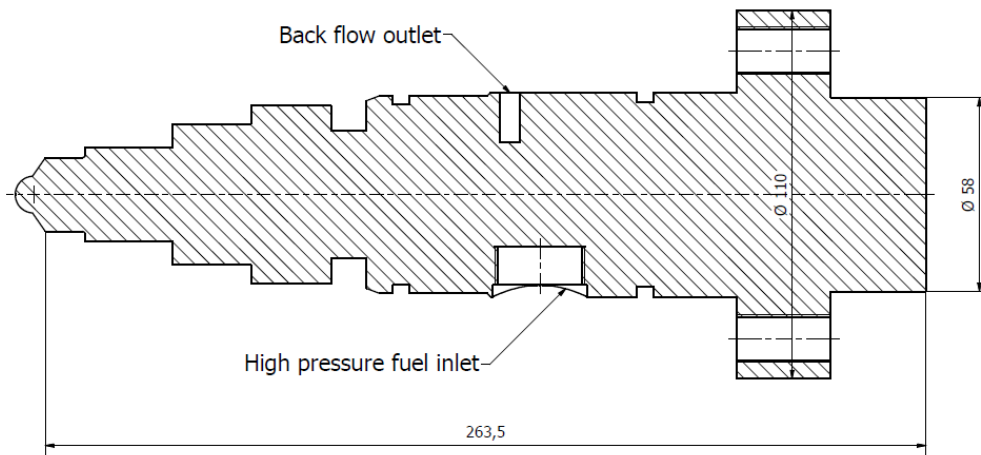


**Figure 3.29:** L'Orange common-rail injector used on the Wärtsilä engine.

The necessity to have a rigid high pressure fuel connection on the body of the injector together with the impossibility to modify the injector to create a direct connection between the back flow outlet and the fuel drain pipe created the need to design a “freely movable” rigid element that would assist the high pressure injector fuel inlet and low pressure back flow outlet. A new nozzle adapter had to be realized because of the different size of the injector nozzle tip ( $\text{Ø}22 \text{ mm}$ ). The nozzle adapter is mounted on the same sensor support that is used with the MTU injector. The L'Orange injector is clamped directly on the new nozzle adapter by two long stud bolts without the need for additional parts (like the tube assemblies for the MTU injector). With this solution it was possible to design the “freely movable” element that served both as a fuel back flow collector and a housing for the rigid high pressure inlet connector (see figure 3.30 and 3.31).

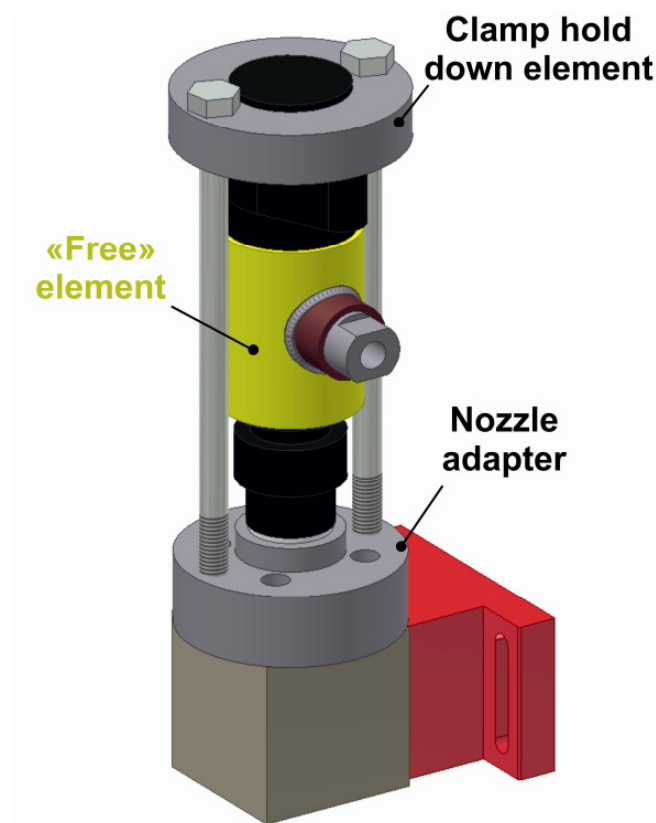


**Figure 3.30:** L'Orange injector adaptor.

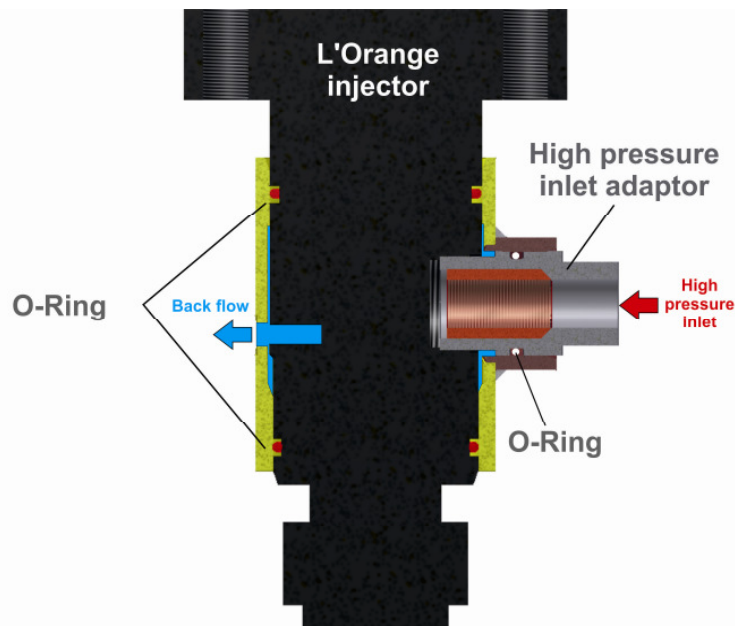


**Figure 3.31:** Section view of the element created to assist inlet and outlet of the fuel to L'Orange injector.

### 3.4.4 Bleeding Valve

The first measurements with the injection analyzer were strongly affected by noise since it was not possible to attain a smooth, constant pressure in the tube between the injections. Different solutions were taken into consideration: Even if some improvement resulted by the replacement of the connection between the two parts of the measuring tube that created an unwanted pressure wave reflection, nothing could explain the erratic noise in the pressure signal. A plausible explanation for this noise was found in the possible presence of air somewhere in the hydraulic circuit of the injection analyzer. In order to improve the pressure signal, a bleeder valve (figure 3.32) was designed and incorporated in the nozzle adapter design to remove the air from the hydraulic circuit (figure 3.33). Again much importance was given to the smoothness of shapes of these elements to reduce unwanted reflections of the pressure waves.

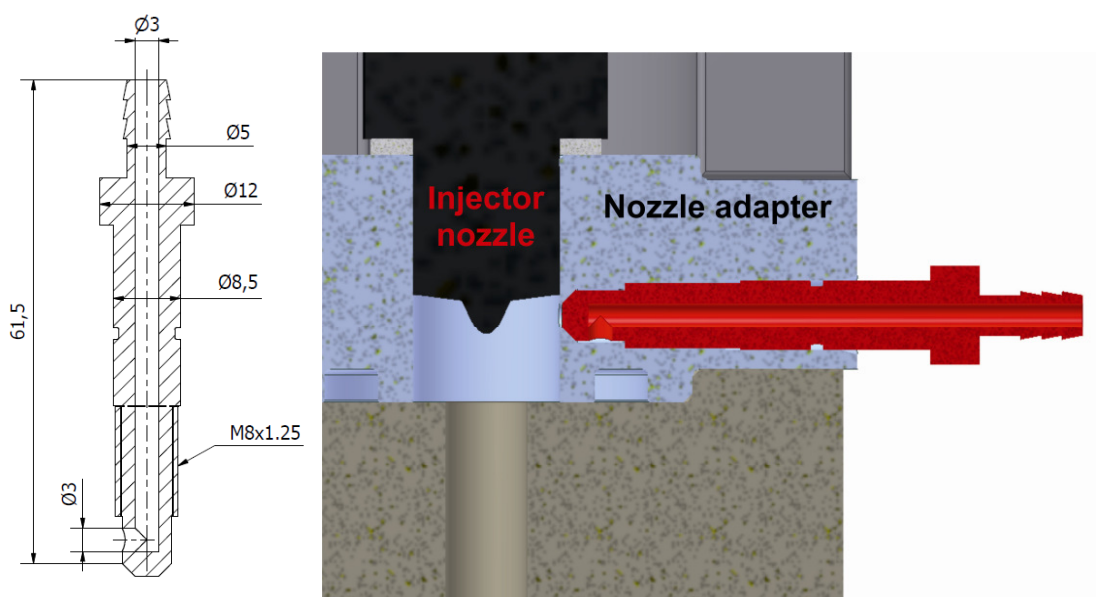


**Figure 3.32 – 3.33:** Bleeder valve mechanical drawing section and 3D section of the bleeder valve mounted on the nozzle adaptor.

The use of the bleeder valve resulted in less noise generation and in a more constant value of the pressure signal between two injections.

## 3.5 Setup

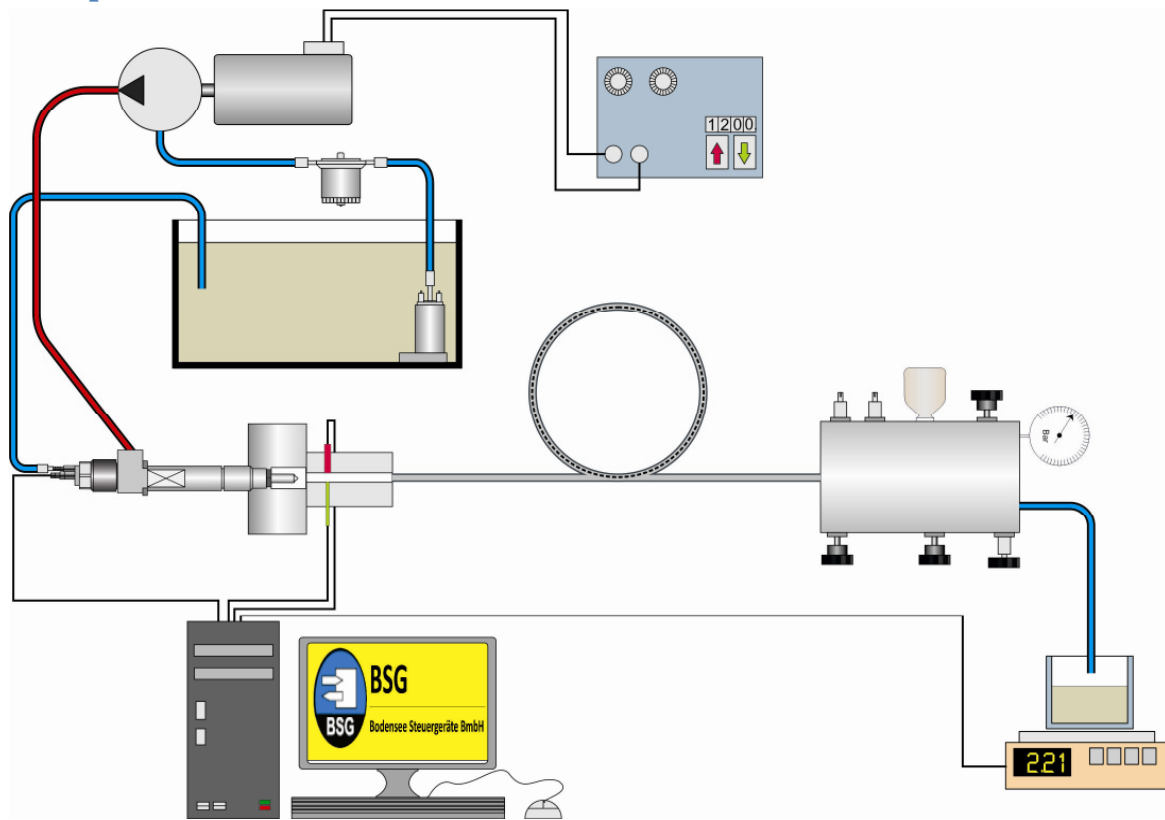


Figure 3.34: Complete setup of the injection analyzer system.

The fuel used in the test rig is the Shell V-Oil 1404, a specially developed calibration fluid for diesel injectors. This fuel is a carefully controlled blend of distilled components meeting narrow viscosity and density ranges to allow accurate calibration and testing of diesel injection systems, it meets the requirement of ISO 4113 and SAE 967. A prerequisite to be able to use this as test fuel was to know the speed of sound in the fuel as a function of fuel pressure and temperature in a range between 20 to 100 bar and 15 to 100 °C respectively. This knowledge is necessary to evaluate the injection rate equations with the actual speed of sound values for all different conditions that arise during the experiments. For the Shell V-Oil 1404 the values are well-known (table 3.3).

Speed of sound values for Shell V-Oil 1404 [m/s]										
		Fuel temperature [°C]								
		-20	0	20	40	60	80	100	120	140
Fuel pressure [bar]	0	1536,95	1454,37	1374,6	1297,64	1223,48	1152,13	1083,59	1017,85	954,92
	50	1558,68	1477,19	1398,72	1323,3	1250,95	1181,72	1115,6	1052,57	992,52
	100	1580,12	1499,67	1422,42	1348,45	1277,8	1210,54	1146,67	1086,13	1028,69
	150	1601,29	1521,82	1445,73	1373,13	1304,08	1238,66	1176,89	1118,66	1063,61
	200	1622,21	1543,66	1468,67	1397,36	1329,82	1266,15	1206,35	1150,28	1097,44
	250	1642,88	1565,21	1491,27	1421,18	1355,07	1293,05	1235,12	1181,07	1130,3
300	1663,32	1586,49	1513,53	1444,61	1379,86	1319,41	1263,24	1211,12	1162,29	

Table 3.3: Speed of sound values for the Shell V-Oil 1404.

The fuel is contained in a 50 litres tank, it is supplied to the high pressure pump by an submersible electric low pressure feeding pump through filters where the temperature of the fuel is monitored as well (3.36). The fuel pressure supplied by the feeding pump can be regulated by a manually adjustable valve (3.37).



*Figure 3.35 – 3.36: The fuel filters with the thermocouple and the three way valve to adjust fuel low pressure.*

The high pressure pump used in the test rig is developed and manufactured by the LAV itself (figure 3.37 and 3.38). This patented high pressure piston pump design (max 2000 bar) controls the fuel pressure resp. the fuel flow by throttling the (low pressure) intake flow which results in a very high pump efficiency (no need for a pressure regulating valve on the high pressure side). The desired pressure value is set on an external control device that monitors the actual fuel pressure with a pressure transducer and controls the throttling valve of the pump to adjust the pressure to the selected value.

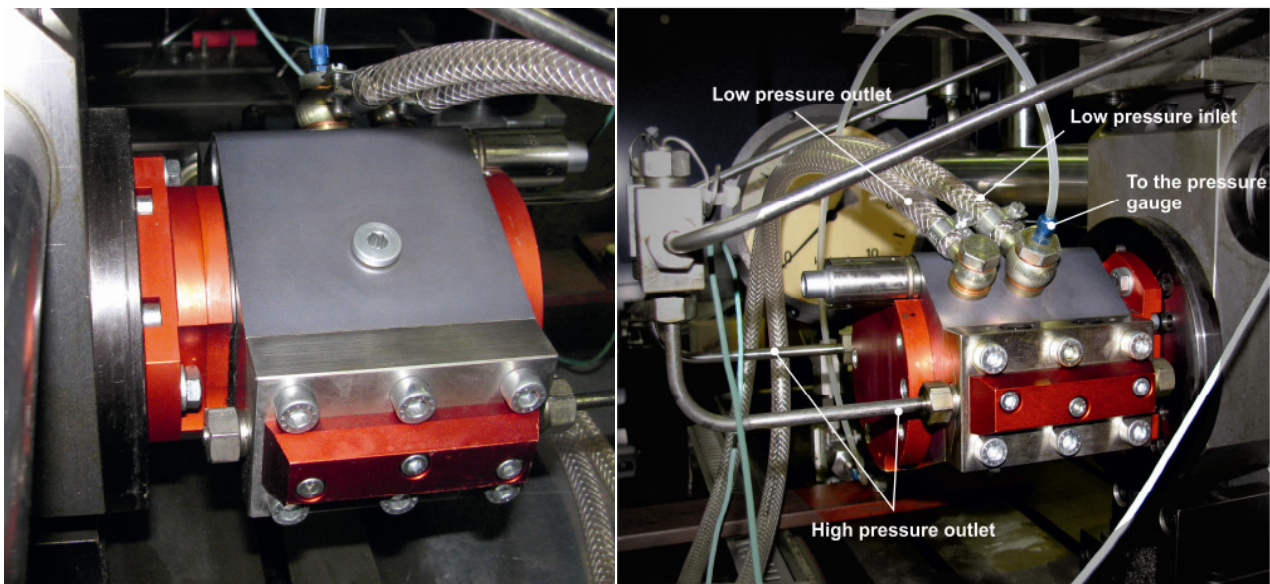


*Figure 3.37 – 3.38: High pressure pump patented at the LAV.*

In order to maintain a steady fuel pressure value the high pressure pump needs to be driven with 600 rpm at least. The pump is directly coupled to a variable speed Landert electric motor of 15 kW. A pump speed of 1600 rpm is chosen for all the experiments.

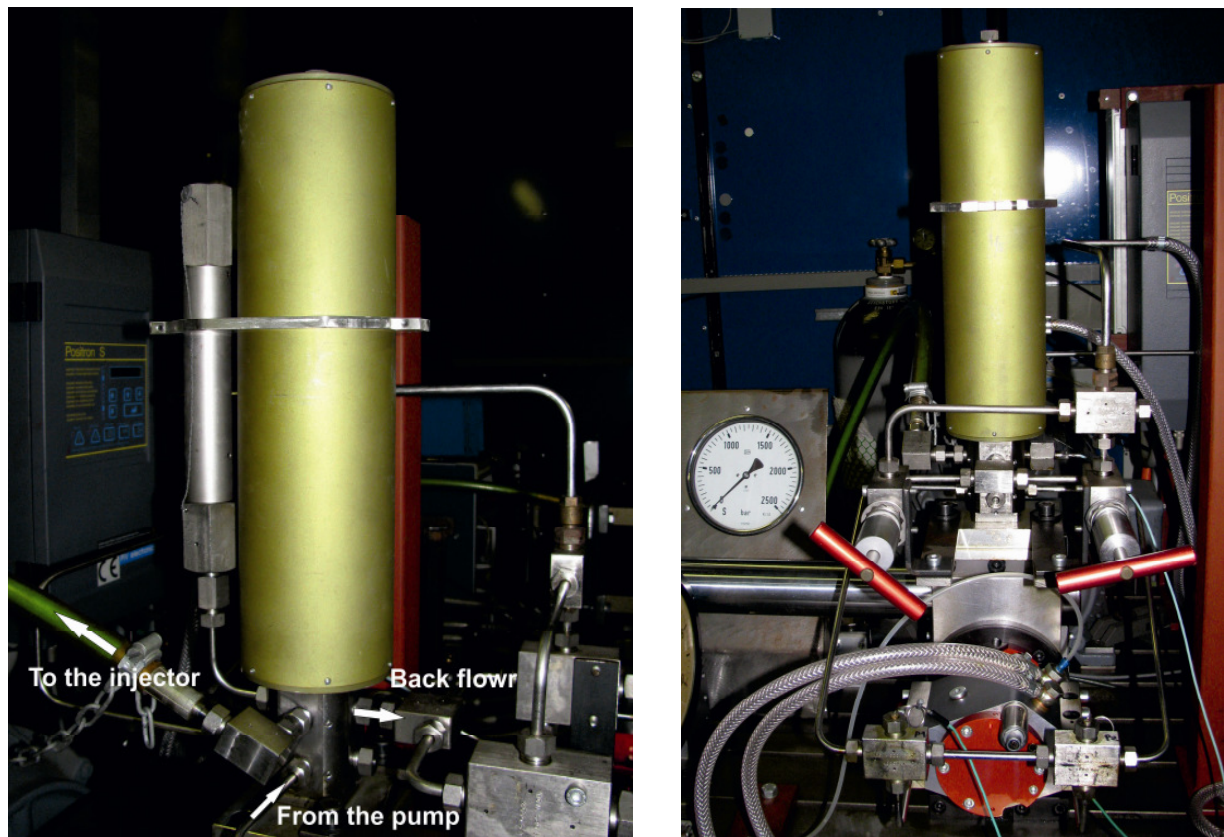


*Figure 3.39 – 3.40: Rail and safety valve of the high pressure pump.*

In order to compare the injected fuel quantity calculated from the pressure wave with another measurement method of the injected fuel quantity, a Mettler Toledo PG-S laboratory balance is used to collect the fuel flowing out of the injector analyzer system. This balance is placed at the end of the follower tube to measure the totally injected fuel mass.

To measure the pressure wave travelling back and forth the hydraulic tube a Kistler quartz pressure sensor (type 6001) for measuring dynamic and quasistatic pressures up to 250 bar at temperatures up to 350°C is used (figure 3.41). The corresponding fuel temperature is measured with a classical type K thermocouple (figure 3.42).

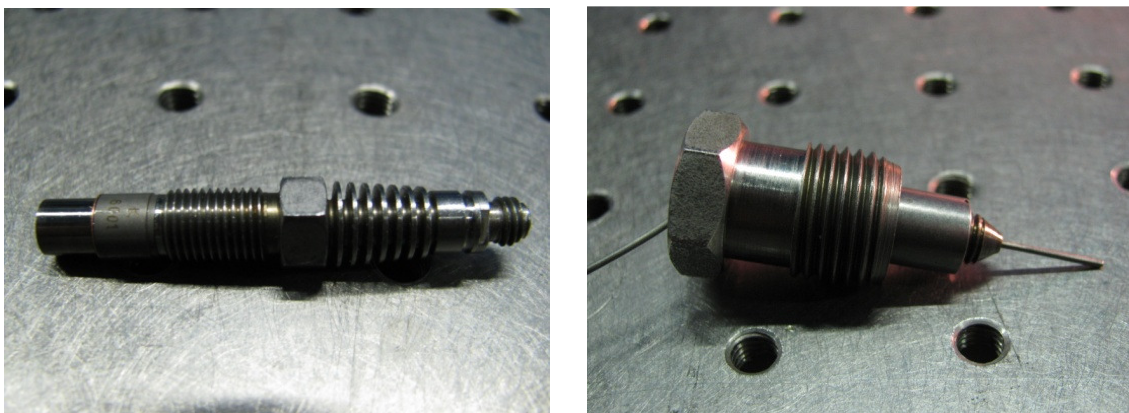


*Figure 3.41 – 3.42: Kistler polystable quartz pressure sensor type 6001 with its connecting nipple and thermocouple type K with its adaptor.*

The electrical current flowing to the injector is recorded with a Yokogawa current probe, type 701932 (max. 30 A) with a bandwidth of 100 MHz.

An Elsys TPCX Transient Data Recorder Module using the Elsys TransAS Version 2.6 software is used for the data acquisition. The TPCX Transient Recorder Modules are fast, high-precision and high-resolution data recorder modules with 8 Single Ended or 4 Differential analog channels, maximum concurrent sample rate per channel 50 MS/s with an onboard memory size of 512 MByte. This system together with the TransAS Version 2.6 software made the data acquisition very fast, easy and reliable.

Using the same PC utilized to control the TransAS software and by means of the BSG application program the injector timing is controlled. The BSG application program allows the user to define the injector solenoid energizing data (current, voltage and duration of the boost and hold phase) and to fully control the timing and the duration of each injection (up to 3 injection events with a combined maximum duration of 5 ms per cycle).

### 3.6 Signal Processing

An important part of the project work is the processing of the acquired pressure signals to calculate the injection rates and the injected fuel mass. Considering the necessity to process enormous amounts of data for each measurement an algorithm that could automatically process all the data sets is absolutely necessary. The algorithm developed in the project is written in Matlab.

As already mentioned, a PC using TransAS data recording modules is used for the data acquisition. The TransAs software can save the acquired data in different file formats (large text files or smaller binary files). Since a Matlab algorithm to convert the binary tpc files in mat<sup>22</sup> files do already exist, all the experimental data are saved in this format. The existing algorithm was improved to get more information from the acquired channels (like channel names) and to better adapt it to the new purpose.

In order to fully characterize the injector performance the following signals were acquired during the experiments:

- ✓ Dynamic pressure in the measuring tube
- ✓ Fuel temperature in the measuring tube
- ✓ Rail pressure
- ✓ Injector current

The aim of the Matlab algorithm (software program) is to allow the selection of all the acquired tpc (transPC data) and txt (Mettler Toledo balance data) data files of a measurement set and then to calculate and return the following results:

---

<sup>22</sup> Binary data container format used by Matlab; may include arrays, variables, functions, and other types of data.

- Injection rate graphical profile for each single injection
- Hydraulic start, end and duration of the injection
- Delays between hydraulic start and end of the injection and injection trigger signal
- Injected mass per shot and standard deviation (calculated from the injection rate profile)
- Injected mass mean (obtained from the balance analysis)
- Difference between measured injected mass and weighed injected mass.

### 3.6.1 Obtaining the Hydraulic Start and End of the Injection

The first goal of processing procedure is to find a way how to automatically identify the **start** and the **end** of the injection from the dynamic pressure signal. By manually observing the traces (figure 3.43) it's easy to identify the start and the end of the injection, but for an algorithm it's difficult to identify those values precisely and reliably for all injection and measurement conditions. For short injection durations a timing error in the order of 1  $\mu$ s could already result in an injected mass error in the order of 20 %! Considering the big amounts of data it is absolutely necessary to have a reliable automatic algorithm.

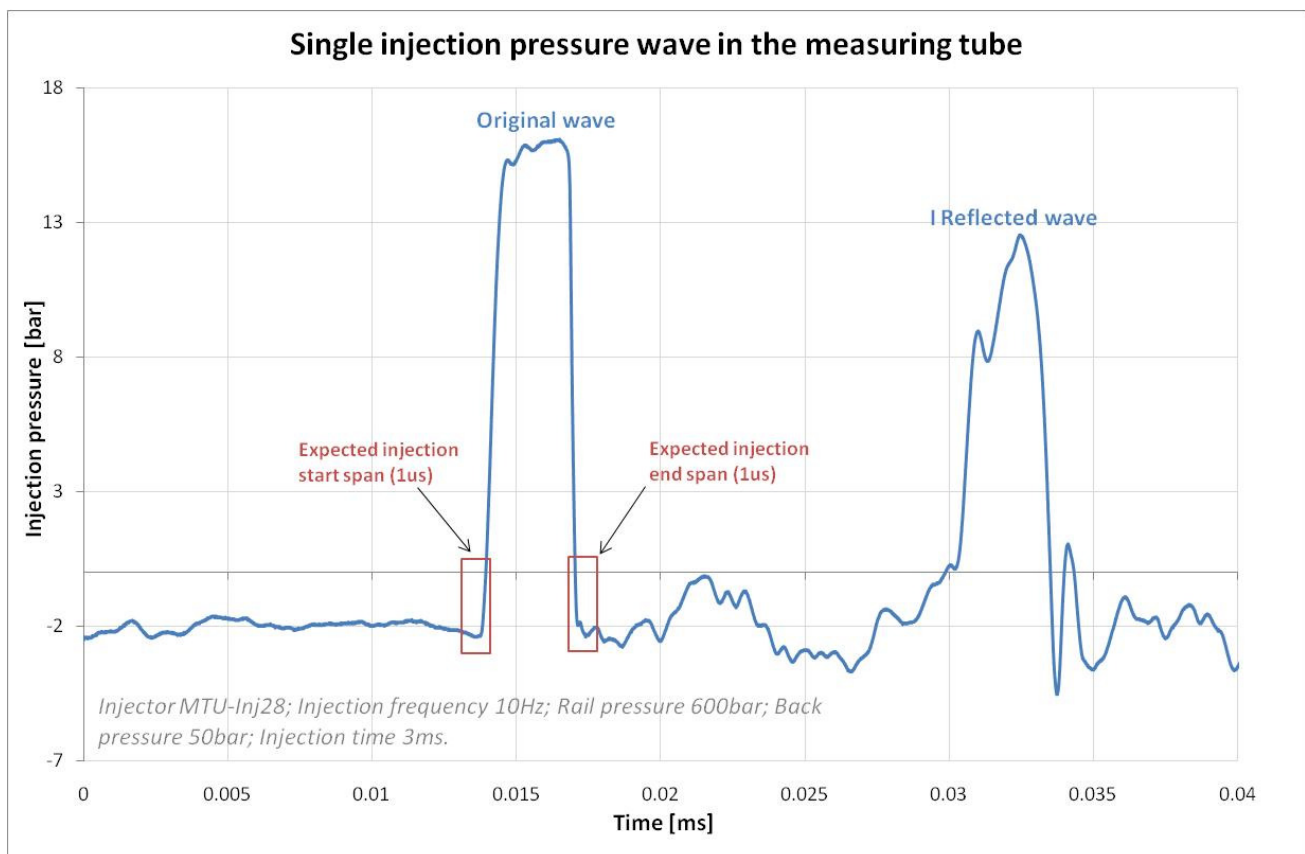


**Figure 3.43:** Possible ranges for the hydraulic start and end of the injection in the acquired pressure trace.

In order to remove the noise from the acquired pressure signal (that could affect the detected start and end of the injection), the Matlab “loess” function is used as a filter (The “loess” Matlab filter is a local regression method that uses weighted linear least squares and a 2<sup>nd</sup> degree polynomial model).

In order to detect the timing of the hydraulic start and end of the injection the first derivative of the filtered pressure signal (figure 3.44) is analyzed and (in spite of the noisy appearance) the injection extremity events are easily defined as the last zero of the function before the first large positive peak (→ representing the rise

of the original pressure wave) and, respectively, the first zero of the function after the first large negative peak ( $\rightarrow$  representing the fall of the original pressure wave).

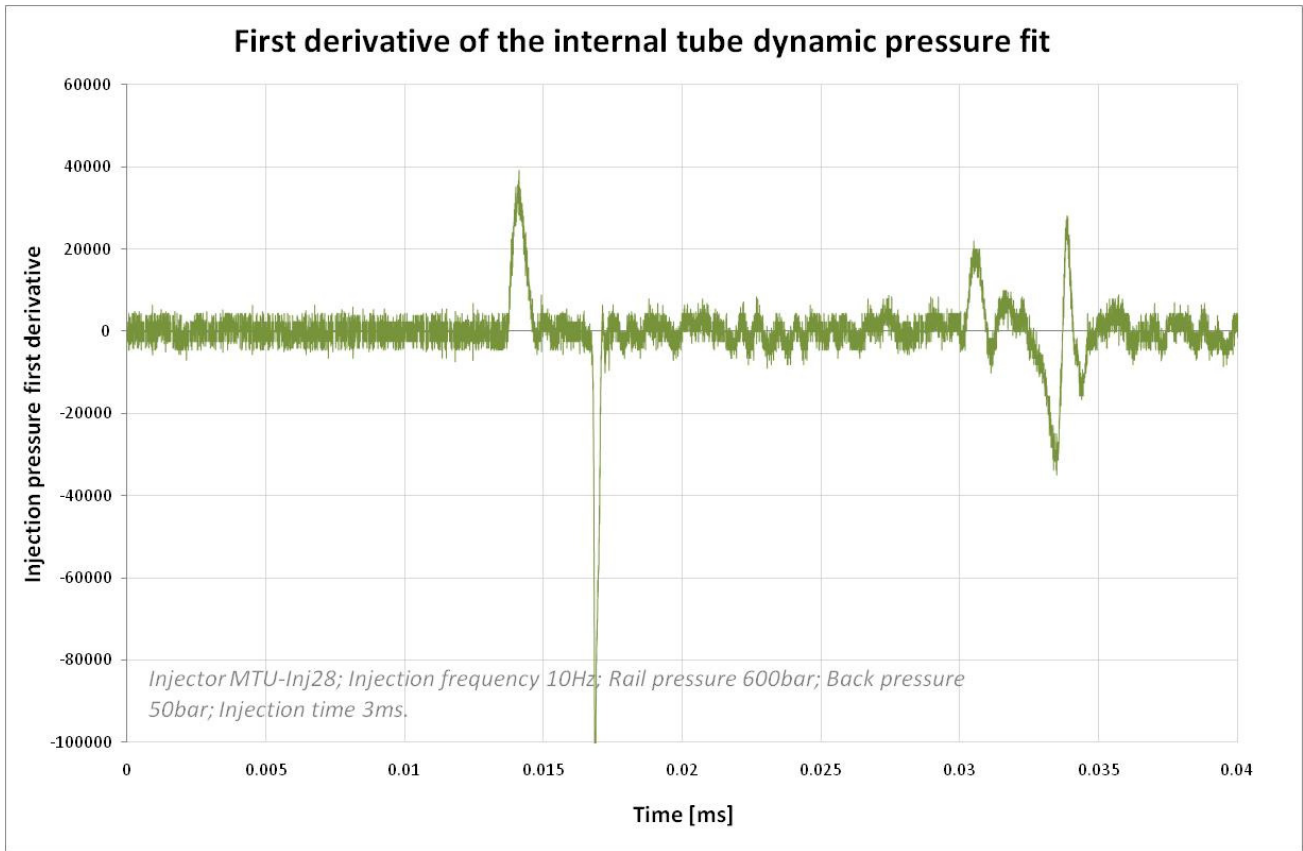


**Figure 3.44:** First derivative of the acquired dynamic pressure trace.

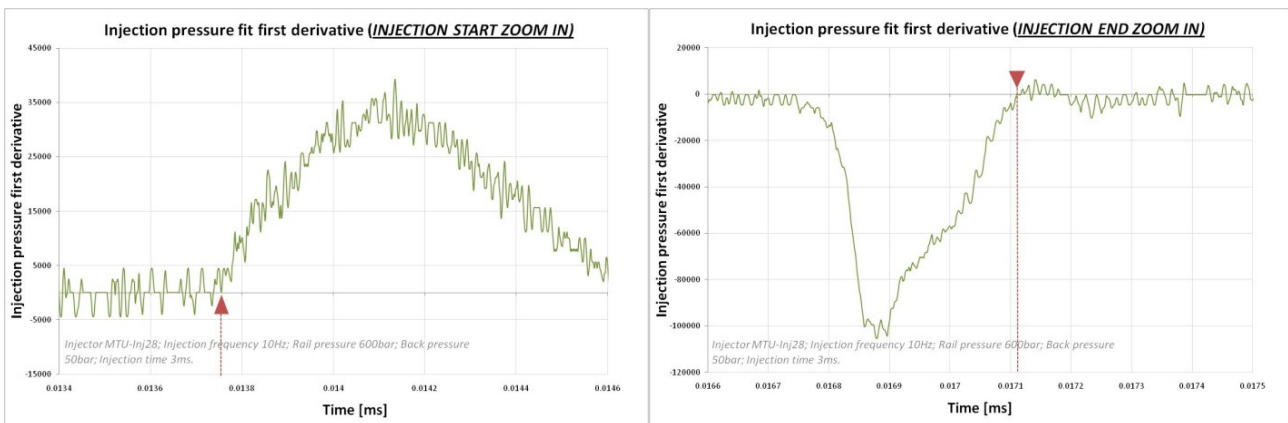


**Figure 3.45 – 3.46:** Two enlarged sections of the graph in figure 3.44 (the first derivative of the dynamic pressure trace) around the injection extremity events.

The zoomed in pressure trace sections of the first derivative of the dynamic pressure show where the algorithm places the start of injection (figure 3.45) and the end of injection (figure 3.46) events.

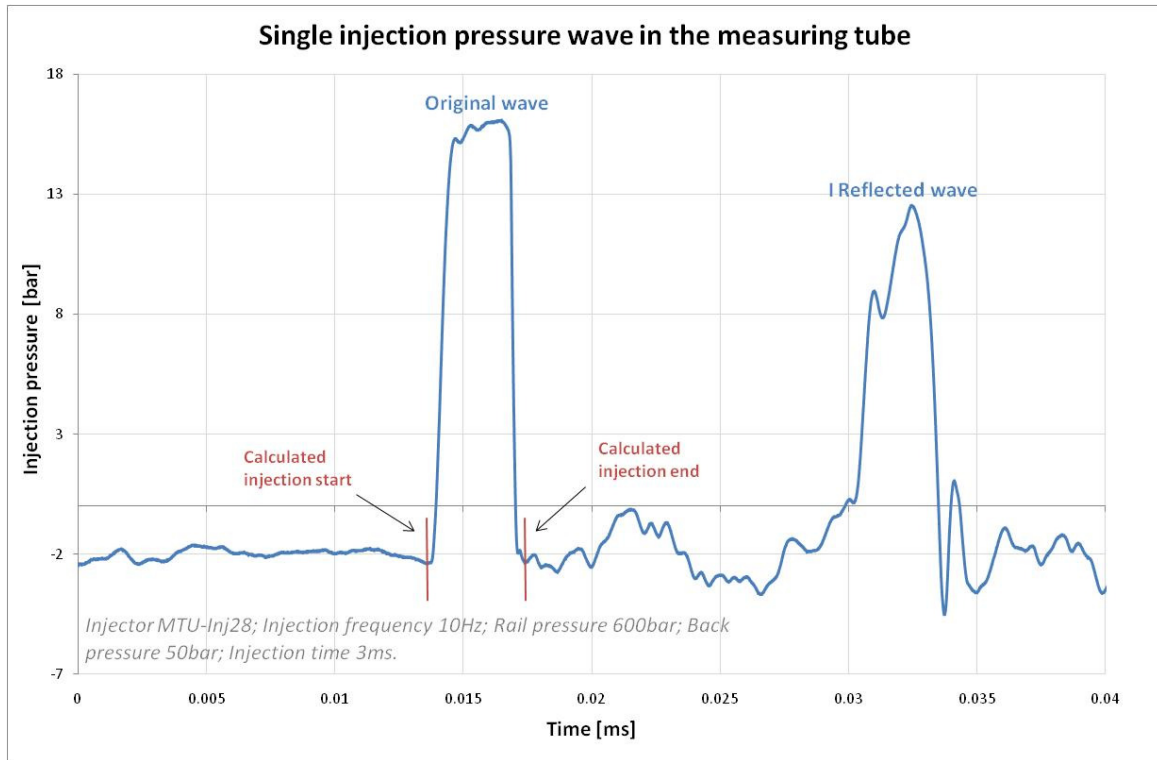


Figure 3.47: Time values of hydraulic injection start and end identified by the developed algorithm.

Since the two injection events are now defined, the hydraulic start and end delays can be easily calculated from the corresponding injection trigger signal as illustrated in figure 3.48.

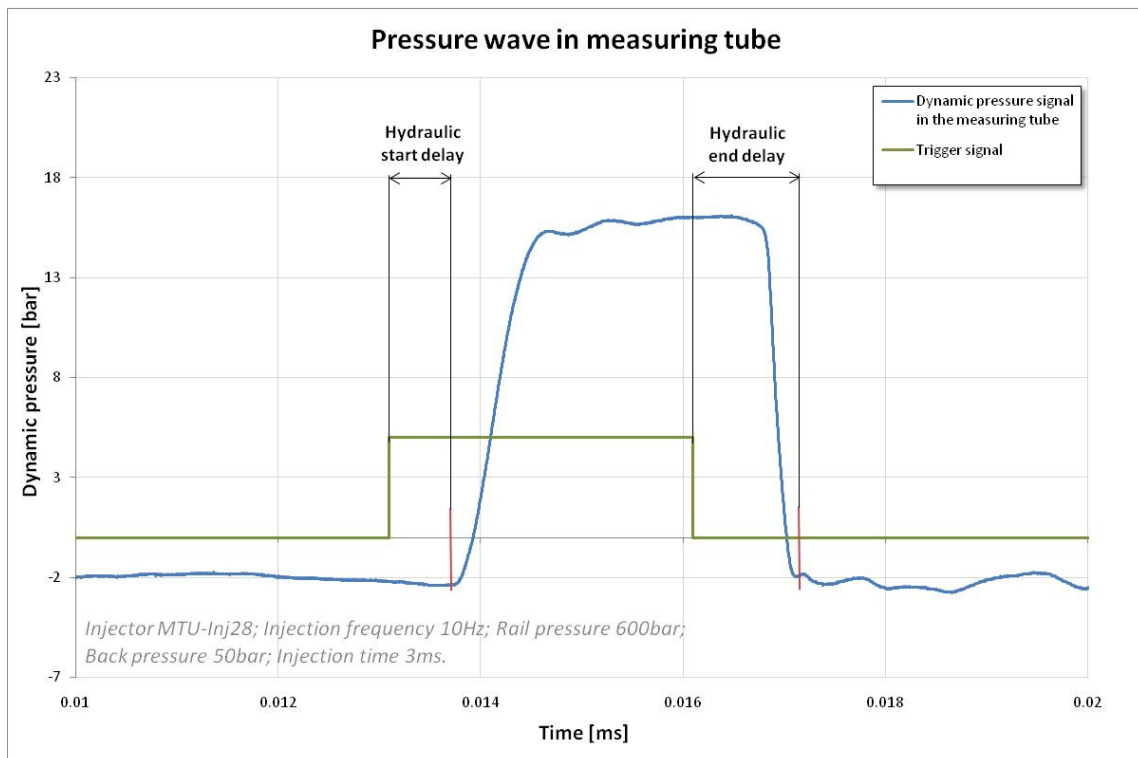
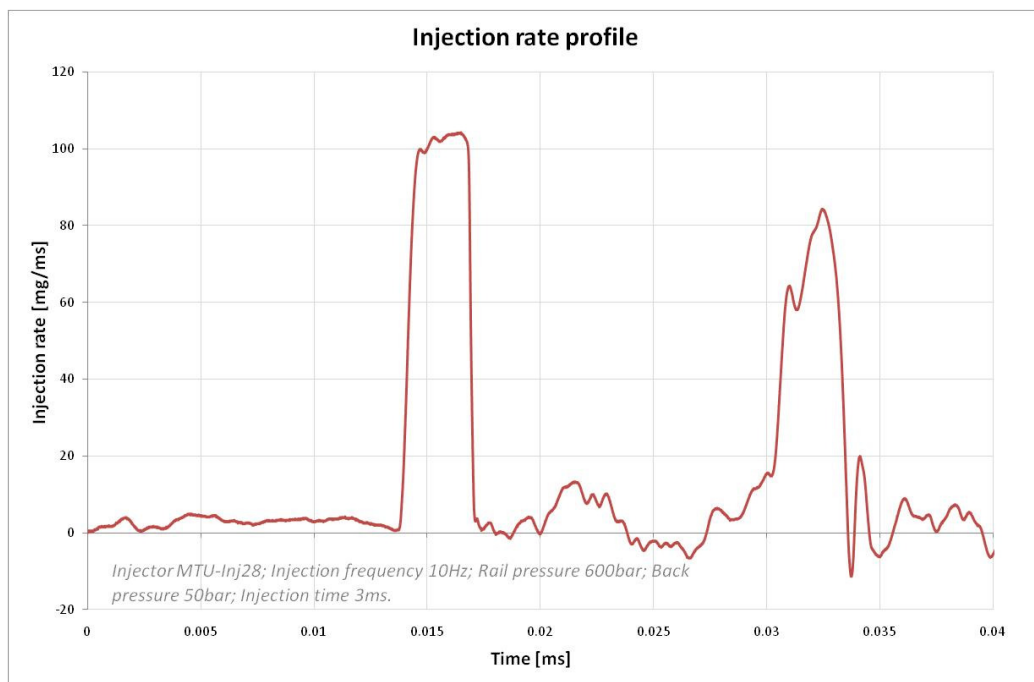


Figure 3.48: Delays between the electronic injection signal and the hydraulic injection events.

### 3.6.2 Obtaining the Injection Rate and the Injected Fuel Mass from the Pressure Trace

The injection rate profile is calculated from the dynamic pressure value (appropriately scaled in order to move trace base line to zero) by using equation 3.5.

Since the cross section of the tube is fixed and the injection duration is very short (the fuel temperature and thus the speed of sound are approximately constant) the injection rate can be simply derived from the pressure trace by multiplying it with a constant factor. (However, between different injections the fuel temperature and thus the factor  $A_{tube}/a$  changes and must be recalculated for each injection event). Due to the constant factor between the dynamic pressure signal and the injection rate the start and end of the injection can be detected directly from the pressure trace instead of from the injection rate profile (figure 3.49).



**Figure 3.49:** Injection rate profile obtained from the dynamic pressure trace by using equation 3.6.

By using the time extremities of the dynamic pressure signal, the injected amount of fuel mass during each single injection event is calculated with the equation (3.6).

### 3.6.3 Obtaining the Injected Fuel Mass from the Back Flow of the System

A second way how to calculate the injected fuel mass is possible by weighing the fuel back flow with a Mettler Toledo precision balance placed at the outflow of the following tube in the injection analyzer system. However, considering the precision limit of the balance in the order of 1 mg, the length (volume) of the tube and the use of a damping system in the follower tube it is impossible to measure the fuel mass of a single injection stroke, but it is possible to measure the mean value over a couple of injection strokes.

The procedure “to weight the injected mass” is based on finding a steady state of the entire measurement (injections with a constant frequency) and especially of the fuel back flow. The balance is attached to a PC in order to acquire the weighing data (with a constant sampling frequency), and as soon as the steady state is reached, the weighing data are saved into a text file during the time of observation.

Since the injection frequency, the observation time and the data sampling frequency (8 Hz) are known parameters the algorithm can calculate the average injected fuel mass per stroke with the following equation:

$$m_{wg} = \frac{[m(T_{obs} \cdot Fr_{data}) - m(1)]}{T \cdot Fr}$$

where:

$m_{wg}$  is the weighed injected mass mean

$T_{obs}$  is the minimum time of observation

$Fr$  is the injection frequency

$Fr_{data}$  is the data sampling frequency of the balance

$m(T_{obs} \cdot Fr_{data})$  is the collected fuel mass weighed by the balance at the end of the observation period (last value transferred to the weighing file in the observation time interval),  $m(1)$  the corresponding collected fuel mass at the beginning of the observation period respectively.

The average of the injected fuel mass measured with the balance is used to assess the accuracy of the newly developed instrument resp. the data processing algorithm by comparing this average injected fuel mass with the value obtained from the injection rate analysis in the algorithm. The difference between these values is called “possible committed error” and is included in the algorithm’s results.

### 3.6.4 Obtaining the Data Processed

In order to map the injection performance over the whole operating range a number of measuring points, marked out by engine speed (injection frequency), rail pressure and electrical injection time are defined. The measurement points used to characterize the MTU injector are shown in table 3.4. For each of these points, the acquired measurement signals and the weighed mass are saved in a tpc and txt data file, both named with the same series of alphanumeric characters that contains the information about injector type and of the measurement point parameters (injection frequency, rail pressure and electrical injection time). In order to get good statistical data a suitable number of injection events (at least 50 injections) are stored in the tpc data file for every measurement point. The result for each measurement point is then obtained by calculating the average values (including statistical data) from all the stored single injection results for this measurement point.

<b>MTU injection measuring points</b>							
		<b>Injection time</b>					
		<i>5 ms</i>	<i>4 ms</i>	<i>3 ms</i>	<i>2 ms</i>	<i>1.5 ms</i>	<i>1 ms</i>
<b>Rail pressure</b>	<i>1600 bar</i>						
	<i>1500 bar</i>						
	<i>1400 bar</i>						
	<i>1300 bar</i>						
	<i>1200 bar</i>						
	<i>1100 bar</i>						
	<i>1000 bar</i>						
	<i>900 bar</i>						
	<i>800 bar</i>						
	<i>700 bar</i>						
<i>600 bar</i>							

**Table 3.4:** Condition of the MTU injection measurement points.

The first version of the Matlab algorithm was realized so that it could process a single pair of data files (the tpc and the txt file of a single measurement point) and then returned all the results of this single measurement point. The measurement results included the mean value and the standard deviation of all the acquired individual injection events. Other information such as the rail pressure trend and the injection trigger signals were also included in the results.

A second revision of the algorithm was needed to improve the speed of the data processing by reducing the necessary human interaction when processing complete measurement sets with many injection parameter combinations. In this version of the algorithm the user is only required to select all the tpc data files from the desired measurement points; it then automatically identifies the measurement point parameters and the corresponding txt data file from the file names and saves all the processed results in a new Matlab structure ordered by the measurement point rail pressure and injection time (see figure 3.50). The balance data sampling frequency is constant and its value is therefore hard coded into the algorithm, but the injection frequency is automatically deduced from the txt data file names. All the graphs resulting from the post-processing are saved in newly created folders named after the measurement point names.

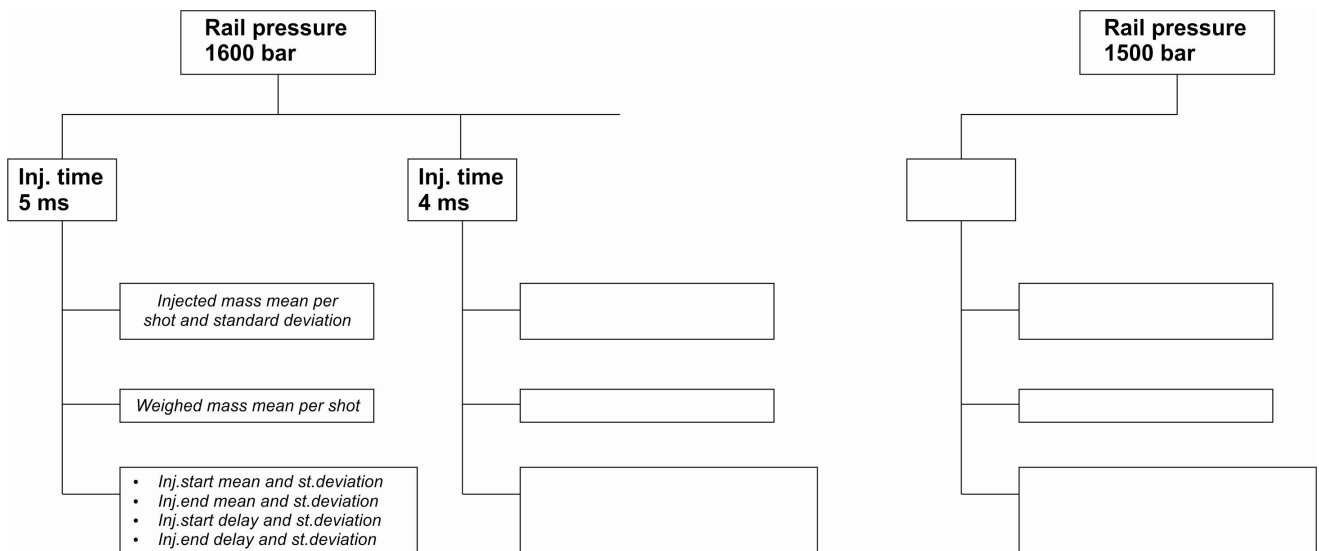


**Figure 3.50:** The Matlab structure layout containing processed results.

## 3.7 Measurement Results

As mentioned in the previous chapters, an assessment of the accuracy of the calculated injected fuel mass can be obtained from the comparison with the fuel mass weighed by the balance. In order to produce a reliable fuel mass feedback value of the injected fuel quantity, it is necessary to achieve a steady state of the back flow out of the following tube during the measurement.

First weighing tests showed that the lower the injection frequency and the lower the injected fuel mass per stroke are, the more erratic the behaviour of the outflow from the injection analyzer is (figure 3.51). This means that for such low frequency and low quantity injection parameters no back flow steady state during the measurements could be achieved.

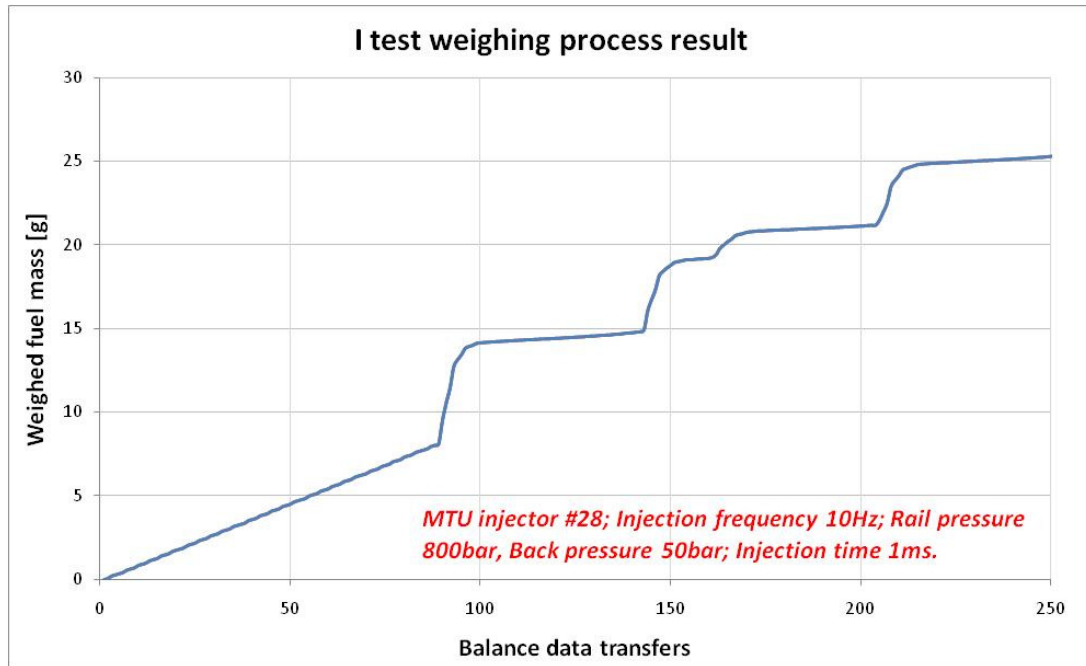


**Figure 3.51:** Result of the weighing process in no-steady-state measurement conditions.

This could be explained by a “stepping operation” of the back pressure valve for very small back flows. Therefore it was considered to use the second configuration of the hydraulic circuit (refer to figure 3.15 in section 3.3.1). However, before rebuilding the analyzer system into this configuration, different solutions for the current setup were attempted: One of these solutions was to move the balance onto a different support in order to inhibit the transmission of the vibrations produced by the injections onto the balance. By allocating the scale on such an isolated support and by using a different balance measurement mode (a balance internal mode proven more suitable for the weighing in of fine powders and small amounts of liquid) a stable back flow weighing value could be achieved for all measurement points (see figure 3.52).

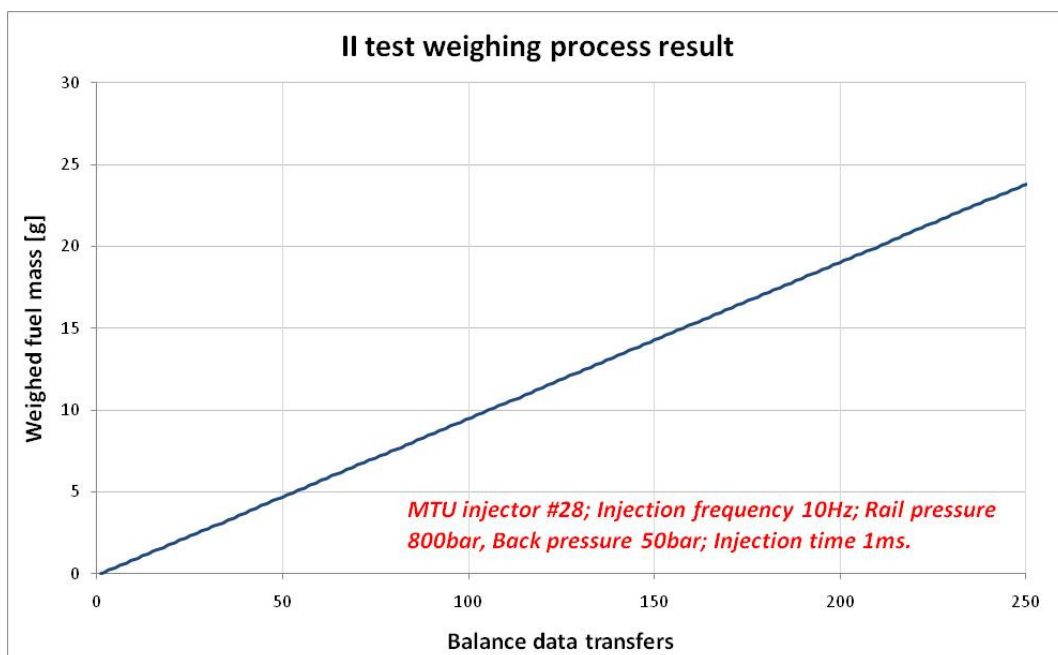


**Figure 3.52:** Result of the weighing process after placing the scale on an isolated support.

In a first attempt to compare the injected fuel mass the temperature of the fuel was not taken into account and thus the speed of sound was supposed to be constant during all the measurements. This assumption resulted in a big difference between the calculated injected mass and the effectively weighted mass, especially for latest acquired injection events. The reason for this difference can be explained as a consequence of a markedly rising fuel temperature during the experiment. As the fuel temperature in the tube increases, the speed of sound in the fuel decreases and the injection rate calculated from the pressure trace is too low compared to the reality (calculation results in too little injected fuel mass injected compared to the reality). Due to the constant value of the speed of sound, the influence of the rising fuel temperature was not taken into consideration, resulting in a too low value for the calculated injected fuel mass.

From then on the temperature of the fuel in the sensor support tube was acquired with a thermocouple and the speed of sound is recalculated based on the measured fuel temperature for each injection. Since the speed of sound depends on the fuel pressure in the tube as well (although to a much lower degree), an absolute pressure sensor should have been used to acquire the current fuel pressure value as well. However, in all the experiments a fixed value of the back pressure (50 bar) was used (adjusted with the back pressure valve and checked with the gauge on the follower tube). As mentioned in previous chapters (3.4.3), the temperature sensor used with the first version of the sensor support was not directly in contact with the fuel and was therefore not able to follow the fast temperature changes in the fuel, resulting in a maximum difference between the calculated injected mass and the weighed mass of around 15 %. With the revised version of the sensor support, where the thermocouple has contact with the fuel (section 3.3.3) the error between the calculated mass and the weighed mass could be reduced, but not completely eliminated.

A second version of the Matlab algorithm was developed to collect all the mass measurement results (calculated injected mass and weighed mass for each single measuring point) and write them into an Excel sheet for further analysis. The following figures show the remaining mass differences between calculated and weighed values of all measurements taken in this project.

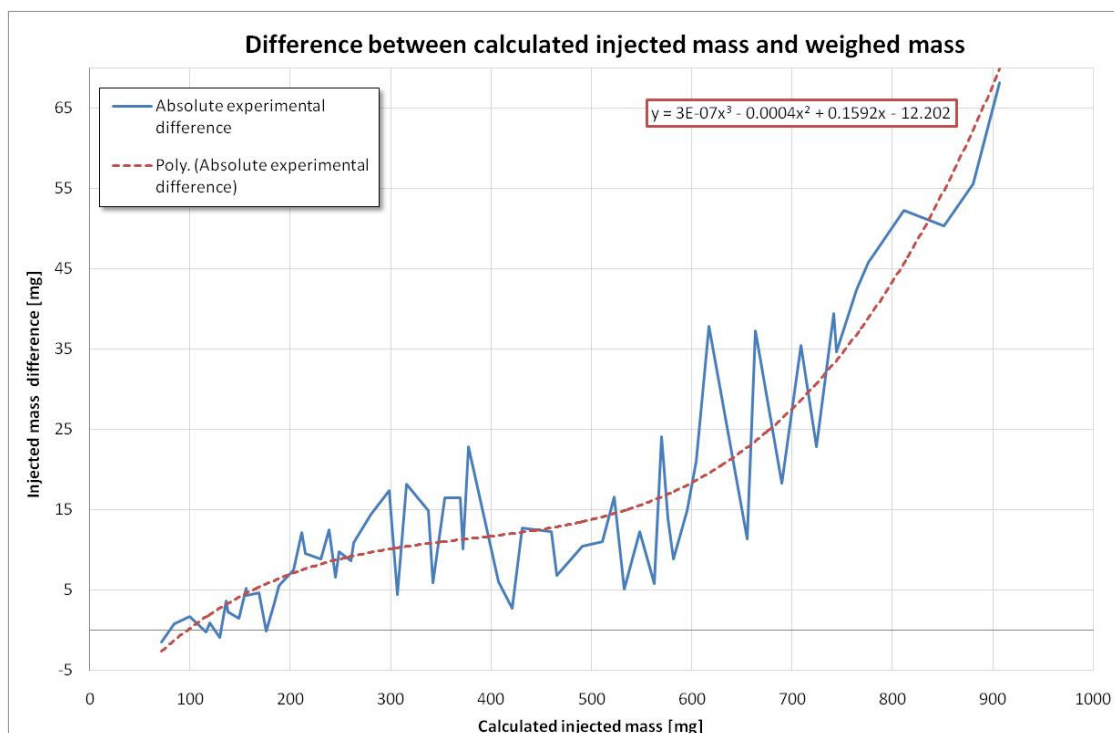


**Figure 3.53:** Difference between the injected masses resulting from the two different procedures.

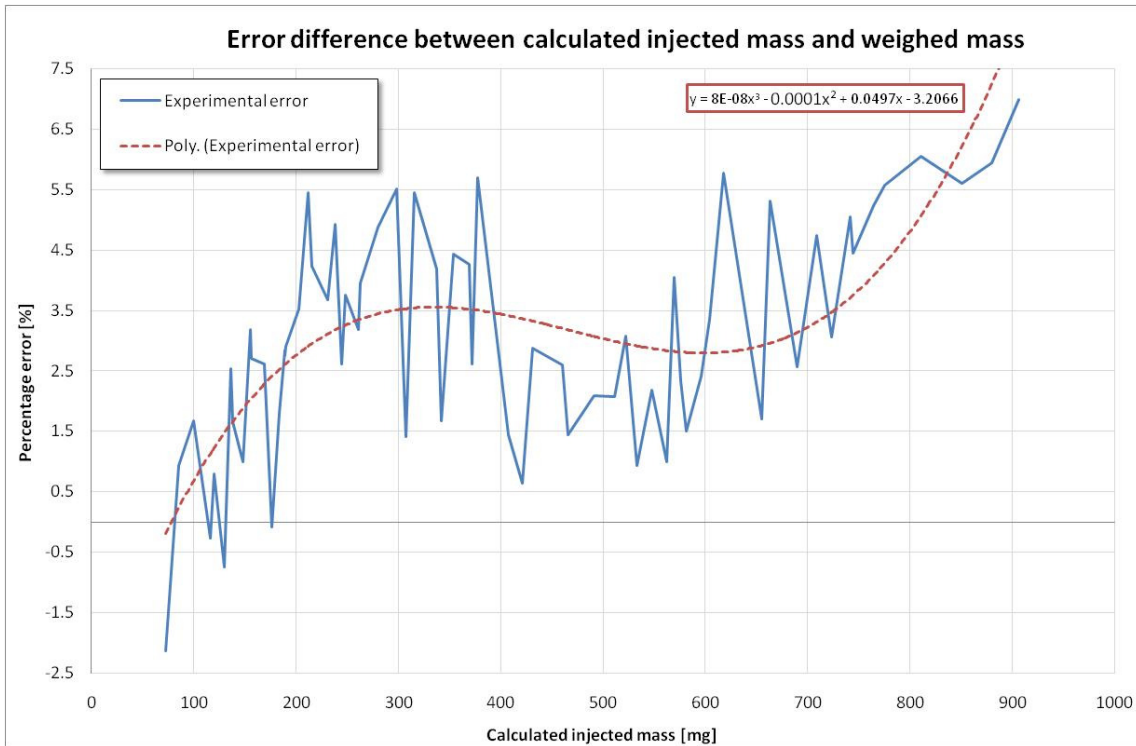


Figure 3.54: Percentage errors between the injected masses resulting from the two different procedures.

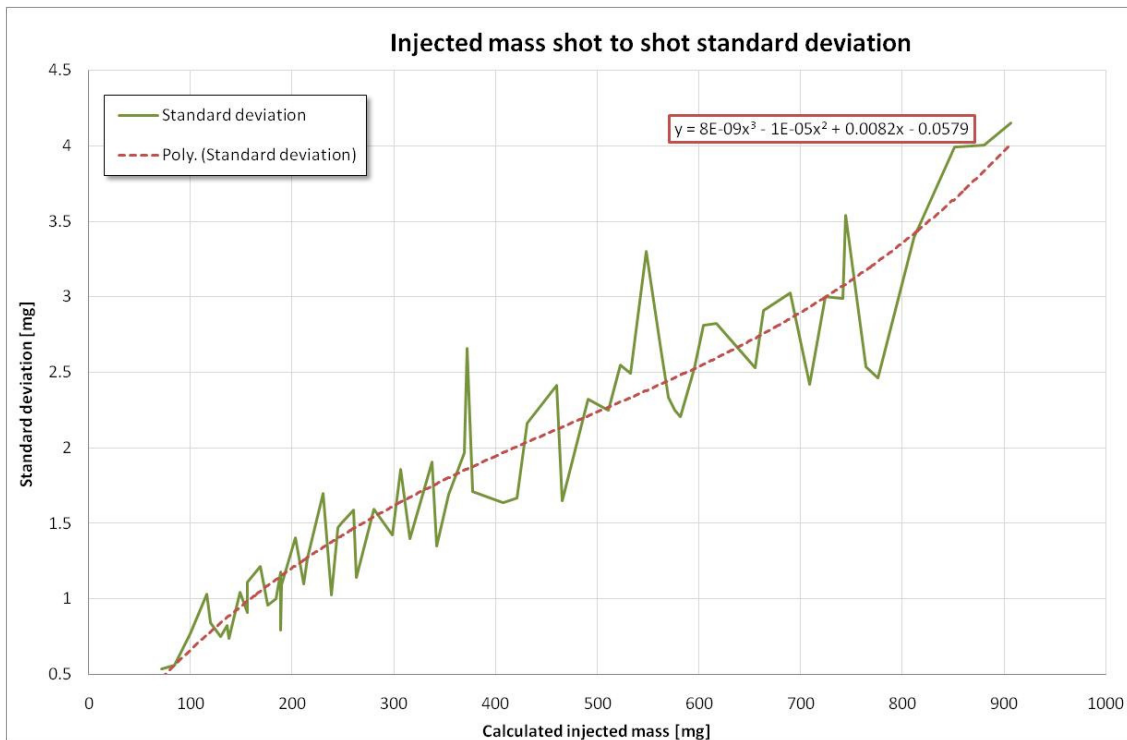


Figure 3.55: Injected mass standard deviation.

Considering the fact that the weighing measurements could not be performed concurrently with the injection rate measurements because of technical problems, and considering the shot-to-shot standard deviation of the injected fuel quantity (figure 3.55), some difference between these values must be expected. It was hoped to find a linear relation between the injected fuel mass error and the injected fuel

mass, but unfortunately the wave-like shape of the percentage error curve makes an easy explanation of the difference impossible. Nevertheless, considering that the resulting difference between the two fuel masses deduced from completely different methods is always lower than 8 %, the achieved results can be considered to be quite good.

The measurement results are finally arranged into Excel sheets to make them easily accessible for the users of the data. In each Excel file the following information is included:

- Injector and fuel details
- Injector solenoid controlling parameters (current, voltage and respectively times)
- A table summarizing injected quantity average for each single measuring point
- A graph showing injected quantity as a function of rail pressure and injection actuation time
- Tables including timing events results as a function of measuring points
- Injection rate profiles

## 3.8 Outlook

Another complete injection rate measurement system based on the Bosch tube principle for measuring injection quantities up to 150 mg per stroke is available in the LAV department (commercial system, sold and manufactured by IAV GmbH). In order to use this system as a reference and to have a further possibility to compare of the measured injected fuel mass, a support to adapt small solenoid diesel injectors on the new injector analyzer was realized (3.57).

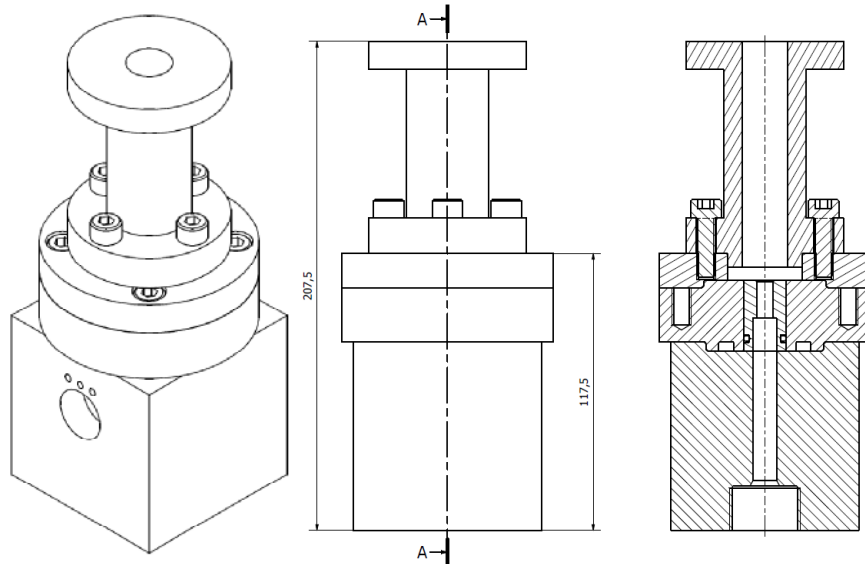


**Figure 3.56:** The support for small solenoid diesel injectors.

Some measurements with the small injector have been performed and the calculated injected mass was compared to the weighed fuel mass in the same way as described in the last chapter. The small injected fuel quantities resulted in an additional reduction of the error between the calculated and the weighed fuel mass to values in the order of 3 % to 5 %.

In the future a comparison between measurement results obtained with the two instruments will be carried out in order to further reduce the possibly committed errors and to increase the accuracy of the newly developed injection rate measuring system.

## 4 Future Fuels for Diesel Engines

### 4.1 Introduction and Objectives

The FVV (Research Association for Combustion Engines) has been promoting research and development in the field of combustion engines since 1956. One of the main goals is to improve the efficiency ratios and emissions of engines and turbines. With the same target, FVV promoted a new research project bringing together, as research partners, the Aerothermochemistry and Combustion Systems Laboratory (Laboratorium für Aerothermochemie und Verbrennungssysteme, LAV)<sup>23</sup> and the Institute for Internal Combustion Engines and Automotive Engineering (Institut für Verbrennungsmotoren und Kraftfahrwesen, IVK)<sup>24</sup>.

The new research project aims at clarifying the influences of chemical and physical properties of synthetic fuels on combustion and emission behaviour under conventional diesel engine operation conditions, in order to define the basis for premium diesel fuels<sup>25</sup>. With this intent seven synthetic blends of components with different chemical structures and with a common matrix obtained by the Fischer-Tropsch (FT) process, were defined and investigated. Results were then compared to a reference diesel fuel following the requirements of EN 590.

Fischer-Tropsch synthesis processes offer the possibility to influence the combustion-relevant chemical and physical characteristics of the fuel by affecting the relative yield of olefins, paraffins and oxygenated products (alcohols, aldehydes, acids and ketones) during the process<sup>26</sup>. Therefore, the identification of the physical and chemical characteristics of the fuel that affect the engine efficiency and emission, represented a central point for the project in order to define suitable basic component for future premium fuels.

In order to evaluate fuels' main differences on the engine, studies were conducted at IVK on a single-cylinder research engine equipped with a common-rail injection system. The performance and emissions of the engine were examined at several representative operating points under various conditions.

To enable a deeper interpretation of the engine investigation results and to fully understand the chain effect produced on load mixture formation, combustion process and pollutant emission due to different physical and chemical characteristic of the fuel, fundamental experiments were performed at LAV. Here two different types of test benches were set up in order to study the injection and early combustion processes. In particular these measurements investigate the fuel behaviour from the injector nozzle through the combustion chamber to the exhaust gas stage. The focal interest of these experiments was to produce a data base of measurement results for all the synthetic fuels, in order to better correlate the effects found in the engine with the most important chemical physical properties.

In this chapter, a brief overview of the entire project is given but the main topic is the injection analysis, which investigates the hydraulic behaviour of the injections. In the following section some details are given about the fuels under investigation. In section 4.2, the experimental setups available for the project are

---

<sup>23</sup> The LAV is part of the Department of Mechanical and Process Engineering at ETH Zürich in Switzerland.

<sup>24</sup> The IVK is part of the University of Stuttgart in Germany.

<sup>25</sup> The here used term "premium diesel fuel" not refers to the standard definition issued by EMA in [58].

<sup>26</sup> This is done by adjusting the temperature, feed gas composition, pressure, catalyst type and promoters of the synthesis process [59].

described. In section 4.3, the fuel injection test bench employed in this work is described in the detail. A summary of the main results of the measurements performed with this test bench is given in section 4.4.

### 4.1.1 Fuels

In coordination with the FVV Working Group, which serves as a discussion forum for the parties involved in the project, a set of 8 fuels was defined. Six of the fuels share a common matrix consisting in a typical Fischer-Tropsch synthetic fuel with high-paraffin basis content. Variants are obtained by further addition of 20 % in volume of paraffins, olefins, naphthens, aromatics and heavy alcohols. A further test fuel with lower boiling range was obtained by a higher proportion of short-chain n- and iso-paraffins. The last fuel is a standard reference diesel according to EN 590.

All fuels were prepared and analyzed by the Institut Francais du Petrole (IFP)<sup>27</sup>. The basic fuel properties are summarized in the table below.

Name		FT1 Boiling range 180-310°C	FT1 + 20 %v naphthens	FT1 + 20 %v iso-paraffins	FT1 + 20 %v olefins	FT2 Boiling range 130-310°C	FT1 + 20 %v mono- aromatics	FT1 + 20 %v heavy alcohols	CEC Reference diesel EN590
Abbreviation		<i>FT-Base</i>	<i>FT-Naph</i>	<i>FT-iPar</i>	<i>FT-Olef</i>	<i>FT-IIBP</i>	<i>FT-Arom</i>	<i>FT-Alc</i>	<i>RDF</i>
Cetane number	-	<b>72.2*</b>	<b>62.7</b>	<b>63.5</b>	<b>66.7</b>	<b>62.4</b>	<b>57.9</b>	<b>62.1</b>	<b>53.2</b>
Calorific value, Lower (H <sub>u</sub> )	J/g	<b>44061</b>	<b>43730</b>	<b>44093</b>	<b>43841</b>	<b>43853</b>	<b>42905</b>	<b>42778</b>	<b>42900</b>
Desity (15°C)	Kg/m <sup>3</sup>	<b>788.1</b>	<b>804.6</b>	<b>789.7</b>	<b>786.7</b>	<b>772.1</b>	<b>807.0</b>	<b>797.7</b>	<b>834.4</b>
Kin. viscosity (40°C)	mm <sup>2</sup> /s	<b>2.354</b>	<b>2.501</b>	<b>2.244</b>	<b>2.261</b>	<b>1.654</b>	<b>1.758</b>	<b>2.817</b>	<b>2.711</b>
HFRR (lubricity) 60°C	µm	<b>334</b>	<b>377</b>	<b>309</b>	<b>342</b>	<b>331</b>	<b>337</b>	<b>424</b>	<b>370</b>
Flash point	°C	<b>89</b>	<b>92</b>	<b>87</b>	<b>93</b>	<b>39</b>	<b>73</b>	<b>89</b>	<b>65</b>
IBP	°C	<b>188.4</b>	<b>189.3</b>	<b>173</b>	<b>194.4</b>	<b>134</b>	<b>185.6</b>	<b>193.2</b>	<b>163</b>
FBP	°C	<b>303</b>	<b>314</b>	<b>337.1</b>	<b>305.6</b>	<b>306.6</b>	<b>306.6</b>	<b>306.7</b>	<b>355</b>
Carbon content	%(m/m)	<b>85.2</b>	<b>85.35</b>	<b>84.85</b>	<b>85.23</b>	<b>84.66</b>	<b>86.11</b>	<b>83.29</b>	<b>86.4</b>
Hydrogen content	%(m/m)	<b>15</b>	<b>14.83</b>	<b>15.24</b>	<b>14.91</b>	<b>15.2</b>	<b>13.99</b>	<b>14.9</b>	<b>13.5</b>
Oxygen content	%(m/m)	<b>&lt;0.5</b>	<b>&lt;0.5</b>	<b>&lt;0.5</b>	<b>&lt;0.5</b>	<b>&lt;0.5</b>	<b>&lt;0.5</b>	<b>1.8</b>	<b>&lt;0.5</b>
H/C	Calc.	<b>2.098</b>	<b>2.071</b>	<b>2.140</b>	<b>2.085</b>	<b>2.134</b>	<b>1.936</b>	<b>2.132</b>	<b>1.862</b>
O/C	Calc.							<b>0.016</b>	

\*) Analysis repeated by SGS, Speyer

**Table 4.1:** Basic fuels properties.

<sup>27</sup> In 2009 IFP changes its name in IFP Energies Nouvelles.

### 4.2 Project Framework Overview

Combustion in any heat engine can be divided into three main phases: Formation of the appropriate mixture of fuel and air, ignition, and completion of combustion. In a diesel engine, the fuel is injected into air that has been compressed to high pressure and temperature. Some of the fuel from the incoming spray jet vaporizes and mixes prior to ignition, forming a pre-mixed fraction of the fuel that ignites and burns as a premixed flame. The remaining fuel in the jet is ignited and burns as a diffusion flame, ideally at the same rate as it is injected.

To obtain a better understanding of the effects produced by fuels' physical and chemical properties on the three main phases of the combustion process, this project looked at the following sequence of steps: Injection, spray formation and evaporation, ignition and soot formation, as well as fuel efficiency and pollutant formation in a running motor. The workload was divided between two research institutes. Three different test rigs were involved: (i) At LAV the first test bench consists mainly of a commercial Bosch tube type injection analyzer and was used to examine hydraulic characteristics of the injection process, from the injection triggering till the outlet of fuel from the nozzle (injection rate, injected quantity, injection times and delays, respectively). (ii) The second test bench built at LAV is a constant volume combustion chamber (high temperature / high pressure test cell – HTDZ) with optical access, equipped with laboratory instrumentation to study spray penetration depth, spray propagation, evaporation, points of ignition and soot formation. (iii) A commercial car engine modified for single cylinder operation was equipped at the IVK to evaluate the fuel properties from the engine's side.

The aim of the project was then, basing on the investigations conducted on the previous mentioned set of synthetic fuels, to tailor the optimal fuel composition for fuelling conventional DI-diesel engine. Referring to basic studies, this is done by gaining the scientific understanding of the mechanisms that influence engine combustion behaviour when fuelled with each synthetic blend. In this way robust basis for generalization and for the understanding of the engine behaviour are created.

The gist of the argument dealt in this section is the framework of the experimental approach used from the two partners of the project to contribute to the collection of the evidences necessary to characterize the effects of fuels' properties on the engine emission and efficiency. Here an overview of the engine test bench, the HTDZ and of the here investigated experimental working points is given. A detailed description of the injection analysis research is given in the following sections of this chapter.

#### 4.2.1 IVK Experimental Approach

The IVK engine tests were conducted on a single cylinder engine. In contrast to using a multi-cylinder engine, this option offers the advantage of accurate control of the air to fuel ratio in the cylinder. A more precise and broader variation of the combustion-affecting boundary conditions is then possible. In this way the engine measurement reproducibility between experiments with different test fuels can be maximized.

The original engine was provided by Daimler AG and it was a 4-cylinder car engine derived from the OM 646 Evo type. In order to obtain the single cylinder version, while keeping the original design of the engine, a new suitable crankshaft was constructed and various modifications of the entire engine geometries were performed. Additionally, the oil and water channels of the cylinder head were machined to ensure a steady supply of lubricant and coolant in the single-cylinder engine operation. The injection system used is a typical Bosch common-rail system. Pressure is supplied by a 3-piston high pressure pump (max. 1600 bar)

connected directly to the crankshaft. A universally applicable ETK ECU interface for development of electronic control unit was used to define the start and duration of the injections.

An overview of the most important data of the single-cylinder engine unit is provided in table 4.2.

<b>Engine test bench</b>	
Displacement	537,4 cm <sup>3</sup>
Bore	88,0 mm
Stroke	44,4 mm
Connection rod length	147 mm
Compression ratio	15,15 (thermodynamic)
Peak fire pressure	145 bar
Max. pressure increase	10 bar/°CA
<b>Injection system</b>	
Injector	Bosch CRI 2.2 MV
– Nozzle	Mini-sac
– Nozzle orifice	7, Ø 0.136 mm
High pressure pump	Bosch CPS3
Max. rail pressure	1600 bar

**Table 4.2:** Technical data of the IVK engine test bench.

A detailed description of the instruments featured in the IVK's test bench can be found in appendix A.

In order to have reproducible and relatively un-influenced engine steady-state operating conditions among the measurements with different fuels, the operating points are pmi-based, as the accuracy of the in-cylinder pressure signal is not affected by frictional losses (which nonetheless affect torque, especially at low load conditions). Therefore the exchange of data between the two project partners took place referring to the operating points based on the indicated power (engine speed – pmi).

3 different motor tests were performed at the IVK in Stuttgart:

- *Single injection tests:* 4 part-load engine operating points (engine speed – pmi defined) were investigated during these tests. The required engine load is obtained by adjusting the injection duration and the rail pressure, while the electric start of the injection is adjusted to achieve a constant centre of the combustion event (defined by HR 50). Inlet air temperature and EGR rate (0 %) are kept constant for all the measurements. The purpose of this test strategy was to determine engine's combustion and emission with the set of fuels.
- *Pre- and main injection tests:* The same 4 part-load engine operating points were again investigated. In this case a pre-injection and a variation of the EGR rate between 0 and 40 % are also performed. The electric start and duration of the main injection is adjusted as above in the single injection tests while the electric end of the pre-injection always happens 1 ms before main injection start; pre-injection duration is adjusted in order to give a constant input of energy ( $m_{pre} \cdot H_u$ ). This

complementary strategy was performed to investigate more realistic engine operating conditions of modern diesel engines and to test the transferability of the knowledge gained in previous experiments.

- *Full load tests:* Two full-load engine operating points were investigated during these tests. The first point (2000 rpm – maximum engine torque) is performed with a pre-injection<sup>28</sup> and without EGR. The second full load point (4000 rpm - predefined value of power) is performed without pre-injection and EGR. In these tests, the electric start of the main injection is again defined to obtain a constant centre of the combustion event (HR 50) while the injection duration is limited by mechanical (peak pressure, pressure rise, maximum exhaust temperature) and combustion ( $\lambda \leq 1.4$ ; FSN  $\leq 3.0$ ) limits.

A summary of the selected engine's operating points can be found in table 4.3.

		Inlet air temperature			EGR - Rate		Rail pressure			Heat release centre		
Engine speed	Load (pmi)	Min.	Base	Max.	Min.	Max.	Min.	Base	Max.	Min.	Base	Max.
<i>Rpm</i>	<i>Bar</i>	°C			%		<i>Bar</i>			°CA after TDC		
1500	2	40	<b>60</b>	80	0	40	500	<b>660</b>	700	8	<b>13</b>	17
2000	2	40	<b>60</b>	80	0	40	550	<b>720</b>	750	9	<b>13</b>	17
2000	6	40	<b>60</b>	80	0	40	700	<b>950</b>	900	10	<b>20</b>	17
2000	10	40	<b>60</b>	80	0	30	800	<b>1050</b>	1000	16	<b>20</b>	23
2000	-	<b>60</b>			0		<b>1400</b>			<b>16</b>		
4000	-	<b>60</b>			0		<b>1600</b>			<b>19</b>		

*Table 4.3: Summary of conditions for the operating points tested on the engine.*

### 4.2.2 LAV Experimental Approach

The aim of the studies carried out at LAV was the characterization of the influence that fuel properties have on the early phase of combustion process. With the intent of study this process, from the outlet of the fuel from the injector nozzle to the spread of the liquid phase, with and without the influence of evaporation, till the ignition and combustion of the fuel/air mixture, including soot formation and soot oxidation in a controlled environment, two different test benches were installed at the LAV laboratory. On one hand a test rig equipped with an injection analyzer manufactured by IAV was used to study the hydraulic behaviour of the injection. On the other hand a constant-volume high-temperature and high-pressure cell (HTDZ) was used to analyze the injection spray, ignition and soot formation.

The HTDZ consists of a cylindrical combustion chamber with a diameter of 110 mm and a depth of 40 mm (figure 4.1). On one side of the chamber there is a central mounting hole for the injector and the gas exchange system opportunely equipped with other sensors. On the opposite side, a large sapphire window

<sup>28</sup> The electric end of the pre-injection always happen 1 ms before main injection electric start and its electric duration is controlled in order to give a constant input of energy ( $m_{pre} \cdot H_u$ )

( $\varnothing$  90 mm) allows the observation of the injection jets and the combustion process. Four smaller windows ( $\varnothing$  48 mm) are installed at the side surfaces, permitting a homogeneous illumination.

The cell and feeding gas (nitrogen or air) can be electrically heated up to 750 K, while the maximum allowed filling pressure (before combustion) is 100 bar. To protect the injection nozzle from overheating a cooling jacket is used. Particularly for this project the cell was also equipped with a hydrogen pre-combustion chamber in order to perform experiments with temperature up to 1000 K.

A detailed description of the high-speed camera and the method adopted to perform these measurements is given in appendix B.

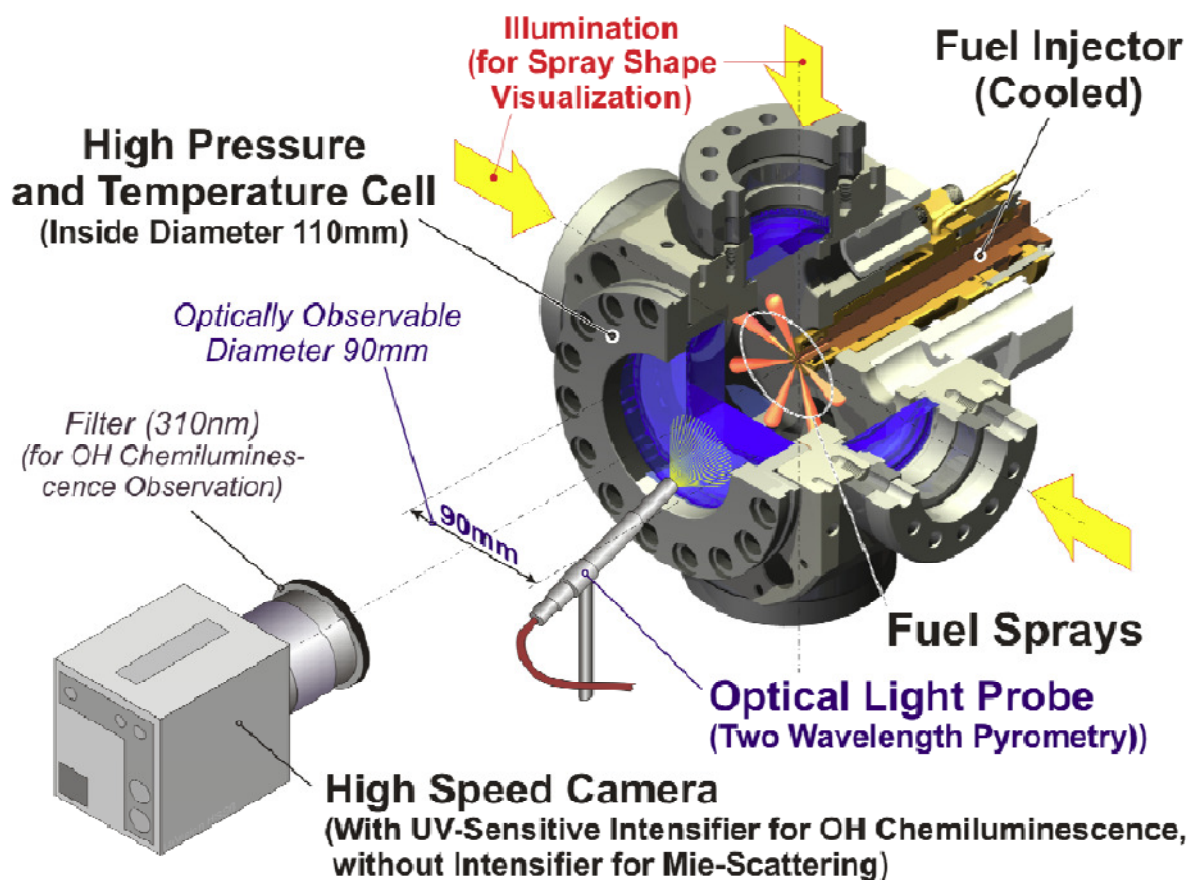


**Figure 4.1:** View of the high-temperature and high-pressure cell of the LAV with the setup for the optical detection of the injection jets [60].

Figure 4.2 shows the temperature-pressure diagram with the measurement points that were defined referring to motor-relevant temperatures and pressures: The temperature of area A (400 K) is still below the boiling range of all the investigated fuels and allows the study of the injection spray propagation without the influence of evaporation. In area B the temperature (650 K) is already over the boiling range of all the investigated fuels and allows the assessment of the injection spray propagation under evaporating conditions. Contrary to points A and B, in the measurement points of area C, the cell is operated with air instead of nitrogen, allowing ignition and combustion of the fuel.

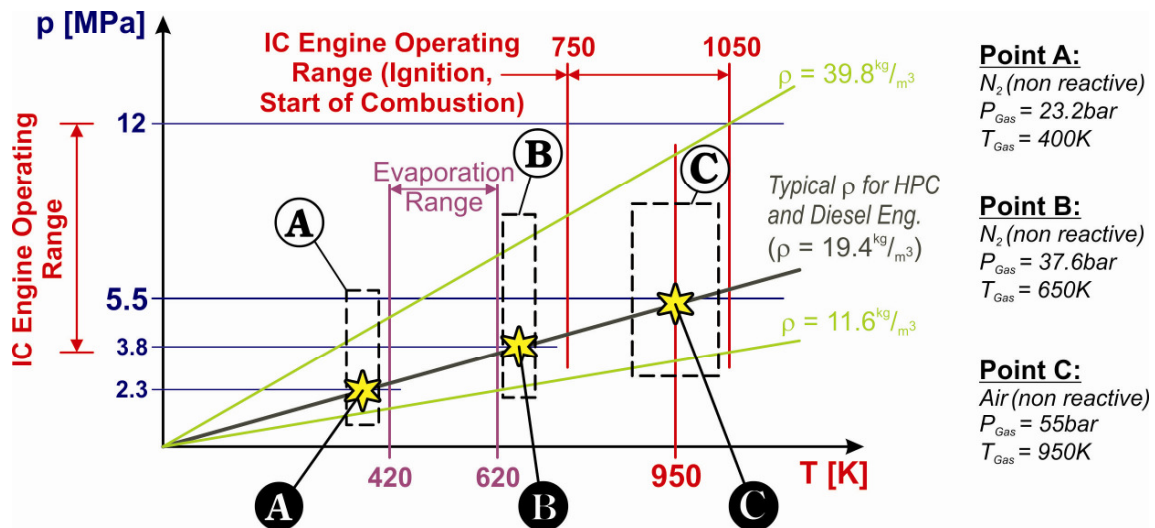


Figure 4.2: Temperature-pressure conditions in the HTDZ for the measuring points: non-reactive, non-evaporating (A), non-reactive evaporation (B), reactive (C) at constant gas density for all conditions [60].

A reactive gas temperature of 950 K at a pressure of 55 bar was chosen for the operating conditions of area C. This cell condition corresponds to the thermodynamic state of the in-cylinder air of the IVK's engine test bench during the start of the injection event.

## 4.3 Injection Analysis Approach

### 4.3.1 Test Bench

In figure 4.3 a schematic overview of the injection analyzer measurement setup is shown.

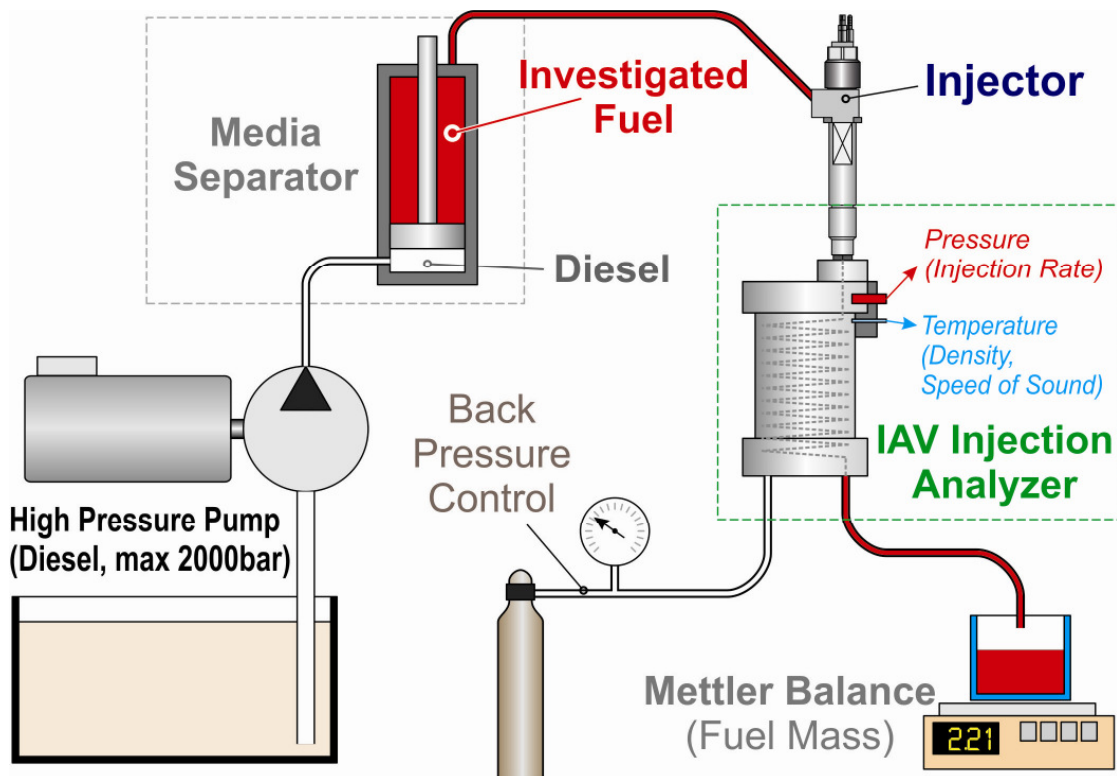


Figure 4.3: Injection analyzer measurement setup.

## The IAV Injector Analyzer

An injection analyzer manufactured by the German company IAV GmbH represents the heart of the test bench. The measurement principle of this device as clearly explained in section 3.3, is based on the detection of the rate of discharge by measuring the pressure wave that is produced by injecting into a predetermined length of a hydraulic tube filled with calibrated diesel fuel.

The injection analyzer consists in two main elements: *the hydraulic unit* and the *control unit (ECU-I)*.

The *hydraulic unit* is the hardware of the measuring device. It houses the injector, the testing fuel and all the sensors to fully define the hydraulic characteristics of the injection event. A sectional drawing and the hydraulic scheme of this unit are respectively illustrated in figure 4.4 and figure 4.5. Different colours are used in the sectional drawing to point out the regions with different pressures; in particular dark blue is used to highlight the region filled with nitrogen. The nitrogen is used to create the fuel back pressure (system pressure) by pressurizing the fuel contained in the measuring device, which is separated from the nitrogen by a sealing plunger (figure 4.4). In this way the fuel back pressure is easily controlled by adjusting the nitrogen pressure.

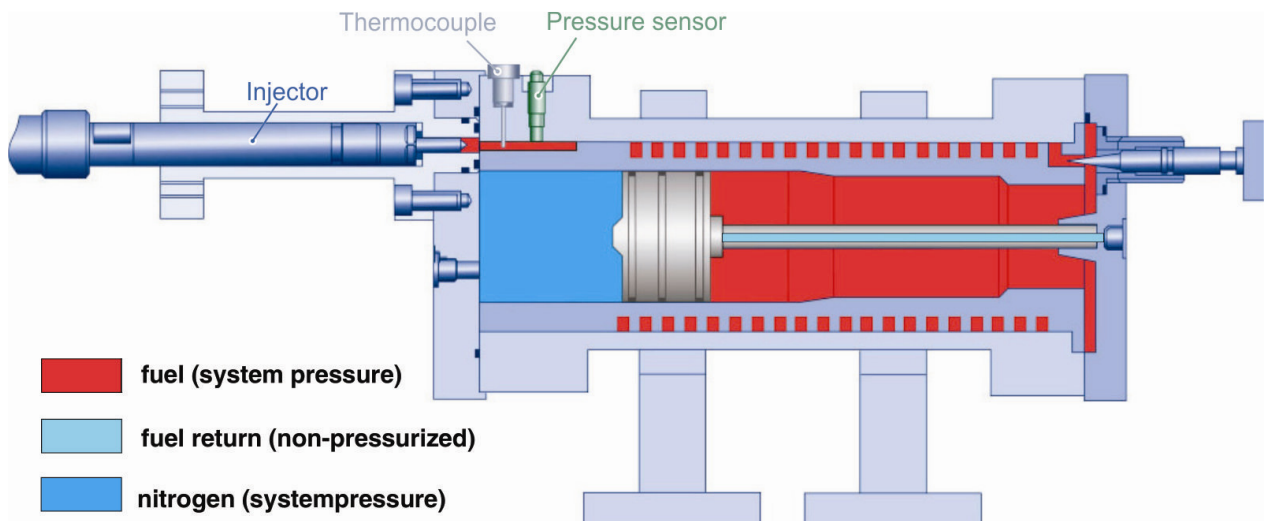


Figure 4.4: Schematic sectional drawing of hydraulic unit [53].

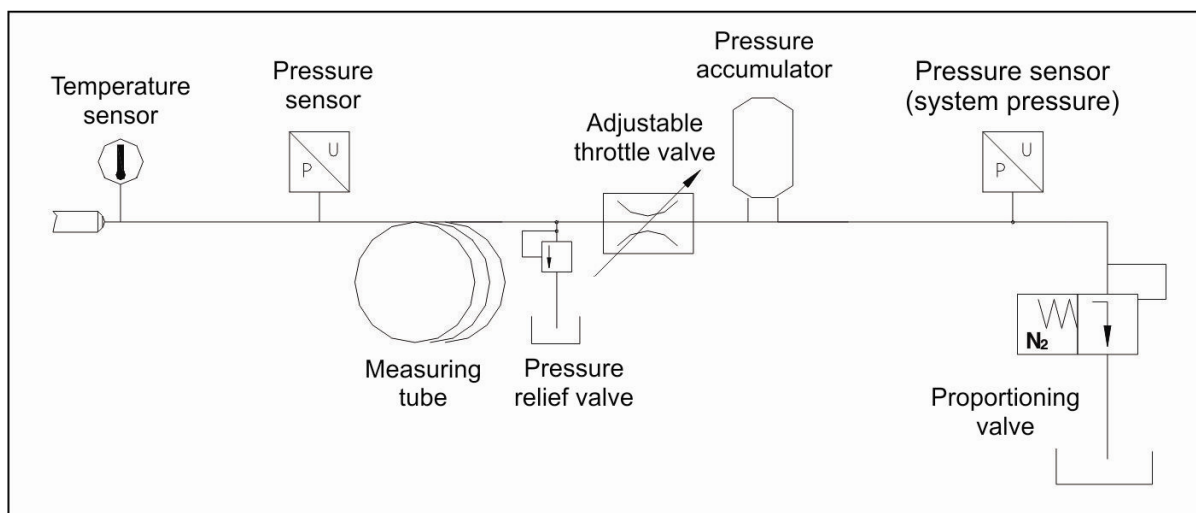


Figure 4.5: Hydraulic circuit diagram of the IAV Injection Analyzer [53].

The *ECU-I* is the control unit of the hydraulic system and is used to monitor, acquire, save and process all the data recorded during the experiment. The control unit accommodates the sensor voltage supply and signal conditioning capability.

Referring to the hydraulic circuit of figure 4.5, the required input signals of the ECU-I during the injection measurements are the pressure signal monitored at the beginning of the measuring tube, the temperature of the fuel in the region where the pressure signal is acquired, the static pressure signal (system pressure) and the injector trigger signal (i.e. the electrical current or voltage used to control the solenoid valve). As the injection analyzer is designed for use on an engine test rig, some additional input signals are also required for the measurements:

- A 1/T signal, representing 1 pulse per 720 °CA (TTL 0-5 Volts). This input is necessary to fix the geometric position in relation to virtual TDC of injection system control.
- A n/T signal, representing 120-3600 pulses per 720 °CA (TTL 0-5 Volts).

There are some other optional input channels implemented for specific purposes: A trigger input for synchronizing the injection analyzer with some other device, or an auxiliary analog input to record an external optional signal (e.g. rail pressure or other).

The only output channel of the device returns an analog output voltage (0-10 V DC) which is proportional to the injected fuel quantity (0-200 mg/stroke).

A dedicated software to operate the ECU-I is installed on a computer used to control and monitor the measurement process, store measurement files and to operate all the electronically-controlled test rig devices.

### *The injector Control System*

The injection analyzer was equipped with the same type of injector used on the IVK engine and HTDZ test bench: A Bosch CRI 2.2 MV mini-sac injector featuring a nozzle with 7 holes with a diameter of 0.136 mm. The solenoid valve of this injector is controlled by the FI<sup>2RE</sup> (Flexible Injection and Ignition for Rapid Engineering). This device is developed by the IAV GmbH for rapid and easy operation of new injectors and ignition systems. In this research the FI<sup>2RE</sup> was used to tailor the energizing profile of the solenoid valve and to perform the injection events as specified from the working point time-recording (a detailed description of the working points follows in section 4.3.2). The performed energizing profile is a 2-step current control actuated with two voltages. Up to five injections per cycle are possible and each injection has:

- Programmable *premagnetisation* (current and duration)
- Programmable *boost phase* (voltage, upper and lower current values, duration)
- Programmable *constant voltage phase* (voltage, duration)
- Programmable *fast current decay* (duration)
- Programmable *holding phase* (upper and lower current values)
- Fast current decay at the end of the holding phase

Figure 4.6 shows two possible energizing profiles obtained with two different values of boost voltage (35 V and 70 V).

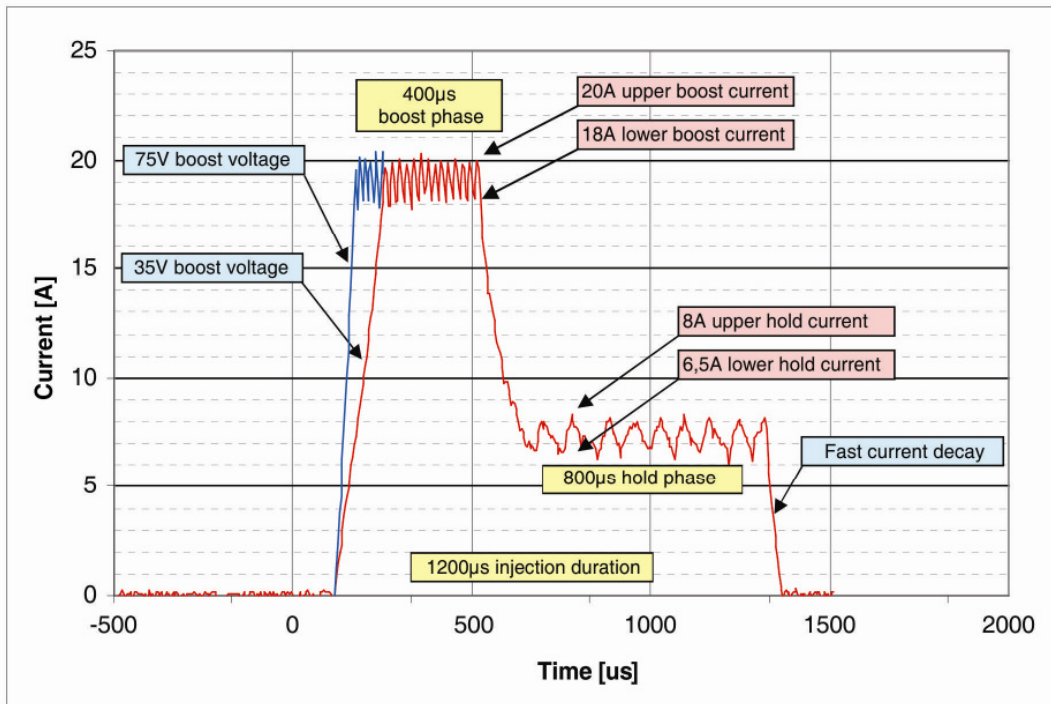


Figure 4.6: Two classical energizing profiles of a common-rail solenoid valve. The two profiles are obtained with two different values of boost voltage (35 V and 70 V) [54].

Since the FI<sup>2RE</sup> is a tool designed to electronically control some engine’s devices (i.e. solenoid and piezo injector, EGR valve, ignition event) during engine operation, the engine encoder signals (camshaft and crankshaft signals) are two necessary inputs. In order to use the FI<sup>2RE</sup> in the applications demanding the simulation of the engine speed (as in this case), a special function permits the FI<sup>2RE</sup> to simulate it, allowing the use of the device without the inputs from the engine encoder. Since this option does not provide the simulated engine crankshaft and camshaft angle positions, needed as input signals for the ECU-I (1/T and n/T signals), an auxiliary quadrature encoder simulator (QES) device was used in the test rig setup.

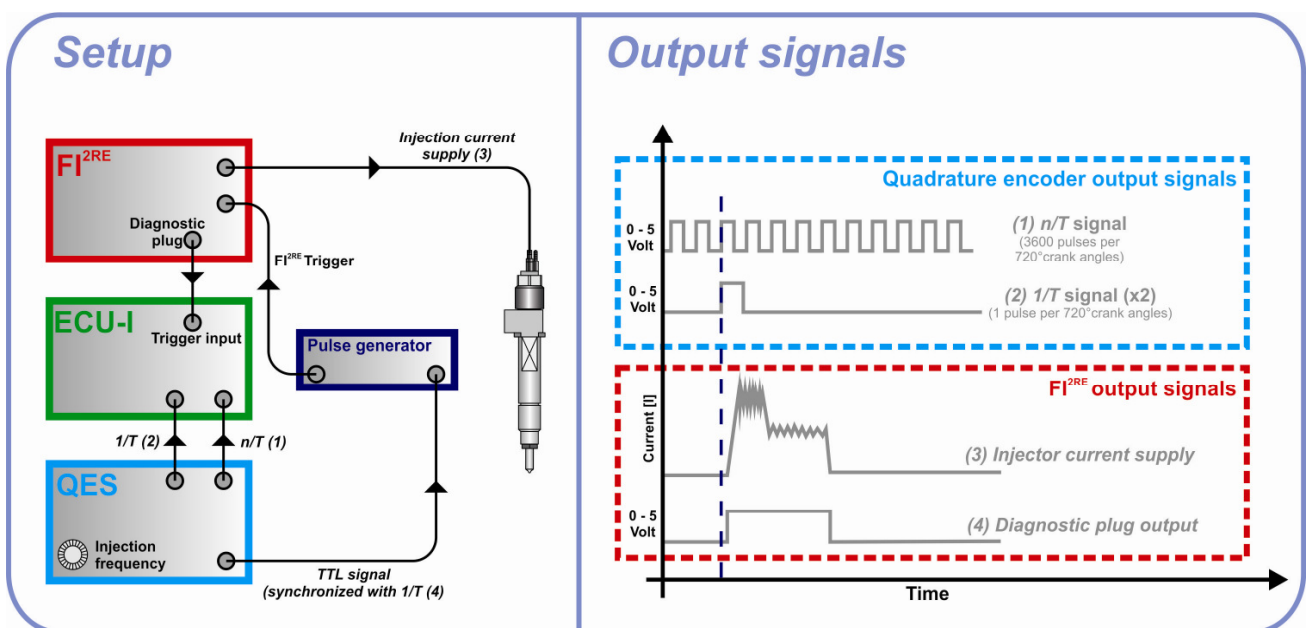
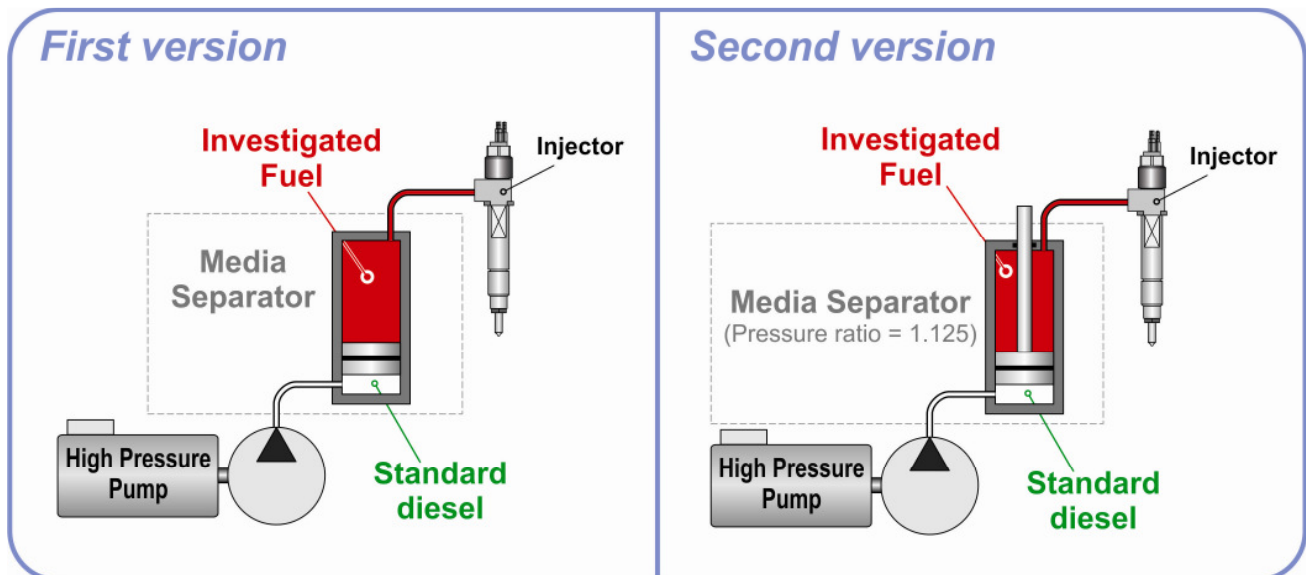


Figure 4.7: The setup used to control the injector.

This device simulates engine speed (thus controlling the injection frequency) by sending the  $n/T$  and  $1/T$  signals to the ECU-I. An additional TTL output (synchronized with the previous  $1/T$  signal) of the quadrature encoder simulator was used to trigger the  $FI^{2RE}$ . The  $FI^{2RE}$ , in turn, sends a pre-arranged current profile to the injector solenoid valve<sup>29</sup>. The additional trigger signal required from the ECU-I was also given from  $FI^{2RE}$  by means of a diagnostic plug, outputting a square pulse proportional in time to the injector current supply. As the QES's TTL output signal does not meet the  $FI^{2RE}$  input requirement (amplitude and clean wave form) an additional device (HP 8116A pulse generator) was used as a go-between ("filter"). An entire overview of the setup and the output signals used to control the injector can be obtained from figure 4.7.

### Fuel Feeding System

Fuel high pressure was obtained by means of the same high pressure pump used to feed the LAV injection analyzer (refer to section 3.5). In order not to load the pump with fuels characterized by different lubricity property and to avoid wasting of the special fuels, the test bench was equipped with a media separator. This element provides a movable seal (plunger) between two liquids that was used to separate standard diesel (feeding the high pressure pump) from testing fuel (see first version draft in figure 4.8).



**Figure 4.8:** Two drafts representing the first and second version of the media separator.

Tests with a first version of the media separator showed problems with the sealing between the two liquids. Analysis with gas chromatography - mass spectrometry (GC-MS) confirmed considerable contamination of the special fuel with the diesel from the pump. For this reason an improved media separator with a new technical solution was designed.

The main difference of the new media separator is the use of a different plunger to separate the standard diesel from the investigated fuel (see second version draft in figure 4.8). This plunger has two different cross section areas on which the fuels press (area ratio = 1.125). With this solution the pressure of the special fuel is higher compared to the pressure of standard diesel during operation and this  $\Delta p$  guarantees an improved sealing.

<sup>29</sup> The external triggering of the  $FI^{2RE}$  to control the time of the injection event is achieved by a  $FI^{2RE}$  special function named "Triggered injection blocks". This function permits external triggering for one or more injections. Once triggered, the injections are started at the angle set for them and for this reason an engine speed must be given to the  $FI^{2RE}$  (either in the form of an external engine speed signal or, as in this case, as an internally simulated engine speed).

New GC-MS analysis ensured the sealing capability of the system (see figure 4.9).

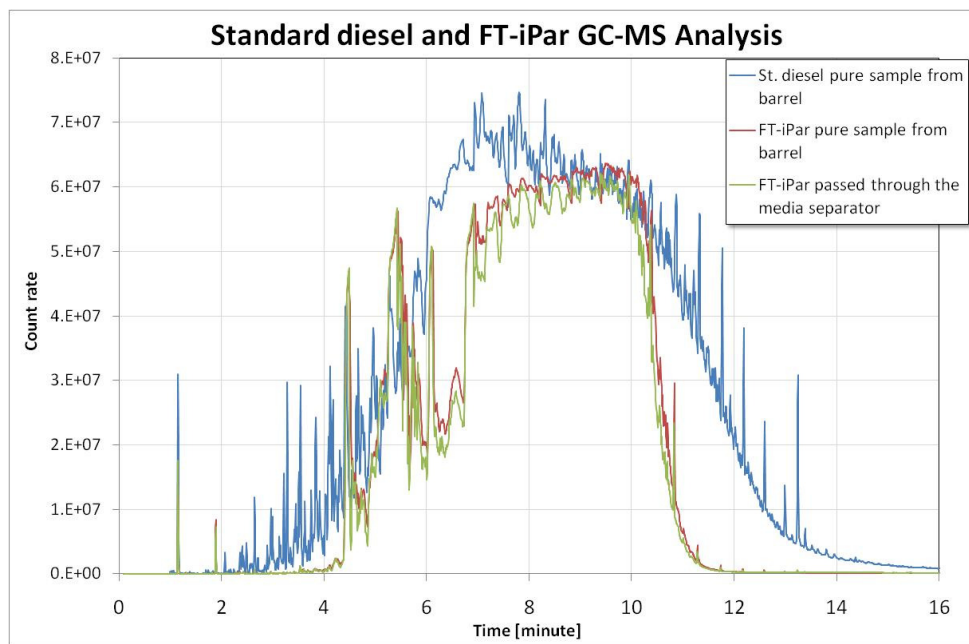


**Figure 4.9:** The superimposition of the chromatography mass analysis of three different fuels samples.

Figure 4.9 shows the results of a chromatography mass analysis obtained with the following three samples of fuels:

- A pure sample (collected from the barrel provided by the IFP) of normal diesel (ISO 4113) used to feed the high pressure pump.
- A pure sample of the synthetic blends FT-iPar collected directly from the provided barrel.
- A sample of the same synthetic blend FT-iPar after having passed through the media separator.

### Additional Devices

An additional pressure sensor was mounted just before the injector inlet in order to check the injector supply pressure and to assure fully reproducible inlet-pressure conditions among all the measurements. A bottle of nitrogen accommodating a manually adjustable cylinder pressure reducer and a pressure-proof hose with appropriate quick-release couplers (for connection to the hydraulic unit) was used to ensure that nitrogen was supplied safely to the injection analyzer. For safety reasons, the cylinder pressure reducer featured an integrated pressure relief valve that limits nitrogen pressure to a maximum of 180 bar. Two pressure gauges for controlling pressure up stream and down stream the cylinder pressure reducer were also accommodated.

A cross-check of the measurement accuracy of the injected mass was given by the readout of a laboratory balance (Mettler Toledo PG-S) placed at the end of the hydraulic circuit which collects the fuel flowing out from the injector analyzer system.

### 4.3.2 Working Points

Basically two main groups of injection conditions were investigated:

**Variable conditions:** These correspond to the injection conditions defined on the engine at the IVK by adjusting the injection system parameters (time and duration of the pre- and main injections and rail pressure) in order to achieve the value of indicated power (engine speed – pmi) predefined for the motor tests. Referring to the 3 types of tests performed on the engine test bench, a map of injection measurement conditions was provided for each of the performed tests and for each of the fuels.

		Working points							
		Engine speed	pmi						
Partial Load Working Points	1500	2	<i>min</i>		<i>max</i>		Rail Pressure Set Point [bar]		
			500		700				
			<i>min</i>	<i>max</i>	<i>min</i>	<i>max</i>	Injection Timing [ $\mu$ s]		
			544	612	467	501			
					43		Back Pressure [bar]		
	2000	2	550		750		Rail Pressure Set Point [bar]		
			516	546	449	481	Injection Timing [ $\mu$ s]		
			45				Back Pressure [bar]		
	2000	6	700		900		Rail Pressure Set Point [bar]		
			666	703	590	613	Injection Timing [ $\mu$ s]		
			58				Back Pressure [bar]		
	2000	10	800		1000		Rail Pressure Set Point [bar]		
801			853	721	773	Injection Timing [ $\mu$ s]			
75				Back Pressure [bar]					

**Table 4.4:** Injection measurement conditions obtained from the “single injection tests” performed on the engine test bench at the IVK.

In table 4.4 is listed an example of the conditions required to characterize the hydraulic behaviour of the injection in the same operating points identified during the “single injection tests” (refer to section 4.2.1). The engine operating points are represented by the *engine speed – pmi*, and each of these engine steady states was obtained by varying the rail pressure and the electric injection duration in a relatively wide range of values. Therefore, each injection condition is identified by the two bounds values of the rail pressure and electric injection duration ranges. The back pressure for the injection conditions is established considering the engine in-cylinder pressure when the injection is performed (triggered). In this manner 4 injection conditions were investigated for each engine steady state of the “single injection tests”.

		Working point		Inlet T	H50	SOPI	DOPI	SOI	DOI	Rail Pressure	Back Pressure
		Engine Speed	pmi	°C	°CA ATDC	°CA BTDC	mics	°CA BTDC	mics	bar	bar
Partial Load	1500	2	60	13	9.3	267	-2.1	445	660	43	
	2000	2	60	13	15.5	260	0.4	431	720	45	
	2000	6	60	20	12.5	245	-2.4	575	950	58	
	2000	10	60	20	12.9	235	-1.9	702	1050	75	

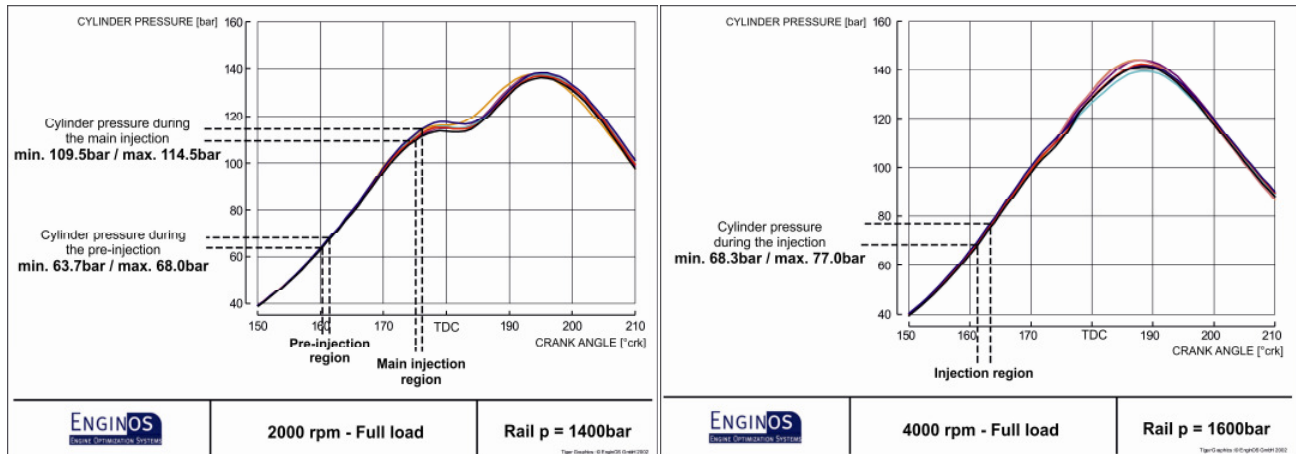
**Table 4.5:** Injection measurement conditions obtained from the “pre- and main injection tests” performed on the engine test bench at the IVK.

“Pre- and main injection tests” were performed at the IVK varying EGR rate, electric duration of the main injection and main injection time<sup>30</sup> (see section 4.2.1). The electric duration of the main injection and the main injection time were varied in a relatively small range for each engine operating point (engine speed – rpm). The rail pressure and electric duration of the pre-injection were instead kept constant for each of these points. Therefore the injection conditions are defined by the *rail pressure – electric duration of the pre-injection* used on the engine and by the average of the values used for the time and electric duration of the main injection. Due to the impossibility to set different back pressure values for the pre- and main injections in the injection analyzer, the back pressure is set equal to the engine in-cylinder pressure at the electric start of the main injection. An example of these injection measurement conditions is shown in table 4.5.

	Working point		Inlet T	H50	SOPI	DOPI	SOI	DOI	Rail Pressure	Back Pressure
	Engine Speed	rpm	°C	%KW n. OT	%KW v. OT	mics	%KW v. OT	mics	bar	bar
Full Load	2000	~22.5	60	16	18.7	232	3.9	980	1400	80
										120
Full Load	4000	~19	60	19	-	-	17.5	930	1600	90
										130

**Table 4.6:** Injection measurement points obtained from the full load test

Since “full load engine tests” were performed with constant rail pressure, electric injection duration (pre- and main) and injection time, these values are used to define the two full load injection conditions. Taking into account the in-cylinder engine pressure during the injections (figures 4.10 – 4.11) and in order to assess the effect of different back pressure on the injection behaviour, two values of back pressures were defined for each of the full load points. Table 4.6 lists an example of these injection measurement conditions.



**Figures 4.10 – 4.11:** Engine in-cylinder pressure during the full load tests.

**Fixed conditions:** A part from the experiments necessary to characterize hydraulic injection behaviour at the operating points of the engine test bench, another set of injection measuring points was defined. These points were defined to obtain a database of intercomparable experimental measurements (among the fuels), and therefore all characterized by the same injection conditions. The reason to have fixed conditions derived from the necessity to enable a deeper interpretation of the effects of fuels’ physical properties on the hydraulic injection behaviour. For this reason two injection durations (0.5 and 1 ms), three rail pressures

<sup>30</sup> Pre-injection time also changes in order to have its electric end 1 ms before main injection electric start.

(500, 1000 and 1500 bar) and one back pressure (50 bar) were selected to be investigated with each single fuel.

Injection Timing [ $\mu$ s]	Rail Pressure [MPa]	Back Pressure [MPa]
500	55	5.0
1000		
500	105	
1000		
500	155	
1000		

*Table 4.7: Fixed injection conditions.*

### 4.3.3 Speed of Sound Determination

As mentioned in chapter 3, in order to obtain reliable results for the measurement of the injected quantity, the speed of sound in the fuel must be well-known for all the measurement conditions. The procedure used to determine the speed of sound under different fuel temperature and pressure is here exposed.

It is proved [52] that the velocity of sound in a fuel corresponds to the velocity of a plane, infinitesimal pressure wave moving along a duct of constant cross-sectional area. The wave could have been generated by a piston moving from rest with a constant infinitesimal velocity or, as in this case, by an injection of fuel at one end of the duct. The basic phenomenon that is utilized to obtain speed of sound values is therefore the pressure wave, generated from the injection, travelling to and fro along the length of the measuring tube till its energy is fully dissipated.

The incident and reflected pressure waves are detected by the pressure sensor at the front end of the measuring tube. Since the length of the tube was determined in previous experiments, the measurement of the time passing between the detection of the original pressure wave and its reflection is used to determine the velocity of the sound in the fuel. The speed of sound is a function of the pressure and temperature of the fuel and the procedure outlined here was used to define the velocity of sound for the fuel conditions (temperature – pressure) at the moment of the experiment.

In order to create a speed of sound map for each fuel, a set of injection rate measurements experiment were done. Each speed of sound map (table 4.8) comprises 4 values of pressure (the 4 values of back pressure specified in the measurement conditions) and 4 values of temperature (covering the range of possible fuel temperature during the measurements) in order to get interpolation curves with a reasonable approximation (the small range of temperature allows a linear interpolation with an error smaller than 1 %). During this set of additional experimental measurements the fuel pressure was easily varied by adjusting the back pressure valve while fuel temperature was attained by adjusting injection frequency, rail pressure and injection duration.

<b>Speed of sound values [m/s]</b>				
<b>Pressure [bar]</b>	<b>Temperature [°C]</b>			
	~25	~32	~37	~44
40				
70				
100				
130				

Table 4.8: The speed of sound map attained for each fuel.

Some former experiments to determine the speed of sound in the fuel resulted in an algorithm (implemented in an Excel sheet by Dr. B. Schneider) that processes injection rate profiles to obtain the value of the sound velocity in the fuel. This algorithm creates two mathematical polynomial curve fits to both the main wave and the reflected wave respectively. Since the reflected wave has a smaller amplitude compared with the original pressure wave (this is due to the partial draining, at the end of the tube, of the fuel transported from the wave, and to the energy dissipated because of the dampening effect of the surface friction on the inner tube wall), the two fits are normalized to equal peak height. The time between the main pressure wave and its reflection is then extracted by the algorithm using an iterative optimization procedure. This procedure consists in shifting the reflected wave fit on the time axis towards the main wave fit until the maximum of the overlap integral between the two areas is found.

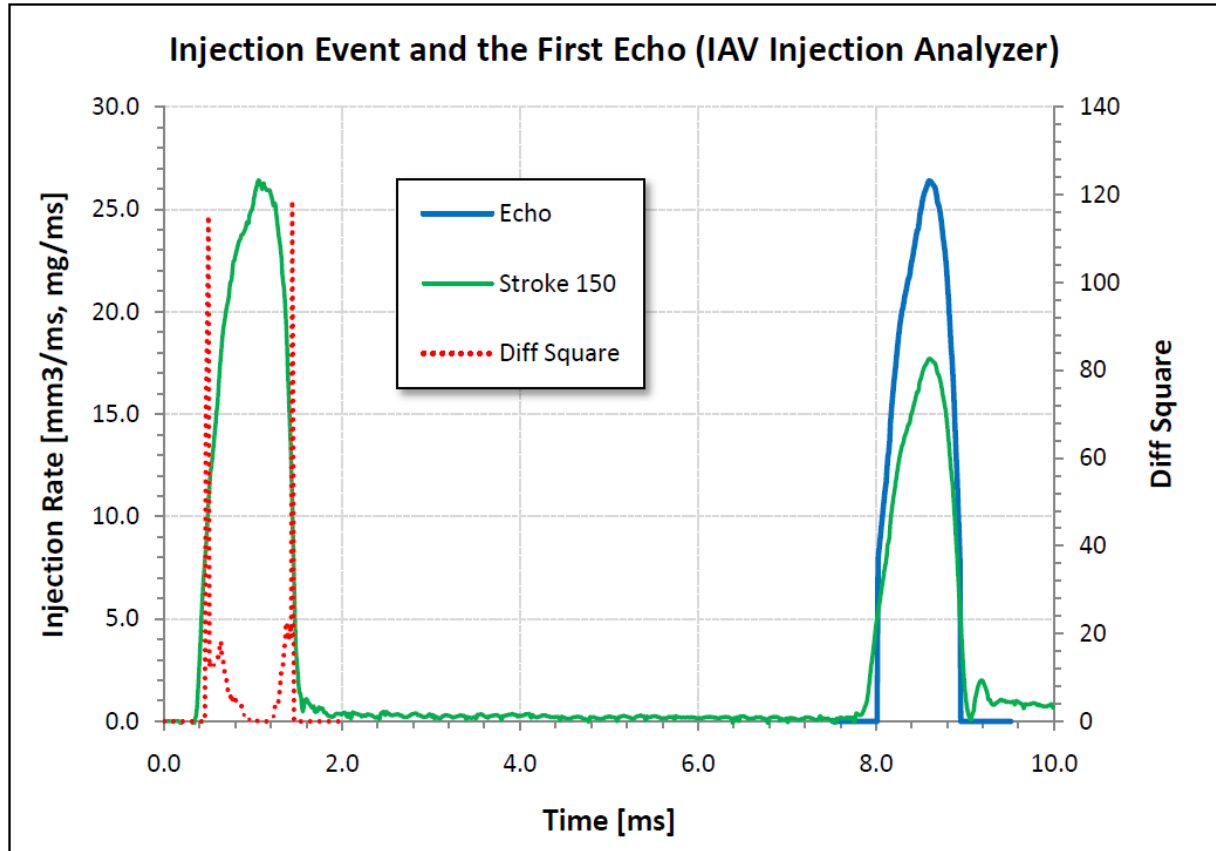
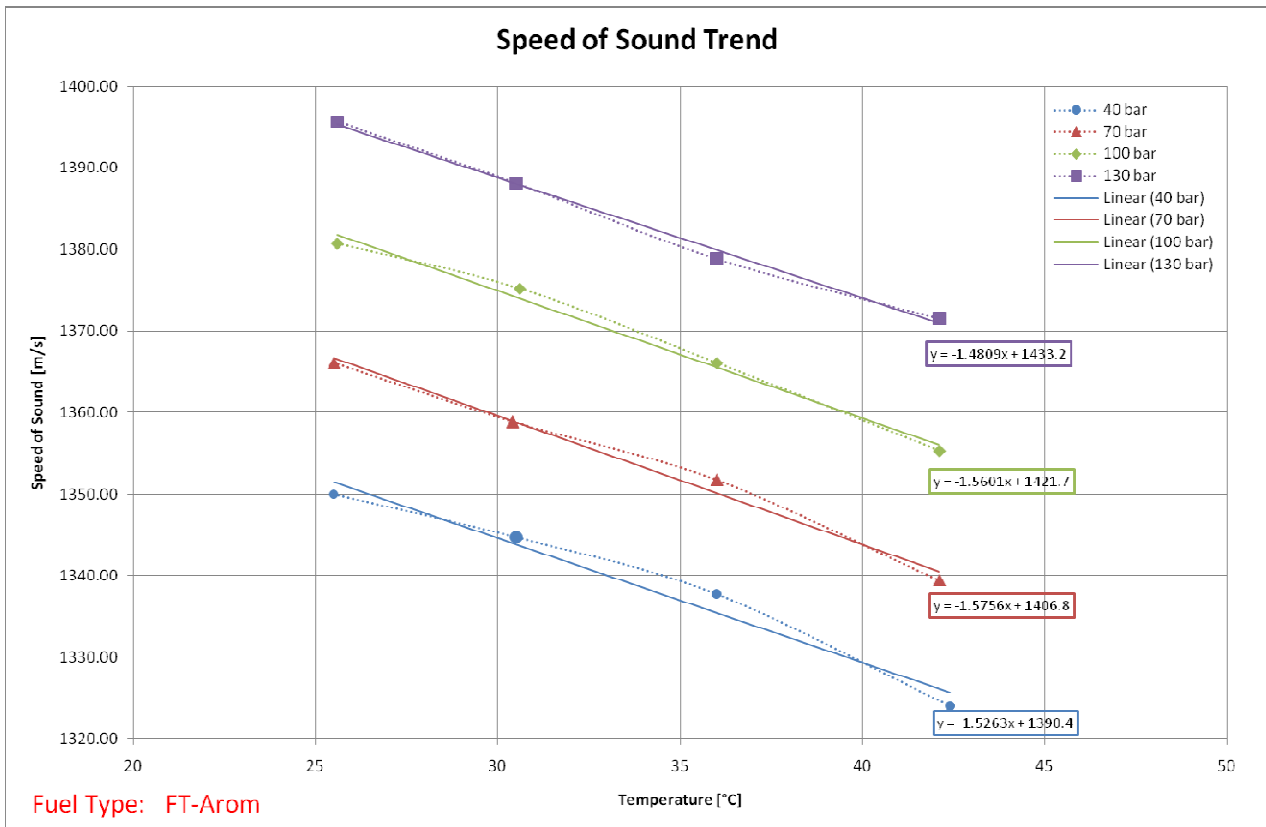


Figure 4.12: The schema of the optimization procedure of the Excel algorithm implemented by Dr. B.Schneider.

By recording the injection rate for a defined fuel pressure – temperature condition, this software allows the calculation of the speed of sound. However, human intervention is needed in the above mention Excel program, making its use very time-consuming. Therefore, an automatic version of the algorithm was implemented using Matlab. This new version permits the processing of thousand of single measurements with minimum human intervention, and directly yields a map of the sound velocity as a function of temperature and pressure.



**Figure 4.13:** Interpolation of the speed of sound values obtained by processing the experimental data with the new Matlab algorithm.

Pressure [bar]	Measured Temperature [°C]			
	25.5	30.5	36	42.4
<b>40</b>	1350.00	1344.72	1337.74	1324.01
<b>40 Lin</b>	1351.48	1343.85	1335.45	1325.68
<b>% Difference</b>	-0.11%	0.06%	0.17%	-0.13%
$y=SOS(P=20,t):$	<b><math>y = -1.5263x + 1390.4</math></b>			

**Table 4.9:** Possible difference (fourth row) between the speed of sound values obtained by the experimental procedure (second row) and by the linear interpolation (third row). The linear interpolation results in the mathematical polynomial expressed in the fifth row.

The assumption of a constant fuel temperature along the entire length of the measuring tube is not fully justified. If the temperature is, in the worst case, off by 15 °C, this would result in an error in the sound velocity of no more than 2 percent which means that the detected injected mass is affected by the same error.

### 4.3.4 Investigational Procedure

In order to guarantee the greatest trustworthiness of the results, the measurement conditions were fully controlled and reproduced during each fuel test. With the same purpose a standardized measurement procedure was always implemented.

The applied procedure can be summarized as follow:

- Cleaning of the test rig from the old fuel.
- Experimental determination of speed of sound for the new fuel, as a function of pressure and temperature.
- Establish stable conditions for the entire setup by running the injector for a few minutes.
- Measurement of a reference point.
- Measurement (with warm-up phases and control measurements at the beginning and end of each series).
- Measurement of a reference point.
- Collection of a sample of the analyzed fuel for future possible analysis (e.g. GC-MS).
- Measurement results post-processing.

### 4.4 Injection Analysis Results

At the moment of this writing not all the HTDZ tests were concluded. For this reason a deep analysis to correlate the data resulted from the hydraulic injection investigation and the measurement results obtained with the engine and HTDZ investigation was not done yet. Nevertheless a study to identify dependencies of the injection rate profile on the fuel's physical properties was conducted.

The process of fuel injection through a nozzle obviously is strongly affected by the fuel's physical properties. They influence the passing of the fuel through the multiple small orifices in the injection nozzle when the fuel is injected at very high pressure into the combustion chamber. Furthermore, the fuel jet must form a spray, i.e. break-up into small droplets<sup>31</sup>, and traverse the combustion chamber in order to reach all parts of the chamber; this phase strongly depends on the fuel's physical properties as well. At the same time, the fuel must vaporize, mix with the air, and start to react. If the fuel jet penetrates too far the fuel interacts with the wall, resulting in degraded mixing, low temperature combustion on the walls, and high emission of unburned hydrocarbon and smoke. If the fuel vaporizes and mixes too close to the nozzle, the mixture will be overly rich, leading, once again, to high unburned hydrocarbons and smoke emissions [55].

The fuel properties that have the greatest effect on the injection are viscosity, density, lubricity and surface tension. Each of these properties may affect the injection process in different ways:

- Viscosity, impacts the fuel spray characteristics through flow resistance inside the injection system and in the nozzle holes. Higher viscosity may result in reduced flow rates and degraded atomization for equal injection pressure.

---

<sup>31</sup> The size of the fuel droplets ranges from approximately ten micrometers to several hundred micrometers.

- Fuel density can affect the mass of fuel injected as all practical diesel injection systems meter the fuel on a volume basis. Increased density may result in higher fuel injection rates due to the direct relationship between mass, volume, and density [55].
- Fuel lubricity affects the capability of the fuel to lubricate the injection system thus affecting the injection performances.
- Surface tension, affects the tendency of the fuel to form drops at the jet-air interface. Increased surface tension may tend to degrade atomization rates<sup>32</sup> [55].

In order to understand the chain effect produced by these properties on the injection process, the injection rate profiles obtained with different fuels under the same measurement conditions (fixed conditions) were compared.

The injection rate profiles for all the studied fuels, performed with an injection rail pressure of 500, 1000 and 1500 bar and an electrical driving time of the injector of 0.5 and 1.0 ms, are illustrated in the figures 4.14 – 4.19.

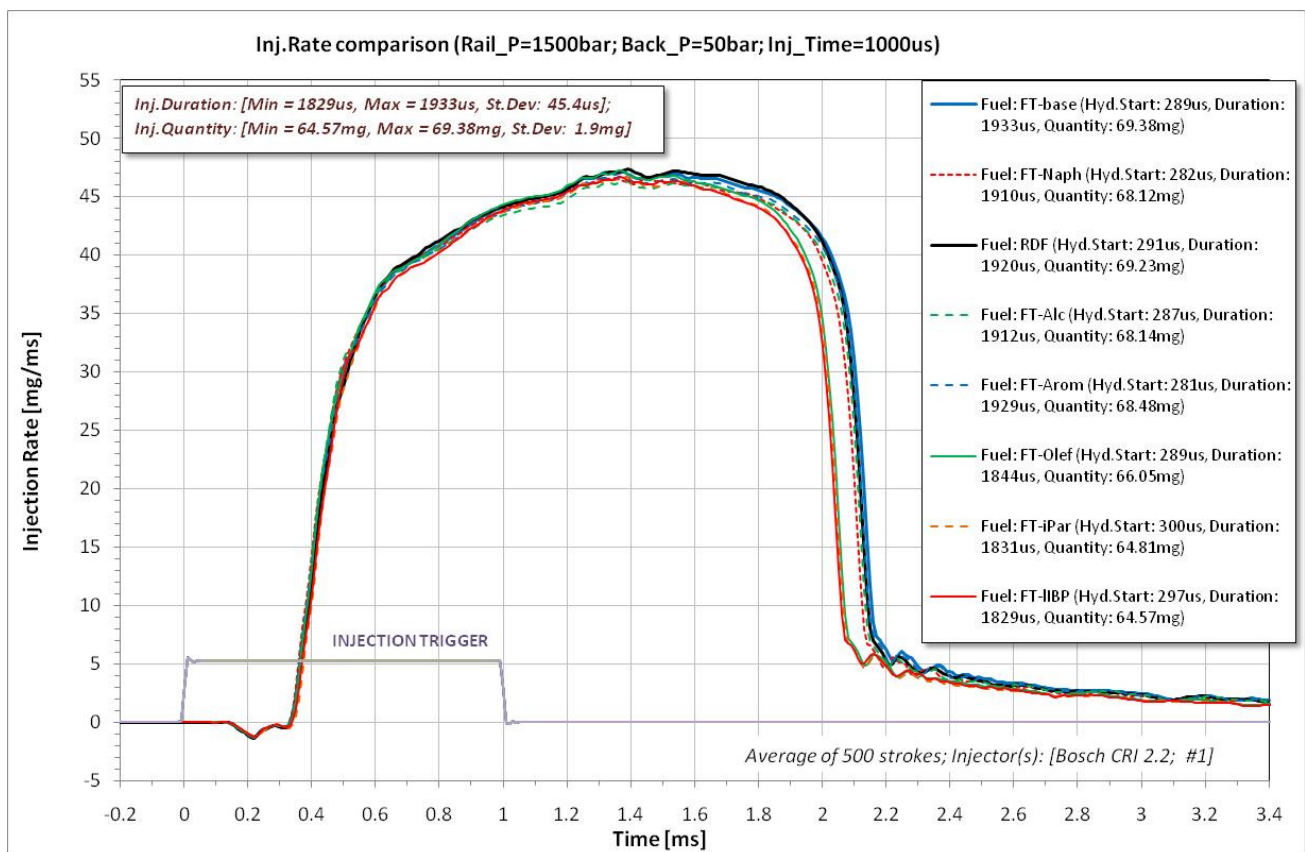


**Figure 4.14:** IR profiles, obtained with the set of fuels, for high rail pressure (1500 bar) and long injection time (1 ms).

<sup>32</sup> It should be noted that the surface tension values of most hydrocarbons are very similar. Based on this fact, surface tension does not play a primary in the jet break-up and atomization process and this is the reason why its effects have not been considered in this work.

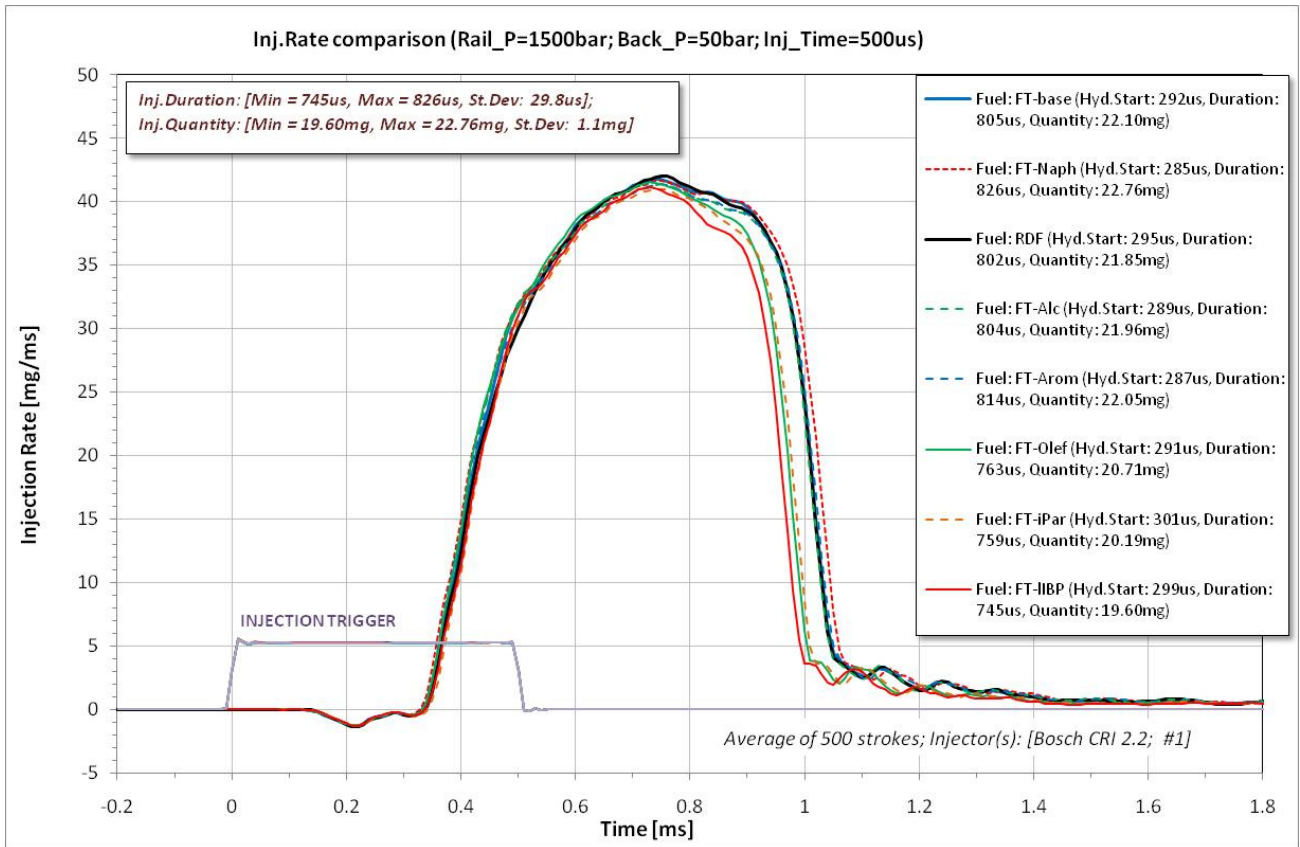


Figure 4.15: IR profiles, obtained with the set of fuels, for high rail pressure (1500 bar) and short injection time (0.5 ms).

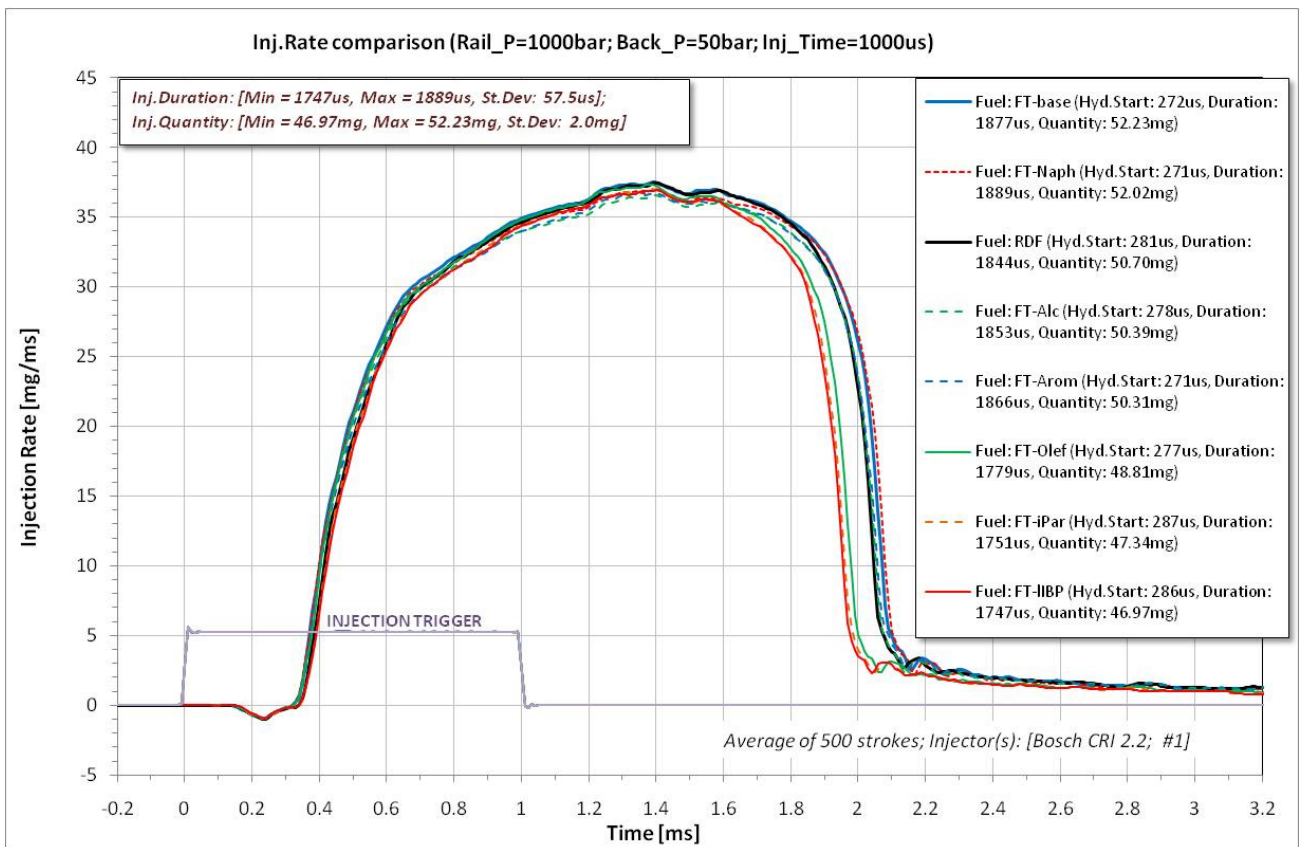


Figure 4.16: IR profiles, obtained with the set of fuels, for medium rail pressure (1000 bar) and long injection time (1 ms).

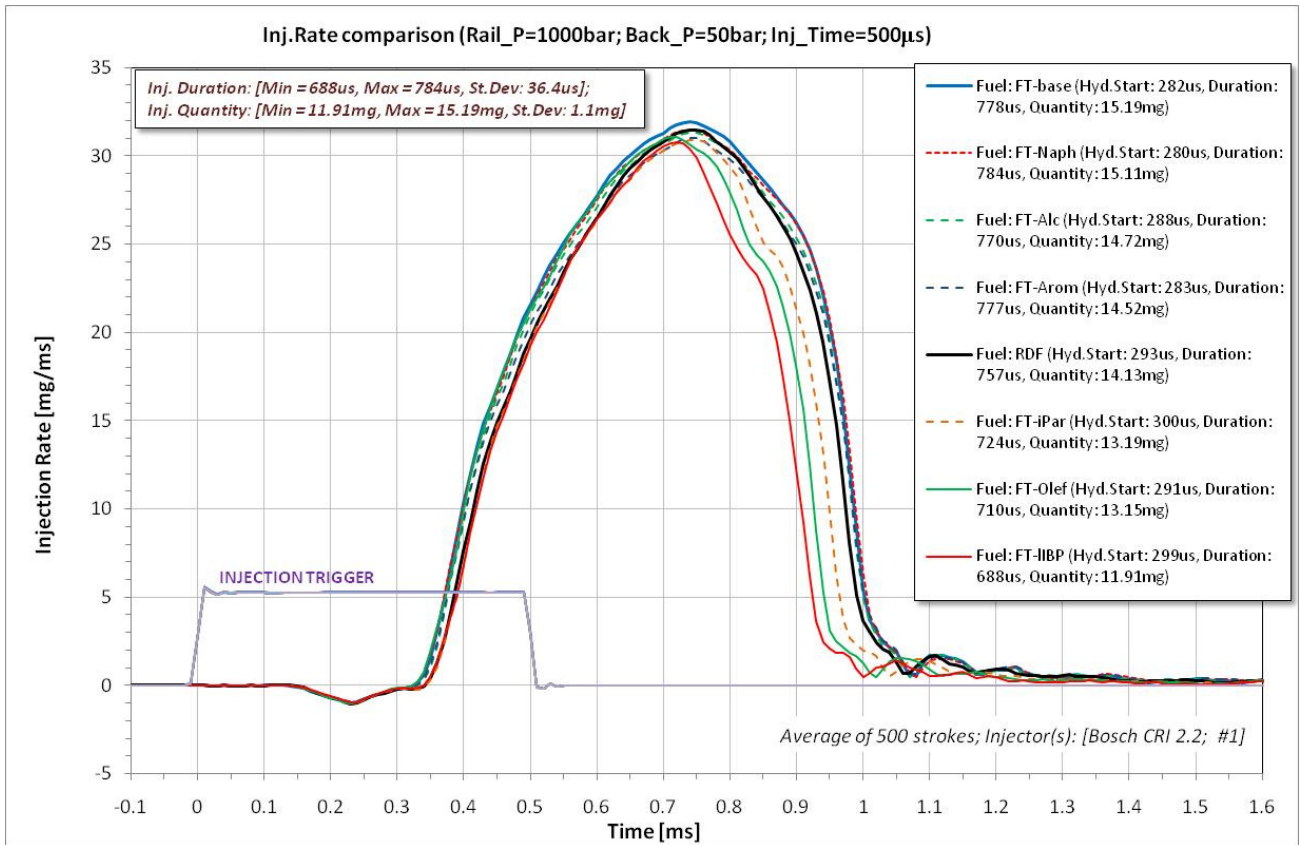


Figure 4.17: IR profiles, obtained with the set of fuels, for medium rail pressure (1000 bar) and short injection time (0.5 ms).

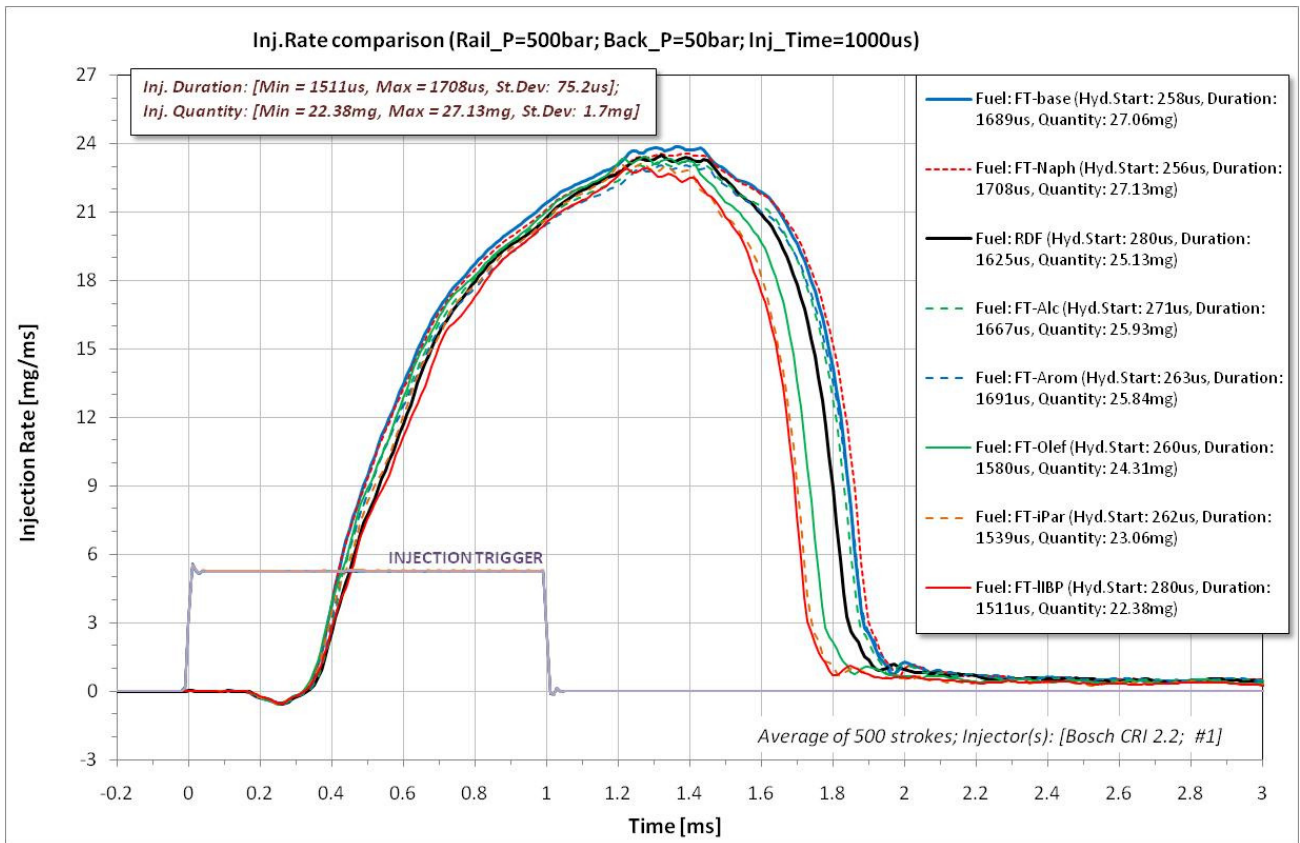
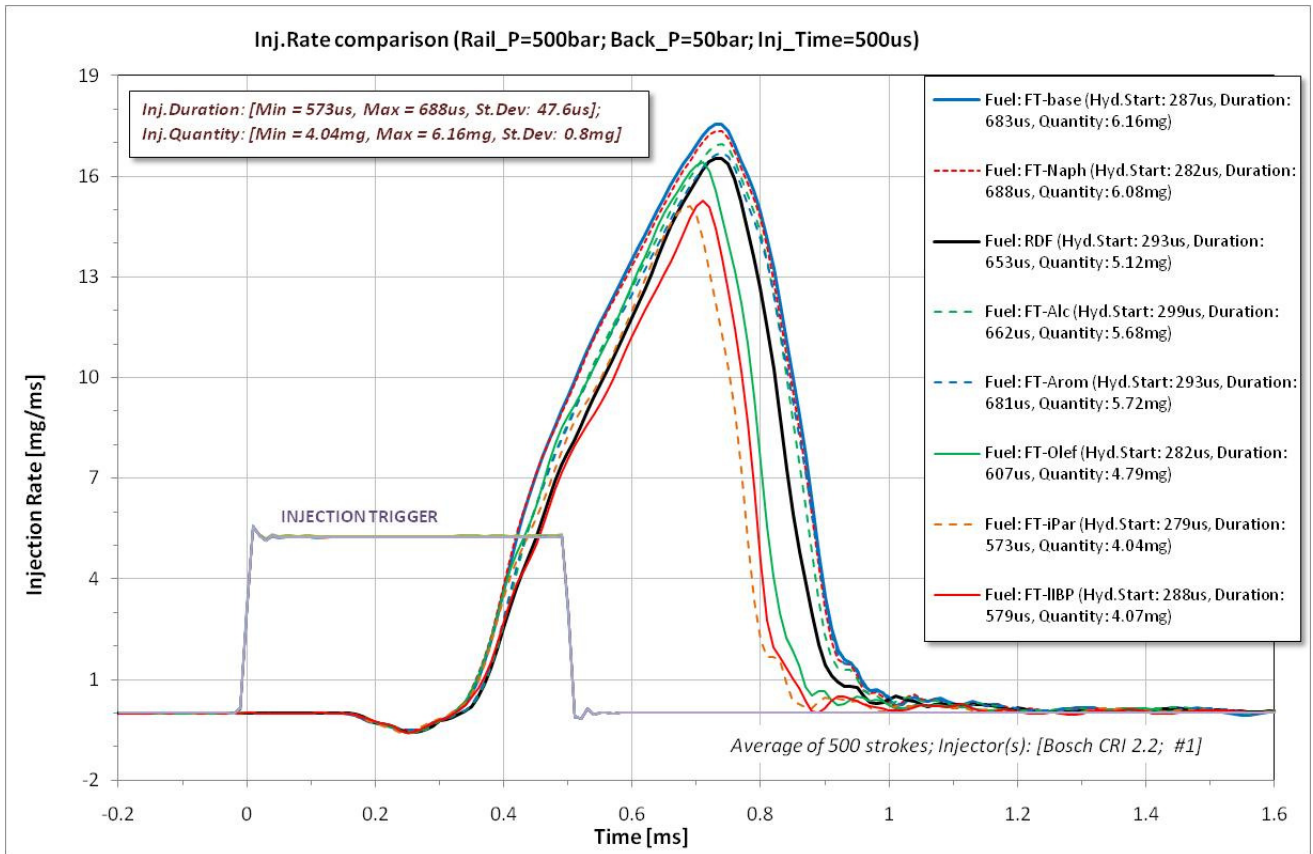


Figure 4.18: IR profiles, obtained with the set of fuels, for low rail pressure (500 bar) and long injection time (1 ms).



**Figure 4.19:** IR profiles, obtained with the set of fuels, for low rail pressure (500 bar) and short injection time (0.5 ms).

The differences in the delays with respect to the electrical start of the injection, as also in the slopes of the rising and falling edges of the injection rate profiles, are hardly perceptible among the fuels. However the hydraulic duration of the injection and the injected fuel mass show differences, most pronounced with short injector driving times and low injection pressures. These differences are summarized in the following table:

	Rail pressure = 500 bar		Rail pressure = 1000 bar		Rail pressure = 1500 bar	
	Inj. driving time = 0.5 ms	Inj. driving time = 1 ms	Inj. driving time = 0.5 ms	Inj. driving time = 1 ms	Inj. driving time = 0.5 ms	Inj. driving time = 1 ms
Hydraulic duration differences [%]	± 9.1	± 6.1	± 6.5	± 3.9	± 5.1	± 2.8
Injected mass differences [%]	± 20.8	± 9.5	± 12.1	± 5.3	± 7.5	± 3.6

**Table 4.10:** Differences in the hydraulic duration of the injection and in the injected fuel mass for the measurement performed with "fixed condition".

Despite a careful and accurate measurement procedure, a relatively high shot-to-shot and day-to-day fluctuation of the measurements was found. The fluctuation increases with shorter injector driving times and lower rail pressures (figures 4.20 – 4.27).

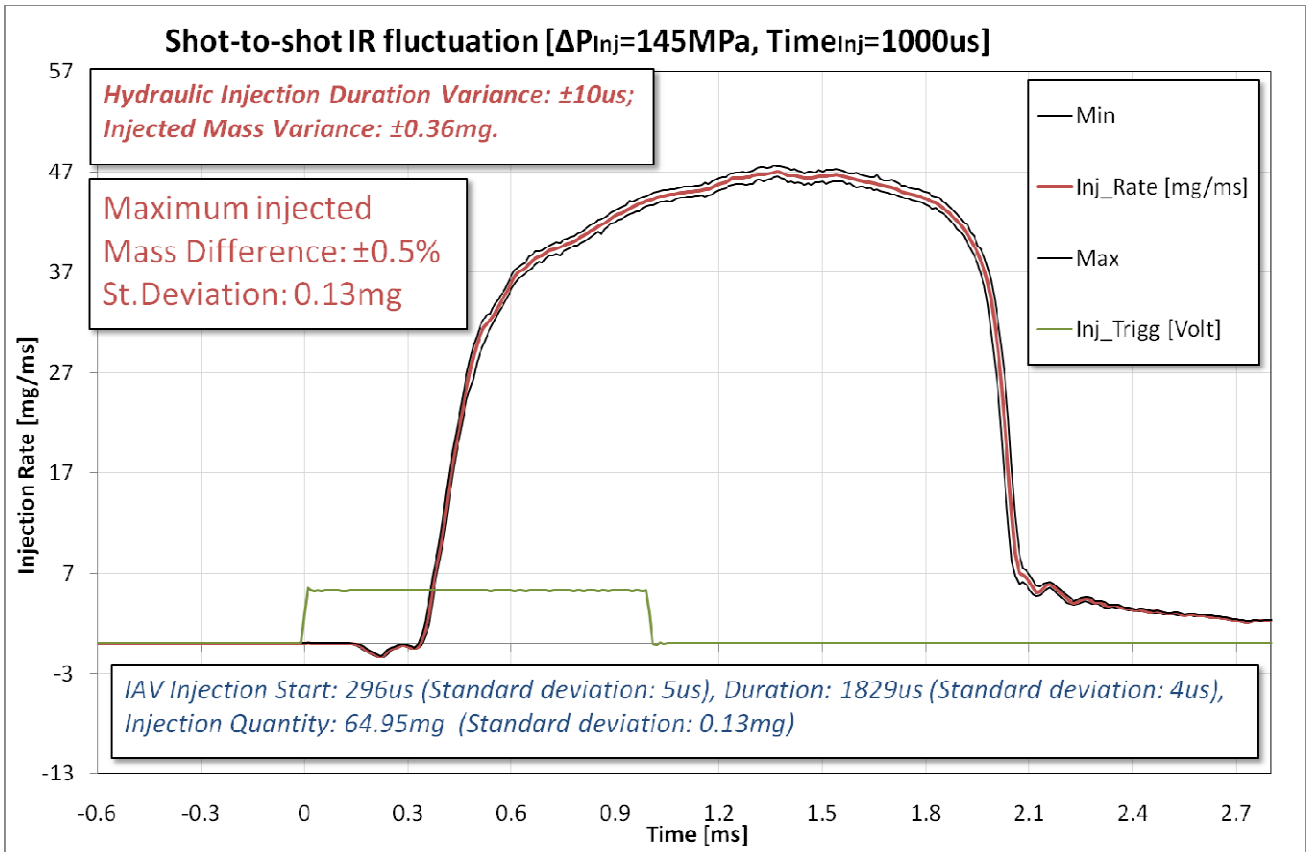


Figure 4.20: IR profile averaged over 500 strokes, for high rail pressure (1500 bar) and long injection time (1 ms).

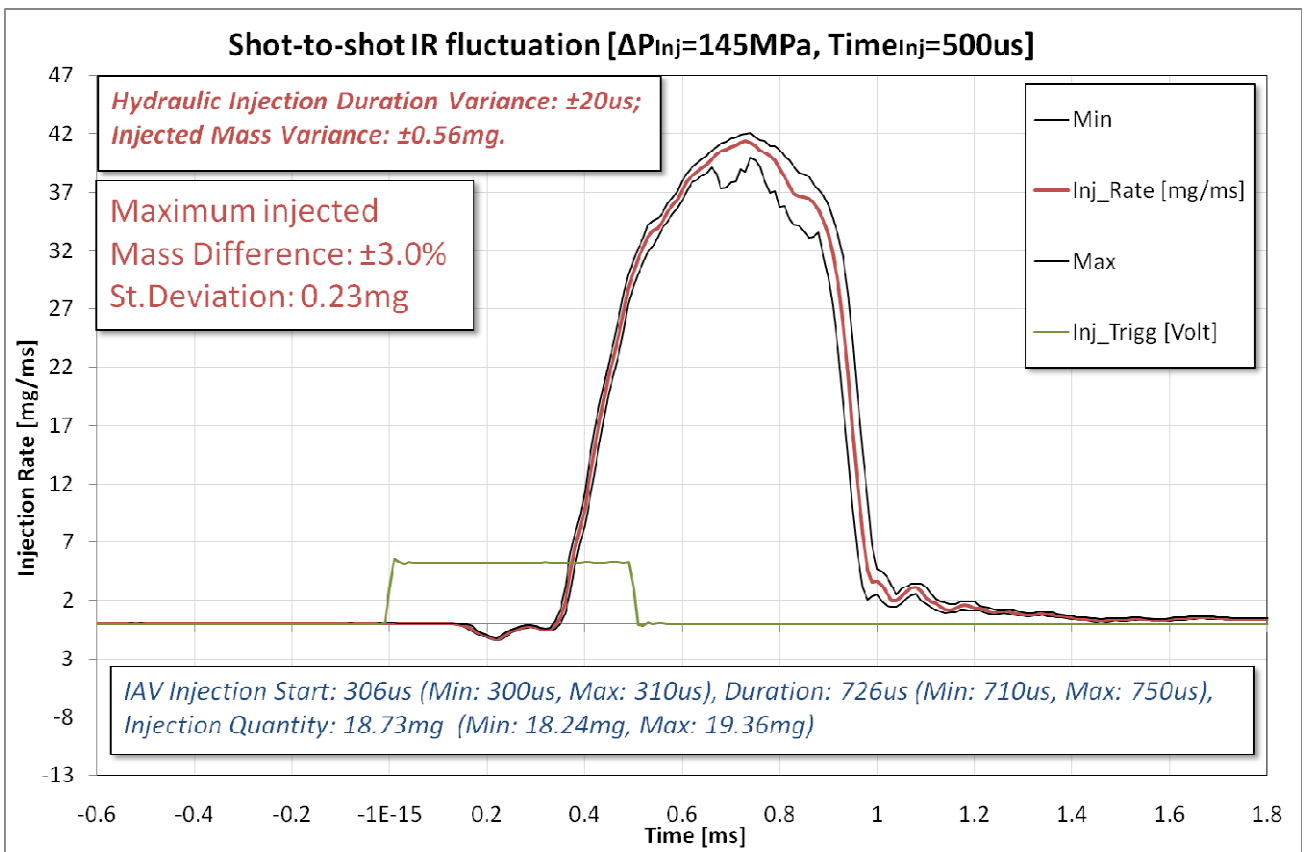


Figure 4.21: IR profile averaged over 500 strokes, for high rail pressure (1500 bar) and short injection time (0.5 ms).

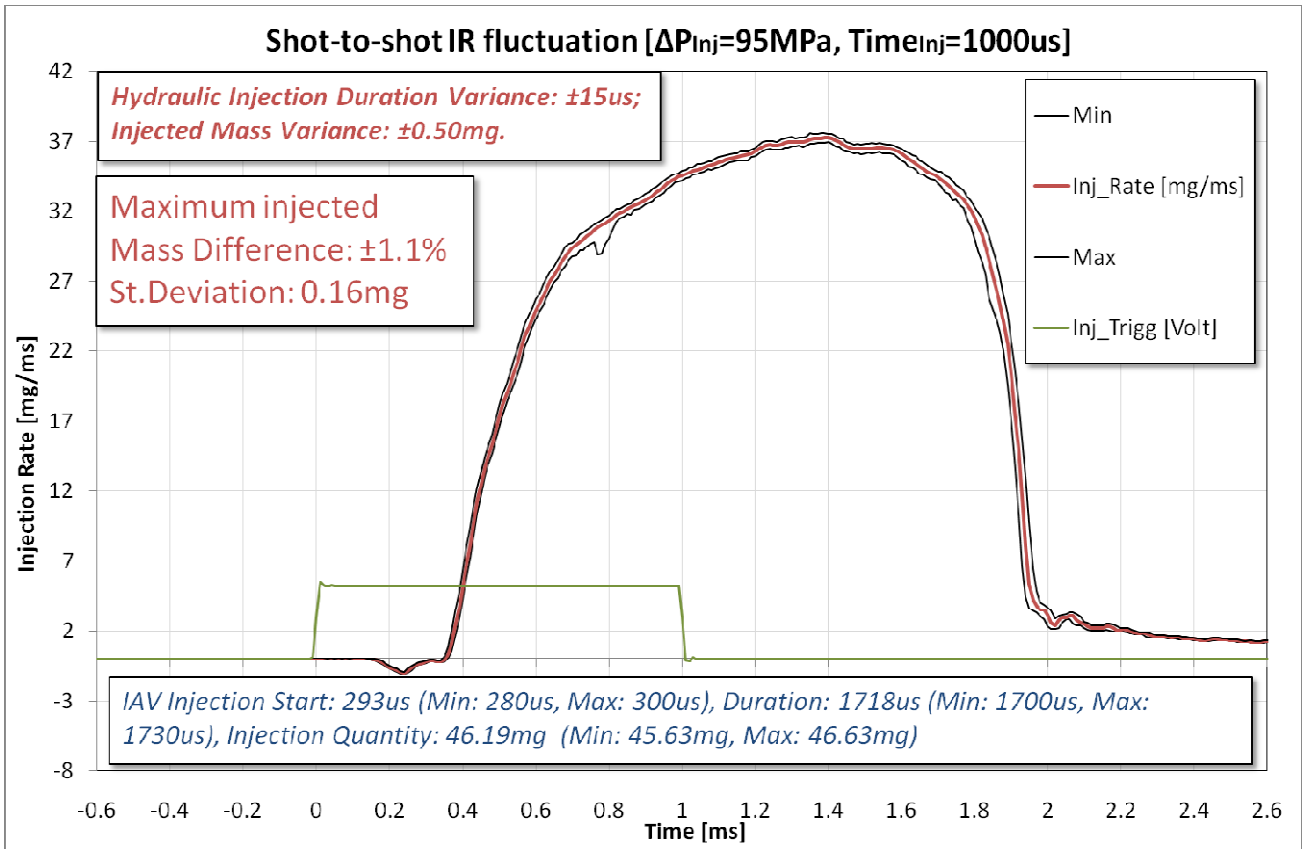


Figure 4.22: IR profile averaged over 500 strokes, for medium rail pressure (1000 bar) and long injection time (1 ms).

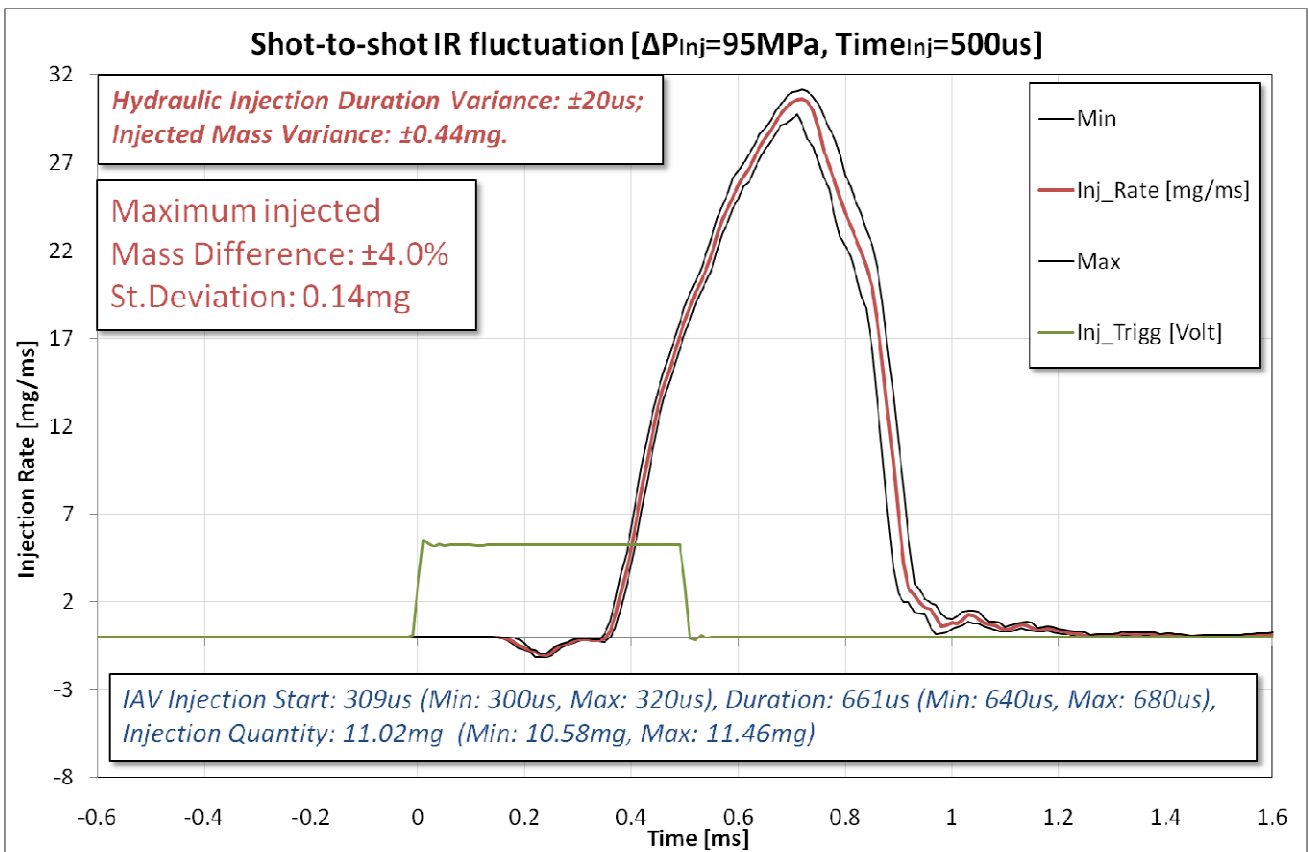


Figure 4.23: IR profile averaged over 500 strokes, for medium rail pressure (1000 bar) and short injection time (0.5 ms).

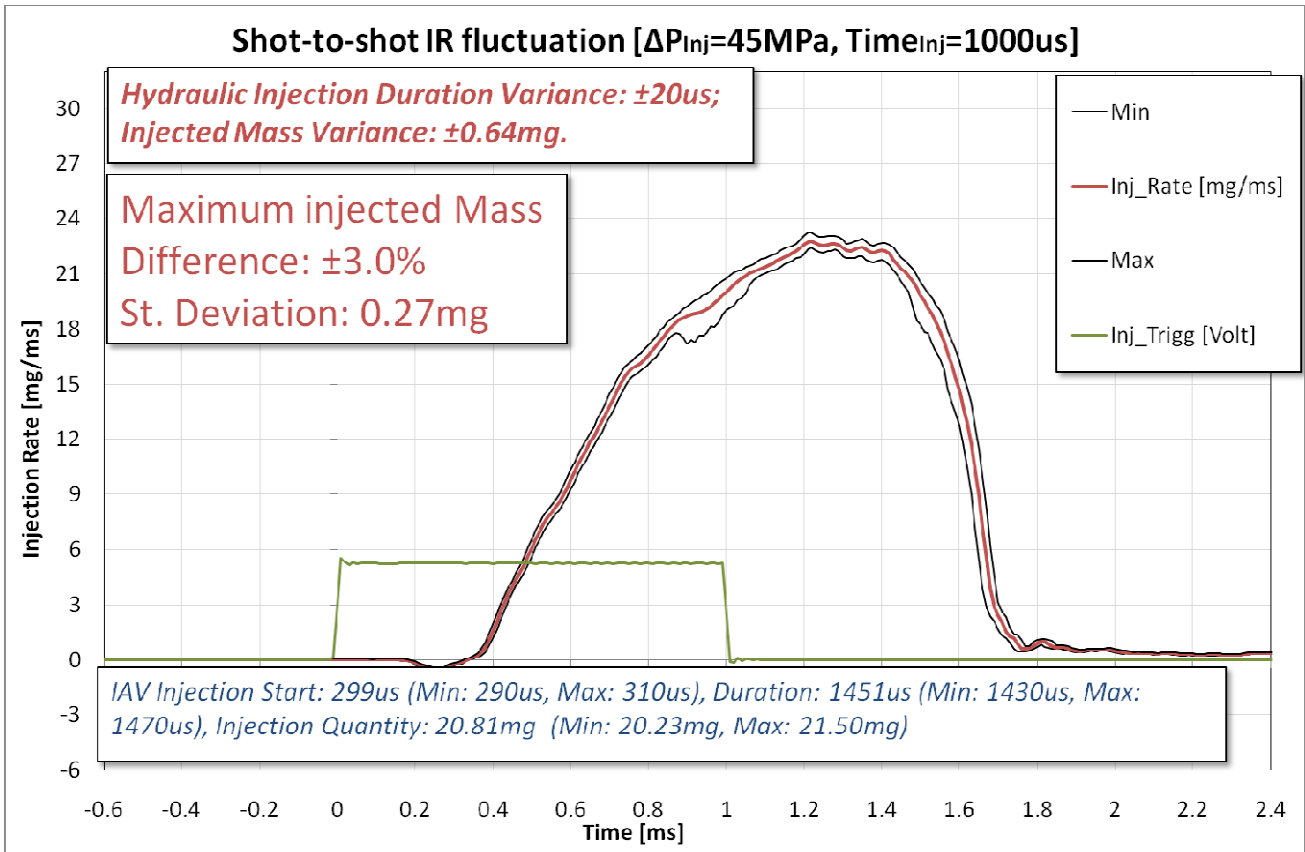


Figure 4.24: IR profile averaged over 500 strokes, for low rail pressure (500 bar) and long injection time (1 ms).

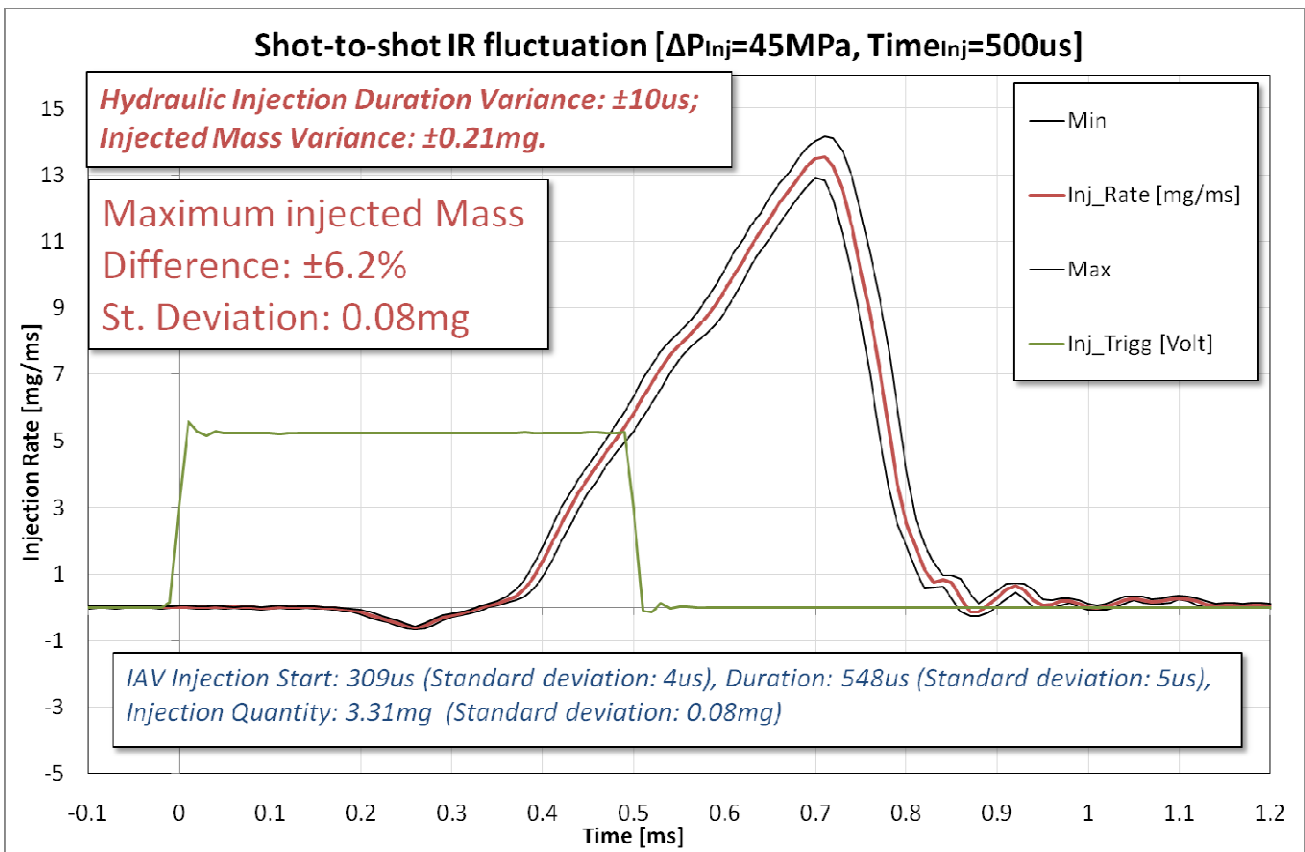


Figure 4.25: IR profile averaged over 500 strokes, for low rail pressure (500 bar) and short injection time (0.5 ms).

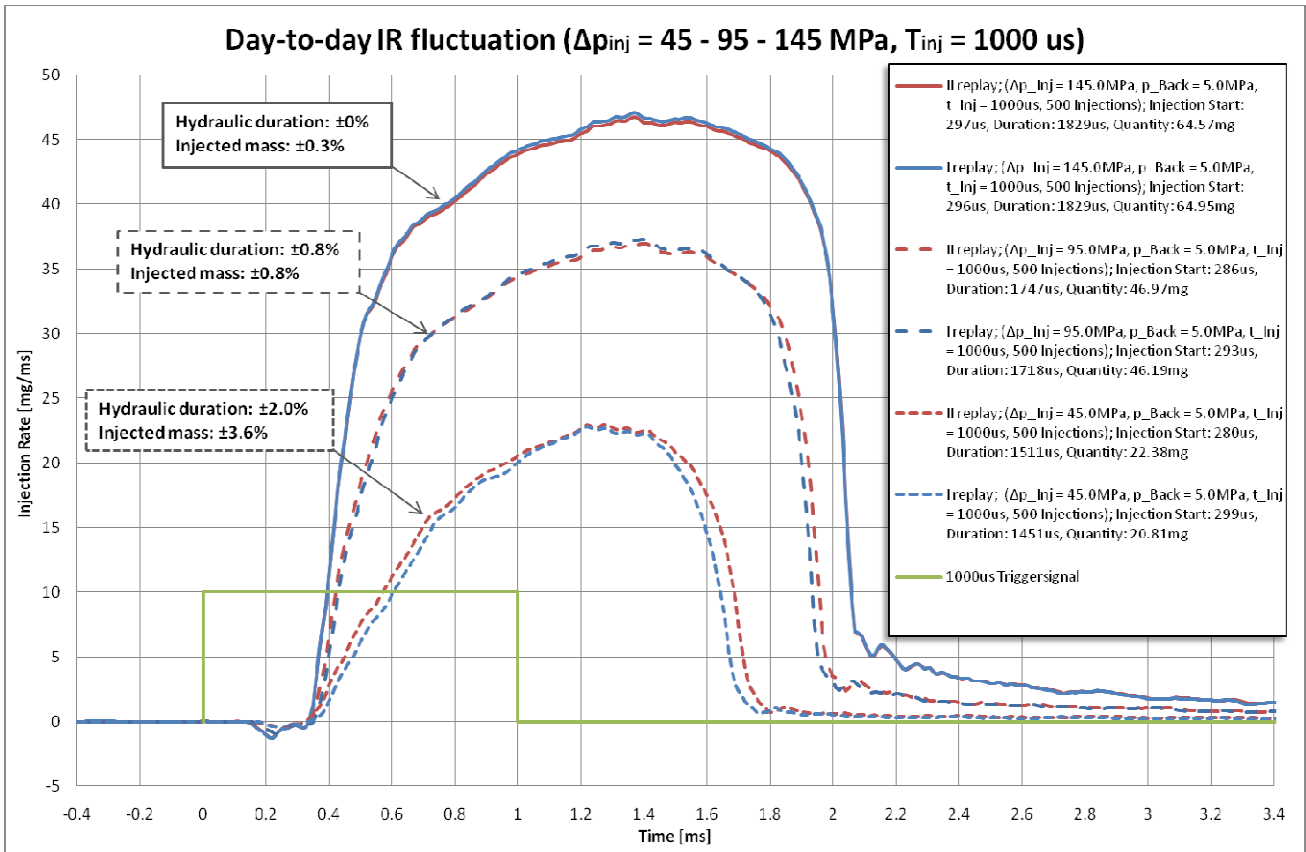


Figure 4.26: IR profiles obtained with the same fuel and under same conditions during different days, for long injection time (1 ms).

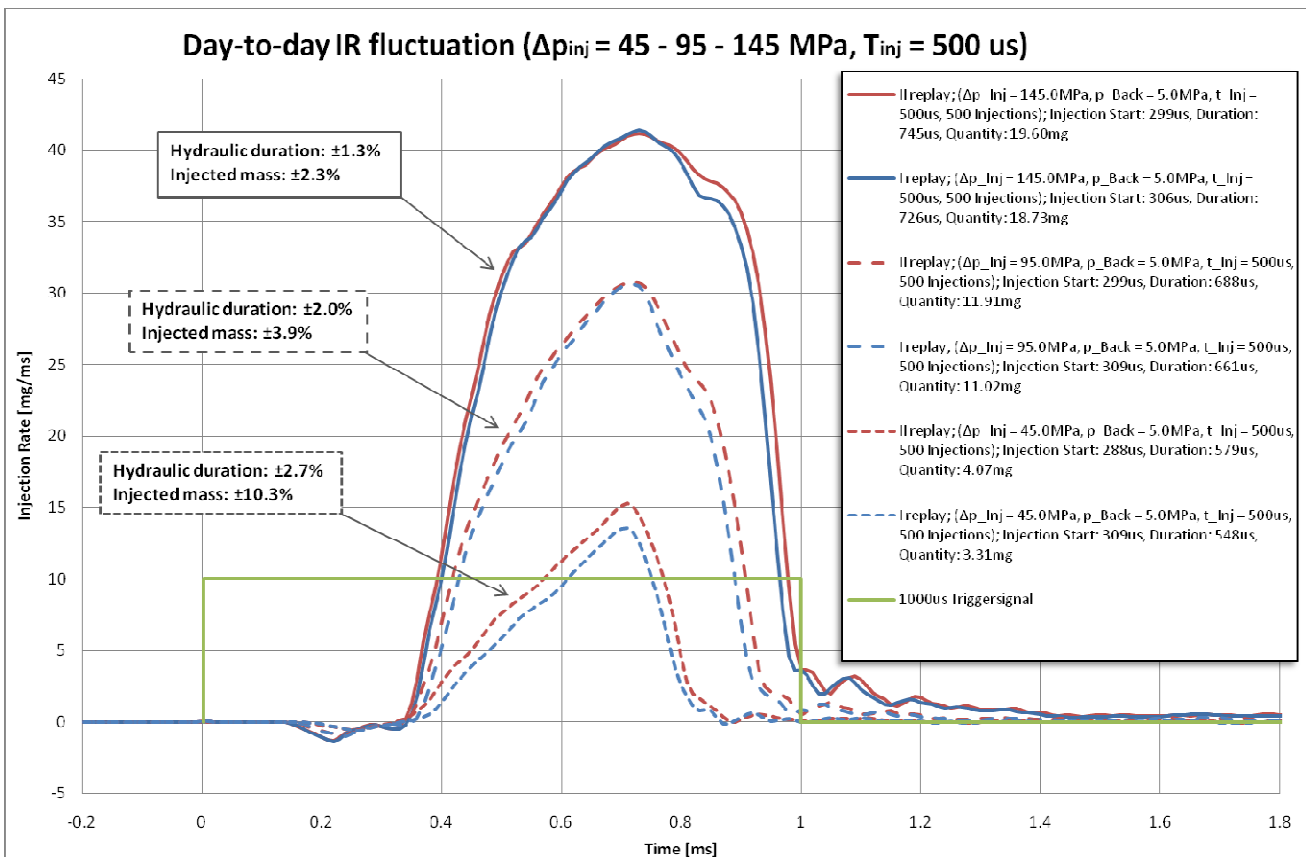


Figure 4.27: IR profiles obtained with the same fuel and under same conditions during different days, for short injection time (0.5 ms).

Considering the highest fluctuation of the measurement results, ranging from 0 % to 2.7 % for the hydraulic duration of the injection and from 0.3 % to more than 10 % for the injected fuel mass, the measurement results could hardly be correlated with the fuels' viscosity and density, and no correlation at all was found with lubricity. As a general trend it appears that the 3 fuels FT-IIBP, FT-iPar and FT-Olef show a short hydraulic injection duration and decreased injected fuel mass. The remaining five fuels differed however only little.

---

## Indexes

### Bibliography

- [1] **Mahr B.:** *Future and Potential of Diesel Injection Systems*, SAE Paper 2002-30-0001, 2002
- [2] <http://www.dieselforum.org>, accessed September 2010
- [3] **Alfieri Ezio:** *Emissions-Controlled Diesel Engine*, Dissertation ETH Nr. 18214, Zurich 2009
- [4] European Automobile Manufacturers Association: *The automobile industry pocket guide*, ACEA Communications department, 2010
- [5] <http://www.dieselnet.com>, accessed August 2010
- [6] **D. J. Patterson, N. A. Henein:** *Emissions from Combustion Engines and Their Control*, Ann Arbor Science Publishers, 1972
- [7] Nevada Mining Association: *NvMA Industrial Hygiene Sampling Manual*, 2008
- [8] <http://www.anl.gov/>, accessed September 2010
- [9] **Dale R. Tree, Kenth I. Svensson:** *Soot Processes in Compression Ignition Engines*, Progress in Energy and Combustion Science Vol. 33 pp. 272–309, 2007
- [10] **M. Lapuerta, R. Ballesteros and J. Rodríguez-Fernández:** *Thermogravimetric Analysis of Diesel Particulate Matter*, Measurement Science and Technology, Vol. 18, pp. 650–658, 2007
- [11] **Heywood John B.:** *Internal Combustion Engine Fundamentals*, McGraw-Hill, 1988
- [12] **Piacentini Marco:** *Fundamental aspects of NOx storage-reduction catalysts for automotive lean combustion engines*, Dissertation ETH Nr. 16830, Zurich 2006
- [13] **B. Bougie, L.C. Ganippa, A.P. van Vliet, K. Verbiezen, N. Dam, W.L. Meerts, J.J. ter Meulen:** *Soot characterization with Laser Induced Incandescence in a Heavy Duty Diesel Engine*, European Combustion Meeting, Louvain la Neuve (Belgium) 2005.
- [14] Landireno corporate university: *Combustibili Alternativi - Caratteristiche, tecnologie, criteri di scelta e prospettive*, 2007
- [15] International Energy Agency (IEA): *Key world energy statistics, 2010*
- [16] U.S. Energy Information Administration (EIA): *Short-Term Energy Outlook*, November 2010
- [17] <http://www.energy.wsu.edu>, accessed October 2010
- [18] <http://www.jmcsd.com>, *Johnson Matthey Catalysts*, accessed August 2010

- [19] **Bertola Andrea G.:** *Technologies for Lowest NO<sub>x</sub> and Particulate Emissions in DI-Diesel Engine Combustion-Influence of Injection Parameters, EGR and Fuel Composition*, Dissertation ETH Nr. 15373, Zurich 2003
- [20] **Mayer, Th. Lutz, Chr. Lämmle, M. Wyser, F. Legerer:** *Engine Intake Throttling for Active Regeneration of Diesel Particle Filters*, SAE Paper 2003-01-0381, 2003
- [21] <http://www.sapia.co.za/>, South African Petroleum Industry Association (SAPIA), accessed October 2010
- [22] **D. J. Aswani, M. J. van Nieuwstadt, J. A. Cook, J.W. Grizzle:** *Control Oriented Modeling of a Diesel Active Lean NO<sub>x</sub> Catalyst Aftertreatment System*, Asme Journal of Dynamic Systems, Measurement, and Control, Vol. 127, Issue 1, March 2005.
- [23] **R. C. Yu, A. S. Cole, B. J. Stroia, S. C. Huang, Ken Howden, Steve Chalk:** *Development of Diesel Exhaust Aftertreatment System for Tier II Emissions*, SAE Paper 2002-01-1867, 2002
- [24] **D. M. Ginter, J. Reuter, W. Taylor:** *Challenges for Diesel Emissions Aftertreatment Catalysts*, North American Catalysis Society (NACS) - 20<sup>th</sup> North American Meeting (NAM), June 2007
- [25] **Oscar Alfonso, Sara Ann:** *Catalytic Plasma Exhaust Converter*, United State Patent Nr. 5942195, August 1999
- [26] **Magdi Khair, Jacques Lemaire, Stefan Fischer:** *Integration of exhaust gas recirculation, selective catalytic reduction, diesel particulate filters, and fuel-borne catalyst for nox/pm reduction*, SAE Paper 2000-01-1933, 2000
- [27] **Katey E. Lenox, R. M. Wagner, J. B. Green Jr., J. M. Storey, C. S. Daw:** *Extending Exhaust Gas Recirculation Limits in Diesel Engines*, A&WMA 93rd Annual Conference and Exposition, Salt Lake City, June 2000
- [28] **Raffael Schubiger, Andrea Bertola, Konstantinos Boulouchos:** *Influence of EGR on combustion and exhaust emissions of heavy-duty DI diesel engines equipped with common-rail injection systems*, SAE Paper 2001-01-3497, 2001
- [29] **M. F. Russell, G. Greeves, N. Guerrassi:** *More torque, less emissions and less noise*, SAE Paper 2000-01-0942, 2000
- [30] **Thomas Koch, Uwe Gärtner, Gerhard König:** *Influence and Potential of Flexible Injection Rate Shaping for Medium and Heavy Duty Diesel Engine Combustion Processes*, International Journal of Vehicle Design, Vol. 41, Issue 1-4, pp. 127-142, 2006
- [31] **Sylvain Mendez, Benoist Thirouard:** *Using Multiple Injection Strategies in Diesel Combustion: Potential to Improve Emissions, Noise and Fuel Economy Trade-Off in Low CR Engines*, SAE Paper 2008-01-1329, 2008
- [32] **M. Badami, F. Mallamo, F. Millo, E. E. Rossi:** *Experimental Investigation on the Effect of Multiple Injection Strategies on Emissions, Noise and Brake Specific Fuel Consumption of an Automotive Direct*

- Injection Common-Rail Diesel Engine*, International Journal of Engine Research, Vol.4, Issue 4, pp. 299-314, 2003
- [33] **Keiki Tanabe, Susumu Kohketsu, Koji Mori, Kenji Kawai**: *Innovative Injection Rate Control with Next Generation Common Rail Fuel Injection System*, Seoul 2000 FISITA World Automotive Congress, Seoul (Korea) June 2000
- [34] **Steven R. Westbrook, Richard LeCren**: *Automotive Diesel and Non-Aviation Gas Turbine Fuels*, Fuels and Lubricants Handbook - Technology, Properties, Performance, and Testing, ASTM International 2003
- [35] U.S. Energy Information Administration (EIA): *Annual Energy Outlook 2006*, 2006
- [36] <http://www.futurecoalfuels.org/>, accessed September 2010
- [37] <http://www.afdc.energy.gov/>, U.S. Department of Energy, accessed October 2010
- [38] **Tomislav Kurevija, Nenad Kukulj, Damir Rajkovic**: *Global Prospects of Synthetic Diesel Fuel Produced from Hydrocarbon Resources in Oil & Gas Exporting Countries*, Rudarsko-geološko-Naftni Zbornik, Vol. 19, pp. 79-86, Zagreb 2007
- [39] ASFE - Alliance for Synthetic Fuels in Europe: *Synthetic Fuels: "Driving Towards Sustainable Mobility"*
- [40] **D. Kusdiana, S. Saka**: *Biodiesel Fuel for Diesel Fuel Substitute Prepared by a Catalyst-Free Supercritical Methano*, Nihon Enerugi Gakkai Taikai Koen Yoshish, pp. 186-187, 2002
- [41] **Jianbing Ji, Jianli Wang, Yongchao Li, Yunliang Yu, Zhichao Xu**: *Preparation of Biodiesel with the help of Ultrasonic and Hydrodynamic Cavitation*, Ultrasonics, Vol. 44, Supplement 1, pp. e411-e414, December 2006
- [42] **Nicholas E. Leadbeater, Lauren M. Stencil**: *Fast, Easy Preparation of Biodiesel Using Microwave Heating*, Energy & Fuels, Vol. 20 pp. 2281-2283, 2006
- [43] Texas Comptroller of Public Accounts: *The Energy Report*, May 2008
- [44] **Robert L. McCormick, Javier R. Alvarez, Michael S. Graboski, K. Shaine Tyson, Keith Vertin**: *Fuel additive and blending approaches to reducing NO<sub>x</sub> emissions from biodiesel*, SAE Paper 2002-01-1658, 2002
- [45] **Tschöke, Helmut**: *Diesel distributor fuel-injection pump*, Robert Bosch GmbH, Stuttgart 1999
- [46] **Joachim Schommers, Frank Duvinage, Marco Stotz, Arndt Peters, Stefan Ellwanger, Katsuyoshi Koyanagi, Helmut Gildein**: *Potential of Common Rail Injection System for Passenger Car DI Diesel Engines*, SAE Paper 2000-01-0944, 2000
- [47] **Ulrich Flaig, Wilhelm Polach, Gerhard Ziegler**: *Common Rail System (CR-System) for Passenger Car DI Diesel Engines - Experiences with Applications for Series Production Projects*, SAE Paper 1999-01-0191, 1999

- 
- [48] **S. Matsuoka, K. Yokota, T. Kamimoto:** *The Measurement of Injection Rate*, Proceedings of the Institution of Mechanical Engineers 1969-70, Vol 184, Nuber 3J, pp.87-94, 1969
- [49] **Bosch Wilhelm:** *Fuel Rate Indicator is a New Measuring Instrument for Display of the Characteristics of Individual Injection*, SAE Paper 660749, 1966
- [50] **Akio Takamura, Susumu Fukushima, Yukimitsu Omori, Takeyuki Kamimoto:** *Development of a new measurement tool for fuel injection rate in diesel engines*, SAE Paper 890317, 1989
- [51] **Glenn R. Bower, David E. Foster:** *A comparison of the Bosch and Zuech rate of injection meter*, SAE Paper 910724, 1991
- [52] **Daneshyar H:** *One-Dimensional Compressible Flow*, Pergamon international library 1976
- [53] IAV GmbH: *Injection Analyzer - Operator's Manual*, 2004
- [54] IAV GmbH: *FI<sup>2RE</sup> - Operator's Manual version 1.6*, 2006
- [55] **Thomas W. Ryan III:** *Diesel Fuel Combustion Characteristics*, Fuels and Lubricants Handbook - Technology, Properties, Performance, and Testing, ASTM International 2003
- [56] **Hartmut Lüders, Peter Stommel, Sam Geckler:** *Diesel Exhaust Treatment - New Approaches to Ultra Low Emission Diesel Vehicles*, SAE Paper 1999-01-0108, 1999
- [57] **Coryne A. Forest, Patsy A. Muzzell:** *Fischer-Tropsch Fuels - Why Are They of Interest to the United States Military?*, SAE Paper 2005-01-1807, 2005
- [58] *EMA Consensus Position, Joint EMA/TMC Pump Grade Specification for Premium Diesel Fuels.*
- [59] **Dry, Mark E.:** *The Fischer-Tropsch Process: 1950-2000*, Catalysis Today, Vol. 71, Issue 3-4, pp. 227–241, January 2002
- [60] **Peter Bloch, Wolfgang Kreutner, Stephan Caruso, Bruno Schneider:** Abschlussbericht Vorhaben 940: Bestimmung optimaler Zusammensetzungen synthetischer Kraftstoffe für konventionelle Diesel-Brennverfahren, FVV Heft R 551, 2010

## Index of Symbols

$a$	Velocity of sound	[m/s]
$A$	Tube cross section area	[mm <sup>2</sup> ]
$dq/dt$	Injection rate	[mm <sup>3</sup> /s]
$Fr$	Injection frequency	[Hz]
$Fr_{data}$	Data sampling frequency of the scale	[Hz]
$H_u$	Lower calorific value	[J/g]
$L$	Length of the measuring tube	[m]
$m$	Mass	[mg]
$\dot{m}$	Mass flow rate	[mg/s]
$m_{pre}$	Pre-injection fuel mass	[g]
$M_{stroke}$	Injected fuel mass per stroke	[mg]
$m_{wg}$	Weighed injected mass mean	[mg]
$p$	Pressure	[Pa]
$Q$	Injected fuel	[mm <sup>3</sup> /s]
$t$	Time	[s]
$T$	Temperature	[°C]
$T_{max}$	Maximum injection period	[s]
$T_{obs}$	Minimum time of observation	[s]
$T_{2L}$	Twice the transient time	[s]
$v$	Fluid velocity	[m/s]
$\rho$	Density	[Kg/m <sup>3</sup> ]
$\lambda$	Air/fuel ratio (fuel-lean mixture $\lambda > 1$ )	

## Index of Abbreviations and Definitions

°CA	Crank angle degree	[deg]
ALNC	Active lean NO <sub>x</sub> catalyst	
ASPO	Association for the study of peak oil and gas	
BTL	Biomass-to-liquid	
CR	Common-rail	
CRT	Continuously regenerating trap	
CTL	Coal-to-liquid	
DI	Direct injection	
DOC	Diesel oxidation catalyst	
DOI	Duration of injection	[μs]
DOPI	Duration of pre-injection	[μs]
DPF	Diesel particulate filter	
EC	Elementary carbon	
EFTA	European free trade association	
EGR	Exhaust gas recirculation	
EIA	Energy information administration (U.S.)	
EPA	Environmental protection agency (U.S.)	
EU	European union	
FSN	Filter smoke number	
FT	Fischer-Tropsch	
GC-MS	Gas chromatography - mass spectrometry	
GTL	Gas-to-liquid	
HTDZ	Hoch-temperatur-druck zelle (high-temperature-	

	pressure cell)	
IARC	International agency for research on cancer	
IC	Internal combustion	
IEA	International energy agency	
IGCC	Integrated gasification combined cycle	
IR	Injection rate	
ISFC	Indicated specific fuel consumption	
LIF	Laser-induced fluorescence technique	
LNC	Lean NO <sub>x</sub> catalyst	
MSHA	Mine safety health and administration	
Mtoe	Million ton of oil equivalent	
NAC	NO <sub>x</sub> adsorption catalysts	
NCRS	Next-generation common-rail system	
NMHC	Non-methane hydrocarbon emissions	
NREL	National renewable energy laboratory	
OC	Organic carbon	
OPEC	Organization of the petroleum exporting countries	
OTL	Oil-to-liquid	
PM	Particulate matter	
PM	Plasma converter	
rpm	Revolutions per minute	[1/min]
SCR	Selective catalytic reduction	
SOF	Soluble organic fraction	
SOF	Soxhlet extraction method	
SOI	Start of injection	[deg]
SOPI	Start of pre-injection	[deg]
TDC	Top dead center	
tpc	TransPC file	
toe	ton of oil equivalent	
VOF	Volatile organic fraction	

## Appendix

### (A) Some Details of the IVK's Motor Test Bench

The test bench is equipped with pressure and temperature sensors, i.e. low pressure transducers (Kistler 4045A) in both inlet and exhaust manifolds and a high pressure transducer (Kistler 6061B) in the combustion chamber are used. The inlet air mass is obtained by means of a thermal mass flow meter (Sensyflow P) that works according to the principle of a hot film anemometer. The injected fuel mass is determined by a gravimetric fuel balance (AVL 733s). Before the fuel is compressed by the high pressure pump, fuel pressure and temperature are adjusted by the AVL Fuel Mass Flow Meter and Fuel Temperature Control (AVL 753C). The emission analysis is made by the external system Pierburg AMA 2000 which is directly connected to the exhaust manifold by a single heated pipe. The concentrations of CO<sub>2</sub>, CO (both analyzed by a NDIR module), NO<sub>x</sub> (CLD type), Hydrocarbons (FID) and O<sub>2</sub> (OXIMAT paramagnetic oxygen analyzer) are determined. An additional NDIR module is used to measure CO<sub>2</sub> content in the inlet manifold in order to calculate the EGR rate.

### (B) Some Details of the HTDZ Test Bench

For the optical detection of the liquid phase propagation of the injection spray under non-reactive, evaporating and non-evaporating conditions, a high-speed camera of the type High speed Star 6 manufactured by LaVision is used. This camera can record up to 5400 frames per second with an image size of 1024 x 1024 pixels (12-bit colours). For the injection spray measurements the field of view is reduced to an image size of 512 x 384 pixels; this image resolution allows a frame rate of 27 kHz (time between two images: 37 μs) to be achieved but only 2 of the seven spray cones are visible in the images. Injection jets are evenly illuminated by halogen lights (through the four side windows of the cell).

The injection spray shape during the injection is then obtained by recording the light scattered by droplets (and other liquid structures) (Mie scattering).

For the OH chemiluminescence imaging under reactive conditions the camera is equipped with a UV-sensitive high-speed image intensifier (IRO). In these measurements, the maximum visible area of the injection jets (Ø 90 mm) is recorded with 512 x 512 pixels, a configuration which allows a frame rate of 20 kHz (time between two images: 50 μs).

The intensity of soot radiation for the three-colours pyrometry is detected through the large window of the cell by an optical probe (Optical Light sample OLP, a prototype from Kistler AG) and is measured at the wavelengths of 680 nm, 790 nm and 903 nm.